

**Optimizing the Combined Effects of TiO₂ and CuO Nanoparticles on CI
Engine Performance and Emissions with Diesel-Methanol Blends Using Box-
Behnken Design**

Lelisa Alemu Gobena



A Thesis Submitted to

The Department of Mechanical Engineering

College of Mechanical, Chemical, and Materials Engineering

Presented in Partial Fulfillment of the Requirement for the Degree of Master's in

Automotive Engineering

School of Postgraduate Studies

Adama Science and Technology University

December, 2025

Adama, Ethiopia

**Optimizing the Combined Effects of TiO₂ and CuO Nanoparticles on CI
Engine Performance and Emissions with Diesel-Methanol Blends Using Box-
Behnken Design**

Lelisa Alemu Gobena
Advisor: Derese Firew (PhD)

A Thesis Submitted to
The Department of Mechanical Engineering
College of Mechanical, Chemical, and Materials Engineering
Presented in Partial Fulfillment of the Requirement for the Degree of Master's in
Automotive Engineering

School of Postgraduate Studies
Adama Science and Technology University

December, 2025

Adama, Ethiopia

CANDIDATE DECLARATION

I declare that this thesis entitled “**Optimizing the Combined Effects of TiO₂ and CuO Nanoparticles on CI Engine Performance and Emissions with Diesel-Methanol Blends Using Box-Behnken Design**” is my own work. That is, it has not been submitted for the award of any academic degree, diploma or certificate in any other university. All sources of materials that are used for this thesis have been duly acknowledged through citation.

Name of student

Signature

Date

RECOMMENDATION

I, the advisor of this thesis, hereby certify that I have read the revised version of the thesis entitled **“Optimizing the Combined Effects of TiO₂ and CuO Nanoparticles on CI Engine Performance and Emissions with Diesel-Methanol Blends Using Box-Behnken Design”** prepared under my guidance by **Lelisa Alemu** submitted in partial fulfillment of the requirements for the degree of Master’s of Science in Automotive Engineering. Therefore, I recommend the submission of revised version of the thesis to the department following the applicable procedures.

Major Advisor

Signature

Date

APPROVAL PAGE FOR M.Sc. THESIS

I/we, the advisors of the thesis entitled “**Optimizing the Combined Effects of TiO₂ and CuO Nanoparticles on CI Engine Performance and Emissions with Diesel-Methanol Blends Using Box-Behnken Design**” by **Lelisa Alemu**, hereby certify that the recommendation and suggestions made by the board of examiners are appropriately incorporated into the final version of the thesis.

Major Advisor/Supervisor

Signature

Date

We, the undersigned, members of the board of examiners of the thesis by Lelisa Alemu have read and evaluated the thesis entitled “Optimizing the Combined Effects of TiO₂ and CuO Nanoparticles on CI Engine Performance and Emissions with Diesel-Methanol Blends Using Box-Behnken Design” and examined the candidate during open defense. This is, therefore, to certify that the thesis is accepted for partial fulfillment of the requirement of the degree of Master of Science in Automotive Engineering.

Chairperson

Signature

Date

Internal Examiner

Signature

Date

External Examiner

Signature

Date

Final approval and acceptance of the thesis is contingent upon submission of its final copy to the Office of Postgraduate Studies (OPGS) through the Department Graduate Council (DGC) and School Graduate Committee (SGC).

Department Head

Signature

Date

College Dean

Signature

Date

School of Postgraduate Studies, Dean

Signature

Date

ACKNOWLEDGEMENTS

I want to start by expressing my sincere gratitude to God Almighty for all of his blessings, grace, and support during this academic journey. Without his divine presence and unwavering support, this achievement would not have been possible. Next, I would like to express my gratitude to my adviser, **Dr. Deresse Firew**, whose insightful advice, unwavering support, and constructive criticism were essential in deciding the direction, scope, and quality of this study. In addition to enhancing my academic skills, his advice has inspired me to advance both personally and professionally.

My profound gratitude goes to **Mr. Chala Ephrem** for his consistent encouragement, thoughtful advice, and senior-level guidance throughout this work. His input has been a critical resource during key stages of my research development. Additionally, I would like to express my gratitude to Addis Ababa Science and Technology University for providing the necessary research infrastructure and laboratory facilities. The availability of such resources was vital for the smooth execution of the experimental work and data analysis. Grateful acknowledgment is extended to **Dr. Melaku Desta** and **Mr. Yewalework Damto** for their committed technical support throughout the engine performance and emission testing. Their practical insights and hands-on support significantly contributed to the success of this study.

Lastly, I extend my deepest appreciation to my beloved father, **Alemu Gobena**, and my dear siblings, whose unwavering support, love, and encouragement have been a constant source of strength. Their belief in my potential has continually motivated me to overcome challenges and pursue excellence throughout my academic journey.

TABLE OF CONTENTS

Contents	Page
CANDIDATE DECLARATION	i
RECOMMENDATION	ii
APPROVAL PAGE FOR M.Sc. THESIS.....	iii
ACKNOWLEDGEMENTS	iv
TABLE OF CONTENTS	v
LIST OF TABLES.....	viii
LIST OF FIGURES	ix
LIST OF ACRONYMS AND ABBREVIATIONS	xi
ABSTRACT.....	xiv
CHAPTER ONE	1
INTRODUCTION.....	1
1.1. Background of the Study	1
1.2. Nanoparticles	3
1.3. Statement of the Problem.....	4
1.4. Objective of the Study.....	5
1.4.1. General Objective	5
1.4.2. Specific Objectives	5
1.5. Significance of the Study	5
1.6. Scope of the Study	5
1.7. Limitations of the study	6
1.8. Organization of the thesis	6
CHAPTER TWO	8
LITERATURE REVIEW.....	8

2.1. Introduction.....	8
2.2. Important Applications of Methanol.....	8
2.3. Physicochemical Properties of Methanol.....	9
2.4. Effects of diesel-methanol blends on performance and emission characteristics of CI engine.....	10
2.5. Summary of related works on diesel-methanol blends.....	14
2.6. The effects of adding nanoparticles to fuel in internal combustion engines.....	15
2.6.1. Fuel Additives.....	15
2.6.2. Stability of nanoparticles in a base fluid.....	16
2.6.3. Effect of metal oxide nanoparticles on performance and emissions of CI engine.....	17
2.7. Response surface methodology for optimizing engine performance and emissions.....	22
2.7.1. Factors (input) and responses (output) in RSM.....	23
2.7.2. Single vs. multiple responses in RSM.....	24
2.7.3. Response surface design for RSM.....	26
2.8. Research Gap.....	30
CHAPTER THREE.....	31
MATERIAL AND METHODS.....	31
3.1. Introduction.....	31
3.1. Materials.....	31
3.2. Methods.....	33
3.3. Design of experiment using Response Surface Methodology (RSM).....	34
3.4. Preparation of diesel-methanol.....	34
3.5. Preparation of Nano-methanol-diesel fuel blends.....	35
3.5.1. Materials and equipment used.....	36
3.5.2. Fuel Preparation Procedure (Example: M10 + TiO ₂ 90 ppm + CuO 60 ppm).....	37

3.6. Engine experimental setup and test procedure	38
3.7. Data analysis	41
CHAPTER FOUR.....	44
RESULTS AND DISCUSSIONS.....	44
4.1. Engine performance and Exhaust emission characteristics	44
4.1.1 Performance Characteristics	44
4.1.2 Exhaust Emission Characteristics	47
4.2. Optimization of engine performance and emissions.....	53
4.2.1 Response surface methodology model (RSM) analysis.....	53
4.2.2. Optimization of engine performance analysis	58
4.2.3. Optimization of engine exhaust emission analysis	64
4.3. Optimizer for response surface methodology	72
CHAPTER 5.....	74
CONCLUSION AND RECOMMENDATION.....	74
5.1. Conclusions	74
5.2. Recommendations and Future Directions	75
APPENDICES	83
Appendix A: Structural, Chemical and Physical Properties TiO ₂ properties	83
Appendix B: Structural, Chemical and Physical Properties CuO properties	84
Appendix C: EDIBON, TBMC 8 model engine dynamometer test setup	85
Appendix D: Originality Declaration Form for Students	86

LIST OF TABLES

Table 2.1 Physicochemical properties of diesel, gasoline, and methanol.....	10
Table 3.1 List of materials and equipments used for the study.....	32
Table 3.2 Range of process factors used in Box Behnken design.....	34
Table 3.3 Specification of the test engine	39
Table 3.4 Experimental test matrix	40
Table 4.1 The brake power data recorded from the test.....	44
Table 4.2 The brake torque data recorded from the test.....	45
Table 4.3 The BSFC data recorded from the test	46
Table 4.4 The carbon monoxide data recorded from the test.....	48
Table 4.5 The carbon dioxide data recorded from the test.....	49
Table 4.6 The hydrocarbon data recorded from the test.....	50
Table 4.7 The nitrogen oxides data recorded from the test.....	52
Table 4.8 Experimental matrix with the results of the engine performance and emission	56
Table 4.9 ANOVA for engine performance.....	57
Table 4.10 ANOVA for engine emissions	57
Table 4.11 Evaluation of ANOVA model.....	58
Table 4.12 Optimization setup	73

LIST OF FIGURES

Figure 2.1 Methanol's primary applications as a source of energy	9
Figure 2.2 A brief summary of FFD.....	27
Figure 2.3 CCD graphical representation	28
Figure 2.4 Three types of CCD.....	28
Figure 2.5 BBD graphical representation	29
Figure 3.1 The comprehensive methodological workflow of the study.....	33
Figure 3.2 Materials and equipment used for nano-methanol-diesel blends preparation	37
Figure 3.3 Ultrasonic cleaner	37
Figure 3.4 blending process utilizing the ultrasonicator	38
Figure 3.5 Schematic diagram of the experimental setup	40
Figure 4.1 Variation of brake power with engine load.....	45
Figure 4.2 Variation of brake torque with engine load	46
Figure 4.3 Variation of BSFC with engine load	47
Figure 4.4 Variation of carbon monoxide with engine load.....	48
Figure 4.5 Variation of carbon dioxide with engine load.....	50
Figure 4.6 Variation of hydrocarbon with engine load	51
Figure 4.7 Variation of nitrogen oxide with engine load	53
Figure 4.8 Surface plot of BT vs engine load and TiO ₂ Nanoparticle	59
Figure 4.9 Surface plot of BT vs engine load and CuO Nanoparticle	59
Figure 4.10 Surface plot of BT vs TiO ₂ and CuO Nanoparticle	60
Figure 4.11 Surface plot of BP vs engine load and TiO ₂ Nanoparticle.....	61
Figure 4.12 Surface plot of BP vs engine load and CuO Nanoparticle.....	61
Figure 4.13 Surface plot of BP vs TiO ₂ and CuO Nanoparticle.....	62

Figure 4.14 Surface plot of BSFC vs engine load and TiO ₂ Nanoparticle	63
Figure 4.15 Surface plot of BSFC vs engine load and CuO Nanoparticle	63
Figure 4.16 Surface plot of BSFC vs TiO ₂ and CuO Nanoparticle	64
Figure 4.17 Surface plot of CO vs engine load and TiO ₂ Nanoparticle.....	65
Figure 4.18 Surface plot of CO vs engine load and CuO Nanoparticle.....	65
Figure 4.19 Surface plot of CO vs TiO ₂ and CuO NPs.....	66
Figure 4.20 Surface plot of CO ₂ vs engine load and TiO ₂ NPs.....	67
Figure 4.21 Surface plot of CO ₂ vs engine load and CuO NPs.....	67
Figure 4.22 Surface plot of CO ₂ vs TiO ₂ and CuO NPs	68
Figure 4.23 Surface plot of HC vs engine load and TiO ₂ NPs.....	69
Figure 4.24 Surface plot of HC vs engine load and CuO NPs.....	69
Figure 4.25 Surface plot of HC vs TiO ₂ and CuO NPs.....	70
Figure 4.26 Surface plot of NO _x vs engine load and TiO ₂ NPs.....	71
Figure 4.27 Surface plot of NO _x vs engine load and CuO NPs.....	71
Figure 4.28 Surface plot of NO _x vs TiO ₂ and CuO NPs.....	72

LIST OF ACRONYMS AND ABBREVIATIONS

AASTU	Addis Ababa Science and Technology University
Adj-R ²	Adjusted coefficient of determination
Al	Aluminum
Al ₂ O ₃	Aluminum oxide
ANOVA	Analysis of variance
BBD	Box-Behnken design
BP	Brake power
BSEC	Brake-specific energy consumption
BSFC	Brake-specific fuel consumption
BT	Brake torque
BTE	Brake thermal efficiency
CCD	Central composite design
CD	Combustion duration
CDC	Conventional diesel combustion
CDE	Conventional diesel engine
CeO ₂	Cerium oxide
CH ₃ OH	Methanol
CH ₄	Methane
CI	Compression engine
CN	Cetane number
CNT	Carbon nanotube
CNG	Compressed natural gas
CTAB	Cetyletrimethyl ammonium bromide
CO	Carbon monoxide
COG	Coke oven gases
CP	Cylinder pressure
CRDE	Common rail diesel engine
CR	CR
CO ₂	Carbon dioxide
CuO	Copper oxide

DI	Direct injection
DOE	Design of experiment
EGA	Exhaust gas analyzer
EGR	Exhaust gas recirculation
EGT	Exhaust gas temperature
Fe ₃ O ₄	Iron oxide
FFD	Full factorial design
GO	Graphene oxide
HRR	Heat release rate
ICE	Internal combustion engine
ID	Ignition delay
M10	10% of methanol and 90 % of diesel
M20	20% of methanol and 80 % of diesel
M30	30% of methanol and 80 % of diesel
MG	Multilayer graphene
MgO	Magnesium oxide
Mn	Manganese
MPPRR	Maximum pressure rise rate
MSE	Mean square error
MWCNT	Multi-walled carbon nanotube
NO _x	Nitrogen oxides
NPs	Nanoparticles
O ₂	Oxygen
PM	Particulate matter
ppm	Parts per million
PRR	Pressure rise rate
R ²	Coefficient of determination
RON	Research octane number
rpm	Revolution per minute
RSM	Response surface methodology
SWCNT	Single-walled carbon nanotube

TDC	Top dead center
Ti	Titanium
TiO ₂	Titanium oxide
ZnO	Zinc oxide

ABSTRACT

Compression ignition (CI) engines continue to be the primary choice for transportation and power generation; however, their extensive use is limited by significant emissions of NO_x, CO₂ and particulate matter (PM), despite progress in engine and fuel technologies. Among various alternatives, methanol has emerged as a promising fuel due to its high oxygen content, elevated latent heat of vaporization, and rapid flame propagation characteristics, all of which support cleaner combustion. In parallel, the addition of metal oxides, specifically titanium oxide (TiO₂) and copper oxide (CuO), has shown potential in enhancing the thermophysical and physicochemical properties of fuel blends, further improving combustion efficiency and emission characteristics. This research focused on the experimental investigation and optimization of the effects of diesel–methanol blends augmented with TiO₂ and CuO nanoparticles on the performance and emission profiles of a CI engine. Fuel blends with 10%, 20%, and 30% methanol (M10, M20, and M30) were created using an ultrasonicator to guarantee consistent nanoparticle distribution. Engine load, TiO₂ concentration, and CuO concentration were chosen as independent variables, and response surface methodology (RSM) was utilized to identify optimal operating parameters. In comparison to baseline operation, the M10 blend demonstrated the most favorable reductions in emissions. Specifically, reductions in NO_x and CO₂ emissions were observed at 7.43% and 5.38%, respectively, when compared to the CI baseline. Under the RSM-optimized conditions of 63% engine load, 90 ppm TiO₂, and 60 ppm CuO, the engine achieved a brake torque of 5.54 Nm, a brake power of 2.11 kW, and a brake specific fuel consumption of 0.356 kg/kWh. The emissions recorded were CO₂ at 3.514% vol, CO at 0.022% vol, NO_x at 167 ppm, and HC at 18 ppm. These results validate that TiO₂/CuO nanoparticle-enhanced methanol blends can significantly improve the performance and emissions of CI engines.

Keywords: Engine, Performance, RSM, Methanol, Emission, Nanoparticles

CHAPTER ONE

INTRODUCTION

1.1. Background of the Study

Global energy sector is witnessing a major shift, largely driven by the necessity to curb environmental degradation and greenhouse gas emissions. Compression Ignition (CI) engines, extensively utilized in transportation and industrial systems, demonstrate superior efficiency when compared to Spark Ignition (SI) engines. Nonetheless, these engines are also significant contributors to air pollution, releasing detrimental substances such as PM, NO_x and CO (Azad et al., 2023). The function of the conventional diesel combustion engine' is based on the mechanism of compression ignition, employing fuels with high reactivity, such as diesel. These fuels are ignited at high temperatures achieved through a carefully regulated mixing process (Azizzadeh Hajlari et al., 2019). Recently researcher indicated that mixing methanol with diesel can reduce emission and improve combustion in CI engines. Renewable fuel obtainable from diverse sources, such as methanol contributes to lower carbon emissions compared to traditional diesel (Karvounis et al., 2023).

The simplest alcohol, methanol (CH₃OH), was first produced by destructively distilling wood. These days, it can be made from a variety of renewable and fossil fuels, including biomass, wood waste, coal, petroleum, natural gas, and marine resources(W. Zhang et al., 2024). Methanol has physicochemical characteristics similar to gasoline and is an easily accessible, safe, and environmentally friendly fuel. It is a promising alternative fuel that can be used directly in SI and CI internal combustion engines. By lowering fuel consumption and raising the CR (CR), contemporary SI engine advancements seek to increase thermal efficiency. However, because of higher combustion temperatures, higher CRs may result in higher particulate matter (PM) emissions (Wang et al., 2020).

Diesel-methanol blends have the potential to improve combustion efficiency and lower emissions in CI engines, according to recent studies. Compared to traditional diesel fuel, methanol, a renewable fuel made from a variety of sources, has a significant advantage in terms of reduced carbon emissions. However, because of its high volatility and low cetane number, which can impair ignition performance, its use in CI engines is frequently restricted(Deka et al., 2024). In response to these limitations, there has been a growing interest among researchers in the integration of

nanomaterials into fuel blends to enhance their properties. Because of their unique physicochemical characteristics, metal oxide nanoparticles like TiO_2 and CuO have become attractive additives for improving combustion. While CuO nanoparticles function as extremely active catalysts that intensify combustion reactions and improve engine performance, TiO_2 nanoparticles' photocatalytic activity helps to improve combustion efficiency and lower exhaust emissions (S PRAKASH VARMA & Venkata Subbaiah, 2024).

Enhancing the incorporation of nanoparticles in diesel-methanol mixtures offers a significant opportunity to boost the performance of CI engines while concurrently minimizing emissions. Under the general heading of response surface methodology (RSM), the Box-Behnken design (BBD) provides a strong statistical framework for optimizing the interaction of multiple variables, enabling researchers to identify the optimal circumstances for increasing fuel efficiency and lowering emissions (Tirkey & Singh, 2023). The current study intends to investigate the combined effects of diesel-methanol blending ratios and concentrations of TiO_2 and CuO nanoparticles on engine performance, emission characteristics, and combustion behavior. Previous research has extensively documented the impact of TiO_2 and CuO nanoparticles on fuel properties and engine performance (Adelkhani et al., 2024). Research indicates that incorporating TiO_2 nanoparticles into fuel blends can significantly enhance their thermal stability, which in turn contributes to greater combustion efficiency (Muniyappan & Krishnaiah, 2024). In a similar vein, CuO nanoparticles have demonstrated the ability to promote the oxidation of carbon-based compounds, effectively minimizing the generation of soot and other harmful emissions. It is expected that the combined impacts of these nanoparticles in diesel-methanol blends would result in significant improvements in engine performance metrics, including improved pollution control and decreased BSFC and higher braking power (BP) (Ramachandran, Krishnaiah, Venkatesan, et al., 2023).

While TiO_2 and CuO nanoparticles exhibit significant promise for enhancing the performance of CI engines, there is a critical need for in-depth investigations that assess their effects across a range of operational conditions. Existing research frequently falls short of providing a thorough analysis of the interactions between these nanoparticles and various fuel mixtures, which could be systematically refined to achieve optimal outcomes. Consequently, this study seeks to address this deficiency by employing the BBD methodology to optimize the synergistic effects of TiO_2 and CuO nanoparticles in CI engines utilizing diesel-methanol fuel blends. The imperative for cleaner

and more efficient fuel alternatives has catalyzed extensive research into the application of nanoparticles within CI engines. The goal of this study is to advance sustainable fuel technologies by improving the performance characteristics of diesel–methanol blends by carefully adding TiO₂ and CuO nanoparticles. It is expected that the results will contribute to a better understanding of how nanotechnology might reduce harmful exhaust emissions and enable cleaner combustion processes.

1.2. Nanoparticles

Researchers are now interested in using nanoparticles (NPs) to improve the physical and chemical features of fuels, increase engine performance and combustion characteristics, and reduce emissions due to the development of nanotechnology. NPs must be used for improvement because alcohol and diesel fuel have certain restrictions. Because of their high surface area-to-volume ratio, quick dispersion, and decreased ignition delay characteristics, nanoparticles are thought to be a novel and promising fuel-borne catalyst that can enhance fuel attributes. Nano additives range in size from one to one hundred nanometers (ul Haq et al., 2024). NPs are incorporated into diesel-alternative fuels in various quantities to improve certain functional characteristics and enhance engine performance. These additives are anticipated to decrease tailpipe emissions and increase the viscosity index of the fuel mixture. Inside the engine and within particulate filters, they aid in raising oxygen concentration, which facilitates more thorough combustion. Additionally, the use of NPs helps to lower the flash point and ignition delay time, resulting in more efficient fuel ignition. They also improve fluid stability, thereby decreasing the likelihood of fuel degradation over time, and reduce wear by creating protective layers on metal surfaces, thus prolonging the lifespan of engine components.

Nanoparticles (NPs) were obtained from a variety of sources including Ferro materials, ceramics, polymeric materials, inorganic compounds, and metal oxides, and their categorization was determined by factors such as material type, size, shape, origin, and occurrence Carbon nanotube NPs (MWCNT and SWCNT), metal-based NPs (such as Ti, Mn, and Al), metal oxide-based NPs (such as CeO₂, MgO, ZnO, CuO, Al₂O₃, TiO₂, CuO, etc.), and magnetic nanofluid NPs (Ferrofluid, notably Fe₃O₄) are some of source of nanoparticles (Mofijur et al., 2024). An ultrasonicator bath was used to prepare the base fuel and nano-additives. The basic fuel was combined with the designated amount of NPs, which ranged from 50 to 200 parts per million, using ultrasonic

vibrations at a high frequency of 40 kHz. Additionally, the length of vibration was set at 40 minutes for a mass fraction of 150 ppm (0.15 g), and 30, 35, 45 minutes for the other three mass fractions: 50 ppm (0.05 g), 100 ppm (0.1 g), and 200 ppm (0.2 g). The NPs' stability and dispersion within the base fuel were improved by this procedure. It was also noted that the NPs remained undissolved in the base fuel; however, it was anticipated that a form of dissociative adsorption could occur between the base fuel and the nano-additives (Soudagar et al., 2018).

1.3. Statement of the Problem

Compression ignition engines, which are widely used in the transportation and industrial sectors, emit dangerous pollutants such carbon monoxide (CO), particulate matter (PM), and nitrogen oxides (NO_x), which greatly contribute to environmental degradation. The use of sophisticated additives and renewable fuels has become more popular due to the growing need for more efficient and clean fuel choices. Although diesel-methanol blends have shown promise in lowering pollutants and improving performance in CI engines, methanol's low cetane number and ignition characteristics pose problems that restrict its useful application in these engines. NPs, such as CuO and TiO₂, have great potential as combustion catalysts that can improve fuel properties and the combustion process as a whole. While CuO helps reduce pollution and improve oxidation reactions, TiO₂ is known for its capacity to promote more thorough combustion. However, little is known about the optimal quantities of these NPs in diesel-methanol blends and how they work in concert to improve engine efficiency and reduce emissions. The possibility to fully utilize these NPs' benefits is further limited by a lack of research examining their interaction effects under various conditions. The goal of this study is to fill the current knowledge gap about the combined impact of TiO₂ and CuO NPs on the emissions and performance of CI engines running on diesel-methanol mixes. The study aims to achieve an ideal balance between enhanced engine performance and decreased emissions by optimizing the inclusion of these NPs using the BBD methodology. It is predicted that the results will provide important new information about how nanotechnology might support cleaner and more effective combustion processes in CI engines.

1.4. Objective of the Study

1.4.1. General Objective

The general objective of this study is to optimize the combined effects of TiO₂ and CuO NPs on the performance and emissions of a CI engine fueled with diesel-methanol blends using Box-Behnken design.

1.4.2. Specific Objectives

The Specific objectives of the study are:

- ❖ To analyze the performance and emission characteristics of the CI engine using a diesel-methanol blend.
- ❖ To evaluate the impact of TiO₂ and CuO NPs on the performance and emissions of a CI engine fueled with diesel-methanol blends
- ❖ To determine the optimal concentrations of TiO₂ and CuO NPs diesel-methanol blends
- ❖ To develop a predictive model for the combined effects of TiO₂ and CuO NPs on CI engines fueled with diesel-methanol blends using BBD.

1.5. Significance of the Study

This research seeks to provide significant insights into the enhancement of diesel-methanol blends incorporating TiO₂ and CuO NPs, a topic of considerable relevance in the realm of sustainable energy and initiatives aimed at reducing emissions. The findings are expected to have the following key implications:

- ❖ It enhances fuel efficiency and engine performance
- ❖ It reduces harmful emissions and advancing clean energy technology
- ❖ It advances nanotechnology applications in combustion engineering
- ❖ It reduces conventional diesel fuel consumption and advocates alternative fuels

1.6. Scope of the Study

The objective of this work is to maximize the combined effects of TiO₂ and CuO NPs on the emissions and performance of a CI engine running on diesel-methanol mixes. In order to assess their effects on engine performance and emissions characteristics, this study methodically investigates different concentrations of TiO₂ and CuO NPs in various diesel-methanol mix ratios using BBD. This study excludes other types of NPs and alternative fuel additives and is restricted to TiO₂ and CuO NPs as the only additions in diesel-methanol mixtures. Furthermore, results may

not be directly applicable to multi-cylinder engines or other engine types without additional validation because it is concentrated on a single-cylinder CI engine configuration.

1.7. Limitations of the study

This study encountered several significant constraints that influenced both the experimental and overall scope of the research. A primary limitation was the lack of access to a fully equipped automotive engineering laboratory of ASTU. Inadequate infrastructure limited access to essential experimental and testing equipment required for comprehensive performance and emission analysis. These shortcomings compelled the research to depend on rudimentary measurement instruments, potentially affecting the precision and dependability of the findings. Another significant challenge encountered was the lack of a particulate matter (PM) emissions analyzer, which rendered it impossible to measure PM emissions. This limitation constrained the study's capacity to deliver a thorough evaluation of exhaust emissions, especially in assessing the environmental implications of various fuel blends. Additionally, the lack of an integrated temperature and pressure sensor within the engine cylinder obstructed the direct measurement of in-cylinder temperature. This shortcoming impacted the accuracy of thermal analysis and impeded a more profound comprehension of combustion characteristics.

1.8. Organization of the thesis

This thesis is organized into five chapters, each of which focuses on a different aspect of the study. The general background and purpose of the study are presented in Chapter 1. The limits of traditional CI engines and the environmental issues related to the use of fossil fuels are briefly discussed at the outset. The advantages of alcohol-based fuels and the function of NPs in improving engine performance are also discussed in this chapter. The problem statement lays the groundwork for the study's approach and describes the main research question. Additionally, the goals, importance, extent, and constraints are all well-defined. The reasoning for combining diesel with methanol and adding TiO_2 and CuO NPs as a possible method to lower emissions and boost combustion efficiency in CI engines is further explained in this chapter. Optimizing nanoparticle dosage for better engine performance and pollution management is the study's primary goal. The literature on diesel-methanol blends, the application of optimization approaches in engine research, and the function of NPs in fuel improvement are all thoroughly reviewed in Chapter Two. It critically evaluates earlier research findings, emphasizing both important findings and gaps that

require more investigation. The synthesis and use of methanol as an alternative fuel, the incorporation of NPs in combustion processes, and their effects on performance and emission metrics are all given particular attention. The experimental approach, including the materials, tools, and fuels employed, is described in Chapter 3 along with the detailed steps taken to guarantee data reliability. The experimental results are presented and interpreted in Chapter Four, which provides a scientific examination of emission data and performance metrics. Last but not least, Chapter Five makes conclusions based on the data, provides helpful advice, and proposes areas for further investigation to expand on the results of this study.

CHAPTER TWO

LITERATURE REVIEW

2.1. Introduction

Due to their excellent fuel efficiency and durability, diesel engines which are well-known for their compression ignition mechanism have been crucial in both industrial and transportation applications. Diesel-methanol blends have emerged as a promising option in this regard, utilizing the renewable properties of methanol while also contributing to lower emission levels. However, the increasing enforcement of strict environmental regulations aimed at reducing greenhouse gas emissions and other pollutants has necessitated the investigation of cleaner fuel alternatives (Malik et al., 2024). The application of metallic NPs to improve the combustion properties of diesel-methanol mixtures and to reduce related problems has been the focus of research. Because of their catalytic activities during combustion, metallic NPs like titanium oxide and copper oxide have demonstrated promise in enhancing engine performance, lowering emissions, and boosting fuel combustion efficiency (Modi et al., 2024).

This literature review aimed to investigate the optimization of metallic nano additives for use in CI engines fueled by diesel and ethanol. This assessment aims to elucidate the most efficient strategies for enhancing engine performance, reducing harmful emissions, and increasing fuel efficiency through a comprehensive synthesis of both experimental and computational studies.

2.2. Important Applications of Methanol

The significant uses of methanol are outlined in the following sections. As illustrated in Figure 2.3, methanol serves as a primary energy source in various key sectors (H. Zhang et al., 2020).

- ✚ Methanol is an essential component in both municipal and private wastewater treatment systems, where it is utilized to purify wastewater and mitigate the formation of 'dead zones' in aquatic environments that result from harmful nitrate concentrations.
- ✚ Methanol is an ideal candidate for use in fuel cell-powered vehicles due to its ability to be converted into hydrogen and carbon dioxide.
- ✚ Methanol serves as a clean-burning fuel that can be utilized in internal combustion engines, either in its pure state, as a blended fuel, or as an additive aimed at enhancing

engine performance while simultaneously lowering emissions. Additionally, it plays a significant role as a key ingredient in the production of renewable biodiesel fuels.

- ✚ Methanol serves as an effective storage medium for organic liquid hydrogen.
- ✚ Dimethyl ether (DME), a significant derivative of methanol, has the potential to serve as a viable alternative for home heating fuel, complementing the use of liquefied petroleum gas (LPG).

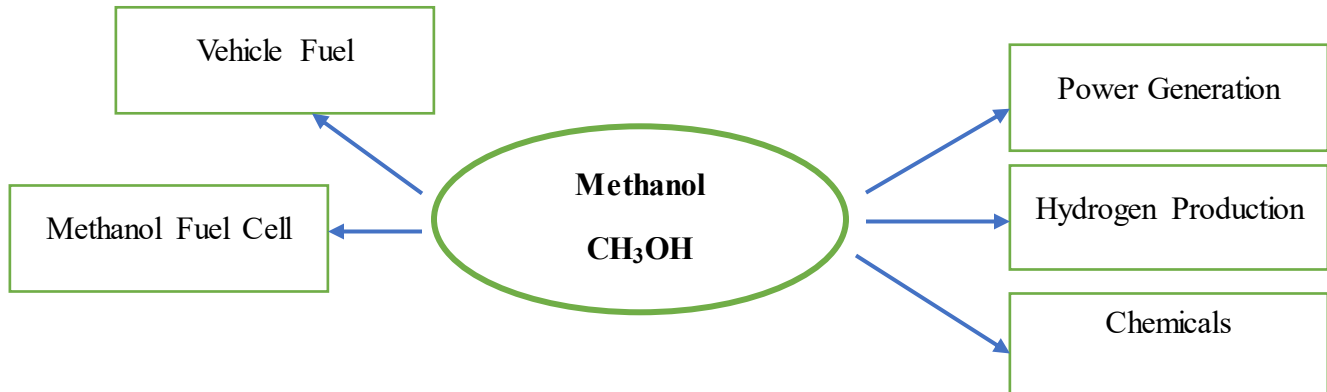


Figure 2.1 Methanol's primary applications as a source of energy

2.3. Physicochemical Properties of Methanol

Methanol has many advantages when used in SI and CI engines, chief among them being its high oxygen mass percentage, excellent octane rating, substantial latent heat of vaporization (L_v), and improved antiknock characteristics. These characteristics contribute to an increase in charge density and volumetric efficiency, which can result in improved torque and overall engine performance. Additionally, methanol exhibits a higher boiling point and greater storage stability than gasoline, attributed to the hydrogen bonding that occurs between its molecules. The higher-octane number associated with methanol allows for its utilization in engines designed for higher CRs. The physicochemical properties of diesel, gasoline, and methanol are detailed in Table 2.1(Sani et al., 2018).

Table 2.1 Physicochemical properties of diesel, gasoline, and methanol

Property	Methanol	Diesel	Gasoline
Boiling point (°C)	65	180-370	27-255
Autoignition temperature (°C)	463	~300	257
Heat of vaporization (kJ/kg)	1162.64	243	349
Low heating value (MJ/kg)	20.1	42.5	42.7
Cetane number	3.8	40-55	0-10
Flash point (°C)	12	65-88	-13 to 45
RON	136	20-30	80-99

2.4. Effects of diesel-methanol blends on performance and emission characteristics of CI engine

Previous research has shown that methanol is a competitive substitute for petroleum diesel in the transportation sector. The transportation industry has become much more important due to the recent boom in industrialization and mechanization. The depletion of petroleum supplies, rising gasoline prices, and increased environmental pollution are all results of this greater reliance on diesel fuel. Alternative fuels, including methanol, are therefore desperately needed to address these issues.

(Hassan et al., 2021) investigated the effects of adding 7%, 14%, and 21% methanol to diesel fuel in a single-cylinder TD 212 diesel engine running at a constant speed of 2000 rpm at different torque levels. Up to 14% methanol was used, which improved engine power output, BSFC, and BTE while lowering noise and exhaust temperature. Methanol's oxygen concentration, which promotes more effective burning, is responsible for these gains. On the other hand, engine efficiency and fuel consumption decreased when the methanol content was raised to 21%. This was probably because methanol has a higher ignition temperature and a lower cetane number. As a result, the study concluded that the best balance for maximizing performance and reducing emissions is a 14% methanol blend.

(Huang et al., 2020) investigated the performance of a 4-cylinder CI engine running at a steady speed of 1800 rpm under various load circumstances using pure soybean biodiesel and mixes of 10% and 20% methanol-biodiesel. The combustion parameters were greatly impacted by the addition of methanol to the biodiesel; at low vs high loads, the peak cylinder pressure and heat

release rate showed different behaviors. In contrast to other operational scenarios with methanol mixes, the ID decreased under low load conditions. The load levels also had an impact on the emission profiles: CO and 1,3-butadiene emissions rose at low loads while they fell at higher loads. Additionally, a higher proportion of methanol in the blends led to an increase in HC and acetaldehyde emissions, while simultaneously decreasing benzene emissions across all tested load conditions.

(Yusaf et al., 2013) investigated the effects of methanol-diesel fuel mixtures (comprising ratios of 0:100, 10:90, 20:80, and 30:70) on the performance of a four-stroke, four-cylinder CI engine across different operational speeds. The findings revealed that a 10% methanol blend led to an enhancement in BTE and a power output increase of up to 70%, alongside the lowest recorded exhaust temperature. Although pure diesel exhibited a lower BSFC, the 10% methanol blend demonstrated significant advantages in both performance and environmental impact. The study indicates that incorporating 10% methanol into diesel fuel could markedly improve engine performance.

(Berber, 2019) in order to reduce the negative environmental consequences connected with diesel engines, methanol is added to diesel fuel at volumetric ratios of 5%, 10%, and 15%. A single-cylinder direct-injection diesel engine is used to assess the different diesel-methanol mixtures. The results of the experiments show that adding methanol to diesel fuel reduces engine torque by a maximum of 13.07% and specific fuel consumption by a maximum of 12.54%. On the other hand, CO and CO₂ concentrations are lowered by 38.4% and 5.04%, respectively, according to the exhaust emission analysis. On the other hand, NO_x emissions increase by 17.1% due to a 3.66% increase in exhaust gas temperature. Additionally, a notable reduction of 39.37% in smoke opacity is recorded when compared to that of standard diesel fuel. While the incorporation of methanol into diesel fuel results in a slight decline in engine performance, the diesel-methanol blends demonstrate a significant and beneficial impact on the environmental issues related to diesel engines.

(Vishnoi et al., 2022) investigated the application of diesel-methanol blends with n-pentanol as a co-solvent to improve phase stability in diesel engines running at different loads. At full load, the blend known as MnP15 which contains 15% methanol and n-pentanol showed better performance parameters, such as higher peak cylinder pressure, a faster rate of heat release, and enhanced brake

thermal efficiency. Notably, the MnP15 blend demonstrated compatibility with unmodified CI engines by reducing emissions of HC, NO_x, and smoke by 34.61%, 3.98%, and 41.29%, respectively. Conversely, blends with more over 20% n-pentanol were shown to be less successful because of their less-than-ideal combustion properties.

(Prashant et al., 2016) investigated various parameters such as ID, PRR, HRR, temperature, and peak cylinder pressure in a turbocharged, inter-cooled four-cylinder diesel generator engine operating on methanol-diesel blends. The findings indicated that an increase in methanol content resulted in extended IDs compared to pure diesel. Additionally, the maximum PRR experienced an increase of up to 19.5%, while the Peak PRR reached up to 9.5% under elevated load conditions. The HRR exhibited considerable variation in methanol concentration, peaking at 78.07 kJ when using a 40% methanol blend at a 10% load, which corresponded closely with the outcomes of the experimental three-factor analysis.

(Vargün et al., 2022) conducted research focused on discovering cleaner alternative fuels and decreasing dependence on fossil diesel by incorporating 20% by volume of methanol (M20), ethanol (E20), and n-heptane (H20) into standard diesel. The experiments were carried out on a 4-cylinder CRDE under different engine loads (40 Nm and 80 Nm) and speeds (1500–1800 rpm). Among the various blends tested, M20 demonstrated the highest BTE of 43% at 1800 rpm and 80 Nm. Additionally, BSFC showed improvement with increased engine load across all blends. In terms of combustion characteristics, M20 demonstrated the highest maximum CP at 114.3 bar, while H20 showed the greatest cumulative heat release of 811.7 J. The use of alcohol-diesel blends resulted in a prolonged ID and a shortened CD when compared to pure diesel (D100). Emission analysis indicated a significant reduction in CO₂ emissions across all blended fuels. HC emissions were observed to decrease with increasing load for all types of fuel. It is noteworthy that M20 and E20 blends led to an increase in O₂ and NO_x emissions, while H20 resulted in a decrease in both. In summary, the study underscored the potential benefits of alcohol and hydrocarbon additives in enhancing engine performance and minimizing specific emissions under particular operating conditions.

(Hasan et al., 2021) investigated the performance and emission characteristics of a compression ignition engine that was fueled with various blends of methanol and diesel under different engine load conditions. Four distinct methanol blend ratios were evaluated and compared against pure

diesel, with a focus on parameters such as BTE, BSFC, and BP. The findings indicated that emissions of HC and CO were reduced with an increase in methanol content, while emissions of NO_x exhibited an upward trend. For example, the highest concentration of HC (40 ppm) was recorded with pure diesel at low load, whereas it decreased to 5 ppm at high load when using a 40% methanol blend (B40). Conversely, NO_x emissions reached a maximum of 640 ppm under high load conditions with B40 and were at their lowest during low load conditions with pure diesel. Additionally, smoke emissions were observed to diminish as the percentage of methanol increased. Regarding performance metrics, pure diesel demonstrated superior results compared to the blends, achieving higher BTE and lower BSFC across all load conditions. Nevertheless, BSFC was significantly elevated with B40 at low load, peaking at 0.75 g/kWh. In summary, blending methanol presents advantages in terms of emissions reduction, particularly for HC, CO, and smoke, although it may lead to a decrease in engine efficiency at higher blend ratios.

(García et al., 2023) examined the combustion characteristics of pure methanol in a light-duty, multi-cylinder compression ignition engine featuring a 19:1 CR, with the objective of evaluating its potential for commercial engine use. Essential performance indicators, including fuel consumption, engine efficiency, and emission levels, were analyzed. The findings revealed that while methanol possesses a lower energy density compared to diesel, it can attain similar combustion efficiency, accompanied by notable decreases in NO_x and soot emissions, thereby underscoring its environmental advantages. Nonetheless, the research also uncovered various obstacles associated with the low auto-ignition characteristics of methanol. Combustion stability proved to be particularly challenging at reduced engine speeds, loads, and during cold starts, primarily due to methanol's elevated ignition energy and prolonged ignition delay. Although methods such as raising the CR and utilizing intake heaters or glow plugs provided some assistance, maintaining consistent low-load operation continued to be problematic. However, at medium to high loads, methanol combustion was more reliably sustained, particularly after the engine attained its operating temperature, indicating that with suitable support systems, methanol could serve as a viable clean fuel alternative for compression ignition engines.

(Z. Zhang et al., 2021) investigated the effects of mixing diesel with different methanol proportions (DM0, DM10, DM20, DM30, and DM40) in a four-stroke engine. A comprehensive model of the diesel engine was created and validated through the use of AVL-BOOST simulation software in conjunction with experimental data. The research examined various parameters, including CP, BP,

BSFC, and the emissions of NO_x, soot, and CO. The research findings indicated that an increase in methanol content led to an enhancement in combustion efficiency, as evidenced by a slight rise in CP (up to 3.17% at 40% methanol). Additionally, there was a notable reduction in CO and soot emissions—specifically, CO emissions decreased by as much as 56.59%, while soot emissions were reduced by 25.28%. Nevertheless, it was observed that engine performance suffered as a consequence. With the rising methanol ratio, both BP and torque experienced a decline (up to 15.45%), and BSFC increased by as much as 17.61%. In summary, although higher methanol blends contribute positively to emission profiles, they simultaneously detract from engine efficiency, highlighting a significant trade-off between environmental advantages and performance.

(Gülcan et al., 2022) A single-cylinder, four-stroke, water-cooled, normally aspirated compression ignition engine was used to study the effects of diesel-methanol-dodecanol blends on engine performance and smoke emissions. Diesel (D100), diesel-methanol (D90M10), and diesel-methanol-dodecanol (D89M10D1) were the fuel blend ratios used in the study. 1% by volume of dodecanol was added to the diesel-methanol blend to solve the phase separation problem. At a constant engine speed of 1800 rpm, the test engine was run under four different loads (6, 12, 18, and 24 Nm). Based on the experimental results, performance metrics like BSFC, BSEC, and brake effective efficiency were computed for each blend at different engine loads. The findings revealed that under low load conditions, the specific fuel consumption increased by a maximum of 8.4% with the addition of methanol to the diesel fuel, whereas this increase was reduced to 3.7% with the inclusion of dodecanol. The addition of dodecanol to the methanol-diesel mixture resulted in the lowest smoke opacity being achieved at low and high loads, specifically at 32.72% and 53.75%, respectively.

2.5. Summary of related works on diesel-methanol blends

The primary objectives of research on the use of diesel-methanol mixtures in CI engines have been to reduce emissions and improve combustion efficiency. While attaining BP and BTE that are either equal to or somewhat lower than those of standard diesel, these blends have shown the ability to reduce PM and CO emissions. Under certain operating conditions, the presence of oxygen in methanol enhances the combustion process, resulting in less soot generation and better fuel efficiency. Nonetheless, challenges persist, including methanol's lower energy density and the

necessity for adjustments to the fuel injection system. Furthermore, research has shown that changing the blending ratios can have a substantial impact on emissions; for example, higher methanol concentrations may improve emission reductions but may also raise NO_x emissions because of higher combustion temperatures. In summary, while the potential of diesel-methanol blends in CI engines is evident, further research is essential to optimize the interplay between performance, emissions, and fuel efficiency.

2.6. The effects of adding nanoparticles to fuel in internal combustion engines

2.6.1. Fuel Additives

Additives, which can be either organic or metal-based compounds, are designed to dissolve readily in fuel, serving primarily to enhance, sustain, and impart advantageous properties to the fuel while ensuring that performance and combustion metrics remain unaffected. These fuel additives, which are usually added in small amounts (between 100 and several thousand parts per million), are essential for improving the quality of different car fuels, such as gasoline, diesel, and biodiesel, and meeting performance standards. These additives help petroleum products comply with environmental emission regulations, improve overall performance, and increase engine combustion efficiency. For diesel, biodiesel, and their blends to have better qualities, fuel additives are crucial. The constraints of biodiesel, which include things like density, toxicity, viscosity, economic viability, solubility of the additives, auto-ignition temperature, flash point, and cetane number, have a major impact on the choice of these additions. Optimizing the gasoline blending process requires taking these factors into account. Oxygenated additives, antioxidant additives, cold flow behavior improvers, cetane number improvers, ignition promoters, and metal-based additives are some of the several types of fuel additives (Srivastava et al., 2018).

Oxygenated Additives: To enhance the combustion properties of fuels exhibiting prolonged ignition delays, small quantities of chemical compounds with elevated oxygen content are incorporated into the fuel. Additives such as methanol, ethanol, biodiesel, dimethyl carbonate, dimethyl ether, sorbitan monooleate, and diethylene glycol diethyl ether are utilized due to their compatibility and ability to blend seamlessly with diesel.

Metal-Based Additives: The combustion properties of fuels can be enhanced through the incorporation of metals and metal oxides in micro- or nanoscale dimensions, utilizing either parts per million (ppm) or weight percentage ratios. Various metals, including Al, Fe, Mn, Mg, Au, Ag,

graphene, Cu, B, and Si, along with metal oxides such as TiO₂, CuO, Co₃O₄, ZnO, CeO₂, and Al₂O₃, serve as effective additives to enhance the physicochemical characteristics of fuels. Additionally, metal alloys like carbon nanotubes (CNT) and magnalium (Mg-Al) are employed as metal-based additives, contributing to improved fuel performance by altering its physicochemical properties.

Cetane number improvers: The cetane number serves as a critical indicator of fuel quality, reflecting its ignition characteristics. Fuels that possess a high cetane number tend to enhance the performance of compression ignition engines. Various additives, including nitroalkanes, nitrates, nitro carbonates, and peroxides, are employed to elevate the cetane number of fuels, thereby optimizing their combustion efficiency.

Cold flow behavior improver: in low-temperature environments, the wax constituents in biodiesel can solidify, forming crystalline structures that negatively impact the cold filter plugging point. To mitigate this issue, the incorporation of specific additives such as ethylene vinyl acetate copolymer, glycerol ketals, glycerol acetates, phthalimide, and succinimide copolymers is recommended, as these substances enhance the cloud point characteristics of the fuel.

2.6.2. Stability of nanoparticles in a base fluid

Due to their large surface area, nanofluids typically have high surface energy, which frequently causes agglomeration and the creation of micro-sized particles before deposition. The achievement of a stable and homogenous suspension of nanofluids is a crucial phenomena for both practical applications and scientific research. Because stability has a major impact on both the thermophysical properties of nanofluids and their function as heat carriers, it is essential in their manufacturing. Many techniques have been reported in the literature to improve the stability of NPs in a base fluid, such as ultrasonication, surface modification, surfactant insertion, and PH correction (Yusof et al., 2020). Several prior studies have explored the effectiveness of ultrasonic dispersion in enhancing and maintaining the stability of NPs. Research conducted by (Rufus et al., 2017) indicated that the stability of nanofluids can be improved by extending the duration of sonication. Their findings demonstrated that increasing the sonication time contributes to a decrease in particle agglomeration. Similarly, (Elsaidy et al., 2021) noted comparable results in their investigations. Both studies concurred that prolonged sonication times enhanced the stability of NPs. Furthermore, (Barai et al., 2022) found that the ultrasonic technique could efficiently

disintegrate particle agglomerates, thereby facilitating a more stable and superior dispersion of NPs within the base fluids.

Chemical substances called surfactants are added to NPs to help reduce the nanofluid's surface tension and improve particle absorption. The use of surfactants for a lower deposition rate has been the subject of some research, however in some cases, using the proper kind of surfactants for the particles is crucial. Only a small number of surfactants have been reported and used in different kinds of nanofluids, according to the literature. These include hexadecyltrimethylammonium bromide/Cetyl trimethylammonium bromide (CTAB), sodium dodecylbenzene sulfonate (SDBS), SDS, polyoxymethylene (10) nonylphenyl ether (TX-10) [34], PVP, salt and oleic acid, and gum Arabic. Nevertheless, incorporating surfactants may lead to certain issues, particularly regarding the efficacy of this approach in enhancing the stability of nanofluids. This limitation becomes evident when considering nanofluids that function at elevated temperatures, as there is a risk of bond degradation between the surfactant and the NPs (Yusof et al., 2020).

2.6.3. Effect of metal oxide nanoparticles on performance and emissions of CI engine

The influence of metal oxide nanoparticle additives, especially TiO_2 and CuO , on the operational efficiency and emissions of CI engines has garnered significant attention in recent research. The incorporation of these NPs into diesel or biodiesel fuels is thought to improve combustion efficiency while simultaneously decreasing the release of harmful emissions. TiO_2 NPs, recognized for their exceptional stability, enhance the combustion properties of the fuel by facilitating superior air-fuel mixing and expediting the oxidation of hydrocarbons, ultimately leading to a decrease in PM and soot. TiO_2 has been found to enhance BTE while simultaneously decreasing CO emissions. In a similar vein, CuO NPs demonstrate catalytic characteristics that facilitate improved combustion, resulting in lower levels of PM, CO, and HC. Nonetheless, it is important to note that elevated concentrations of these metal oxide NPs can lead to an increase in NO_x emissions, attributed to the rise in combustion temperatures. Research has also shown that the advantages in performance and the reduction of emissions are influenced by factors such as the concentration of NPs, as well as the engine's load and speed.

(Gharehghani et al., 2019) studied the concurrent use of water and cerium oxide NPs in a diesel-biodiesel fuel mixture was experimentally examined to assess its impact on the performance and emission characteristics of a single-cylinder diesel engine, which was operated with a start of

injection set at 20 degrees before top dead center. The results obtained indicated that the B5W7m fuel emulsion (comprising B5 with 7% water and NPs) improved brake thermal efficiency by over 13.5% and 6% when compared to B5W7 and B5, respectively. Additionally, the B5W7m formulation led to a reduction in BSFC by 8% and 23% relative to B5 and B5W7, respectively. The CO emissions were significantly lowered with the use of B5W7m, showing reductions of 42% and 3% in comparison to B5W7 and B5, respectively. The enhancements in combustion performance can be attributed to the catalytic properties of cerium oxide NPs. Conversely, the incorporation of 90 ppm CeO₂ into the B5W7 formulation resulted in an increase in NO_x emissions by approximately 14%; however, this level remained 21% lower than the NO_x emissions produced during B5 combustion.

(Ma et al., 2024) assessed the impact of integrating different forms of carbon-based NPs—graphite oxide (GO), multilayer graphene (MG), and carbon nanotubes (CNT)—at various concentrations into diesel-methanol mixtures on the combustion and emission properties of a DI diesel engine across different load scenarios. The findings revealed that all nano-fuel mixtures improved combustion, as demonstrated by elevated peak CP, heightened peak HRR and diminished ID and CD. In terms of performance, the incorporation of carbon NPs led to enhancements in BTE and a decrease in BSFC. Among the various additives evaluated, GO exhibited the most beneficial effect on combustion, followed by MG and CNT. Emission assessments revealed notable reductions in CO, HC, and smoke opacity when utilizing nano-fuels, with CNT proving to be the most effective in diminishing CO and HC levels, while GO was the most efficient in reducing smoke opacity. A slight increase in NO_x emissions was noted. In summary, the research underscores that carbon-based nanomaterials can substantially enhance methanol-diesel blends, thereby improving their viability for applications in internal combustion engines.

(Parida et al., 2024) investigates the effects of adding TiO₂ NPs to a mixture of diesel and Karanja biodiesel on the emissions and operating efficiency of a direct injection compression ignition engine. The results showed that adding TiO₂ NPs reduced the exhaust gas temperature and improved brake thermal efficiency. However, it was observed that changes in the fuel-air combination, which resulted in incomplete combustion, increased emissions of hydrocarbons and carbon monoxide. Because of the lower oxygen levels in the combustion chamber, the addition of NPs led to a significant decrease in nitrogen oxide emissions. Particulate matter emissions were also reduced by the presence of NPs, which acted as catalysts for the oxidation of soot particles.

(Vigneswaran et al., 2021) investigated how TiO₂ NPs affected a monocylinder diesel engine's performance, combustion properties, and emissions when using water-in-diesel (DWS) emulsion fuel. The results show that the TiO₂-infused emulsion gasoline (DWT3) reduces CO, HC, and smoke emissions by up to 32.98% and improves brake thermal efficiency by 5.65%. Nonetheless, it is significant that NO_x emissions rise by 16.26%. In conclusion, the usage of TiO₂-enhanced emulsion fuel shows promise as a substitute that doesn't require any changes to the engine's current hardware.

(Srinivasan et al., 2021) studied the effects on a single-cylinder diesel engine's operating efficiency, combustion parameters, and emission profiles of adding alumina and TiO₂ NPs to neat biodiesel (B100) at concentrations of 25 ppm and 50 ppm. The results show that the fuel blended with TiO₂ (B100T50) improves BTE by 5.2%, reduces BSFC by 10.56%, and significantly reduces CO, HC, and smoke emissions by up to 44%. It is significant, yet, that NO_x emissions increased by 21%. In conclusion, adding nanoparticle-enhanced biodiesel improves engine performance and reduces emissions while the engine is running at full load.

(Koca et al., n.d.) investigated the effects on a three-cylinder, four-stroke diesel engine's operating performance and emissions characteristics of adding TiO₂ NPs to diesel fuel at concentrations of 25 ppm, 50 ppm, and 75 ppm. The results show that, at a 25% load condition, the addition of TiO₂ NPs can improve brake thermal efficiency by up to 15.12% and reduce BSFC by 13.36%; however, this change significantly raises exhaust gas temperature. Notably, CO₂ and NO_x emissions increase by 5% and 11.44%, respectively, at maximum load, indicating that although TiO₂ nanoparticle addition increases combustion efficiency, it also raises NO_x emissions.

(D'Silva et al., 2015) explored how adding optimal concentrations of TiO₂ NPs to diesel fuel in a compression ignition engine affected a number of characteristics, including density, flash point, viscosity, and calorific value. The results show improvements in fuel properties, with the addition of TiO₂ resulting in a 22% decrease in BSFC and an increase in BTE under peak load circumstances. Further emission analyses show significant reductions in CO by 25% and HC by 18%, highlighting TiO₂'s potential as a useful additive for enhancing performance and lowering emissions.

(Nanthagopal et al., 2017) investigated the effects of adding ZnO and TiO₂ NPs to Calophyllum inophyllum biodiesel in a four-stroke, twin-cylinder, water-cooled, direct injection diesel engine.

Titanium dioxide and zinc oxide concentrations of 50 ppm and 100 ppm were combined with distilled water using an ultrasonication method to form the nanofluids. Using a mechanical stirrer, four different Calophyllum inophyllum nano emulsions were created: 93% Calophyllum inophyllum biodiesel, 5% ZnO and TiO₂ nanofluids, and 2% span 80. All four Calophyllum inophyllum nano emulsions were used to study the compression ignition engine's characteristics, and the results were compared to those of pure Calophyllum inophyllum biodiesel and conventional diesel at different engine loads. Due to the large surface-to-volume ratio of the NPs, which promote quick evaporation and better atomization, the diesel engine operating with CIME nano emulsions increased brake thermal efficiency by 5–17% when compared to pure CIME fuel at maximum brake power. Furthermore, CIME nano emulsions had far lower CO and HC emissions than both pure biodiesel and regular diesel fuel. For all CIME nano emulsions, the NO_x emissions were marginally higher than those of normal diesel fuel but still lower than those of pure Calophyllum inophyllum biodiesel. Additionally, compared to both pure biodiesel and diesel fuels at all engine loads, the smoke emissions from the diesel engine were significantly reduced for all CIME nano emulsions. The combustion characteristics, including in-cylinder gas pressure and heat release rate, were enhanced by the addition of NPs to pure Calophyllum inophyllum at all engine loads. In conclusion, it is evident that the incorporation of NPs into biodiesel significantly improves performance characteristics, yielding notable enhancements in performance and minimal emissions.

(Senthil Kumar et al., 2020) investigated diesel fuel's emission characteristics by adding TiO₂ NPs to a single-cylinder, four-stroke CI engine. The goal of this research is to reduce the harmful tailpipe emissions that pure diesel compression ignition engines create. Using an ultrasonicator, diesel fuel was mixed with TiO₂ nano additions at concentrations of 50 and 100 ppm. The TiO₂ nano addition was added in order to enhance diesel's combustion characteristics and lower its exhaust emissions. The results of the experiment showed that the fuels examined in this study did not require engine changes. Additionally, employing both the base and modified fuels resulted in a consistent combustion process and no discernible physical harm to the engine's components. It was determined that the addition of 50 and 100 ppm of TiO₂ NPs to diesel resulted in a notable decrease in CO, HC, NO_x, and smoke emissions.

(Perumal & Ilangkumaran, 2018) researched how CuO-NPs added to pongamia methyl ester biodiesel (PME-B) affected a diesel engine's operating, combustion, and emission characteristics.

For this study, a single-cylinder, four-stroke, DI diesel engine with a 17.5:1 CR was used. The findings showed that adding NPs enhanced engine performance in terms of BTE and decreased BSFC. Additionally, the NPs considerably reduced the emissions of smoke, CO, and NO_x. Their smaller size and larger surface area, which allowed for a more efficient mixing of fuel and air, were associated with improved combustion properties.

(D'Silva et al., 2017) Investigated the effects of incorporating CuO NPs at concentrations of 10, 30, and 50 mg/l into a B20 biodiesel blend derived from pongamia pinnata, focusing on performance metrics and emissions in a CI engine. The findings indicate that the highest concentration of CuO (B20+50 mg/l) results in a 2.75% improvement in brake thermal efficiency and a 4.85% reduction in BSFC when compared to the B20 blend without additives. Furthermore, the B20+50 mg/l CuO formulation significantly decreases smoke emissions by 20% and NO_x by 2.63%, although it does exhibit a slight increase in HC emissions. CO emissions show a minor decline across all tested CuO concentrations, with the B20+50 mg/l variant demonstrating the most favorable overall performance.

(Surendrababu et al., 2022) Investigated the incorporation of CuO NPs at concentrations of 50 and 100 ppm into a diesel blend derived from pumpkin seed oil methyl ester (PSOME20) to enhance engine performance and minimize emissions in a CI engine. The findings indicate that the introduction of CuO NPs into the PSOME20 blend results in a 2.3% improvement in BTE and a 6.4% reduction in BSFC. Furthermore, the addition of CuO NPs leads to a notable decrease in the emissions of HC, CO, and smoke, while also promoting improved combustion characteristics, as evidenced by increased HRR and CP.

(Naik & Kumar, 2018) Assessed the viability of nano diesel as a fuel for CI engines by examining blends of Al₂O₃ and CuO NPs at a concentration of 0.006% by weight in a single-cylinder, four-stroke CI engine. The findings indicate that Al₂O₃ nanodiesel significantly enhances engine performance compared to CuO nanodiesel, achieving a reduction in BSFC of 1.4% and decreasing HC, CO, and NO_x emissions by 13.3%, 12.17%, and 8.75%, respectively. While CuO nanodiesel also contributes to performance improvements, it results in smaller reductions in emissions, specifically 6.3% for HC, 7.11% for CO, and 2.6% for NO_x.

(Ağbulut et al., 2021) The study evaluated the direct effects on engine combustion, performance, and emissions of adding sizable volumes of copper oxide (CuO) NPs (particle size < 77 nm) to

regular diesel. Fuel blends containing 1000 ppm and 2000 ppm CuO were tested at engine speeds ranging from 2000 rpm to 3000 rpm in 250 rpm increments using a single-cylinder, naturally aspirated, direct-injection, air-cooled diesel engine. CuO NPs enhanced fuel thermal conductivity and encouraged more thorough burning by providing extra oxygen and serving as a combustion catalyst. Consequently, when CuO-doped fuel was used instead of pure diesel, exhaust gas temperatures, carbon monoxide (CO), unburnt hydrocarbons (HC), and nitrogen oxides (NO_x) emissions all dropped. For the 1000 ppm and 2000 ppm mixes, CO emissions decreased by roughly 14.6% and 20.8%, HC by 6.2% and 13.4%, and NO_x by 4% and 4.7%, respectively. Additionally, the adjusted fuels reduced BSFC (BSFC), improved brake thermal efficiency (BTE), and raised the heating value. CuO NPs also shortened the ignition delay by speeding up combustion reactions. Crucially, suspensions-maintained stability up to 2000 ppm without clogging the fuel filters in the engine.

(Kalaimurugan et al., 2023) To assess the effect of fuel-borne fuel additives in the form of copper peroxide (CuO₂) NPs in a variable CR engine running at a fixed speed and fueled with a diesel and biodiesel fuel blend, an experimental investigation was carried out. The investigation considered the dispersibility of CuO₂ NPs in a B20 biodiesel fuel blend typically made from Neochloris oleoabundans methyl ester and diesel fuel. The fuel samples were made with increasing amounts of 25, 50, 75, and 100 ppm of CuO₂ NPs. These fuel samples were marked B20, B20 + 25 ppm, B20 + 50 ppm, B20 + 75 ppm, and B20 + 100 ppm. In this investigation, fuel properties such as viscosity, density, cloud point, calorific value, and pour point were measured without making any engineering changes in a variable CR engine at a fixed engine speed. For determining the performance of a variable CR engine fueled with diesel and biodiesel fuel added with increasing amounts of 25, 50, 75, and 100 ppm of CuO₂ NPs, parameters like exhaust gas temperatures, BSFC, brake thermal efficiency, and exhaust emissions of hydrocarbons, carbon monoxide, nitrogen oxides, and smoke concentrations were calculated. The variation in these parameters clearly proved that biodiesel and diesel fuel added with NPs enhanced functional benefits like improved burning efficiency and decreased exhaust gas emissions in comparison with B20 fuel.

2.7. Response surface methodology for optimizing engine performance and emissions

Optimization is the process of selecting the process parameter to produce the desired result. Under a variety of restrictions, optimization determines the optimal answer for the given aim. Single-

objective and multi-objective optimization are both possible. Two approaches can be used for optimization. First, the global maxima or minima in the plotted result can be located using the graphical method. The latter is the gradient approach, which determines the maximum or lowest gradient by utilizing the gradient of the objective function. In the search space or design space of the design vector, the two approaches locate the maxima or minima. a number of forecasts and optimization strategies were used to look at the emissions and engine performance. One tool for prediction and optimization used to examine engine characteristics is RSM(Rajendran et al., 2023).

RSM is a sophisticated mathematical and statistical approach employed in the design of experimental studies. Its primary objective is to enhance the response variable that is influenced by several independent factors. The second-order polynomial equation presented in Equation (2.1) serves as a predictive model for the output response, incorporating the various input variables into its formulation (Veza et al., 2023).

$$Y = b_0 + \sum_{i=1}^k b_i x_i + \sum_{i=1}^k b_{ii} x_i^2 + \sum_{i < j}^k b_{ij} x_i x_j + e \quad (2.1)$$

Where Y is the response; x_i and x_j are factors; b_i and b_{ii} are the 1st order and the 2nd order coefficients, respectively; b_0 denotes the intercept; b_{ij} is the model linear coefficients (for the i and j variables); k is the number of factors studied in the experiment and e is the error related with output.

Although originally designed for chemical applications, the use of RSM has now broadened to encompass various other domains, including mechanical engineering and the automotive industry. In the context of ICE, the RSM methodology is primarily employed to enhance the performance and reduce the emissions of both gasoline and diesel engines. Nevertheless, in light of the rising apprehension regarding the depletion of fossil fuels and their associated environmental challenges, the application of RSM for optimizing engine performance and emissions is increasingly gaining traction within biofuels research.

2.7.1. Factors (input) and responses (output) in RSM

The correct identification of the input, or independent, variables is the first and most important step in using Response Surface Methodology (RSM), since these parameters have a significant impact on the modeling process as a whole and the outputs that are produced. A review of earlier RSM-based research on internal combustion engines (ICEs) running on alternative fuels reveals

that operating conditions like engine speed, engine load, compression ratio, and fuel blending ratio are frequently chosen inputs. Carefully determining the operating ranges for these factors, which are usually determined based on previous experimental investigations, is equally important. Unreliable results and limited practical relevance can result from choosing variables or their ranges incorrectly. Selecting output parameters that accurately represent engine performance, combustion characteristics, and emission behavior is essential on the response side. Therefore, to guarantee the accuracy and utility of the analysis, careful and logical selection of both independent variables and response parameters is necessary prior to applying the RSM approach (Veza et al., 2023).

2.7.2. Single vs. multiple responses in RSM

Problems with one or more responses can be solved using Response Surface Methodology (RSM). Nevertheless, multi-response optimization adds more complexity because it is harder to find the ideal set of factor levels that meets all of the model's goals. Convergence issues may occur when the number of responses surpasses the constraints. As a result, a balance must be achieved by prioritizing the most important response variables and establishing reasonable goals. Before looking at curvature effects, a factorial design is typically used in practice to assess the primary effects and interactions. Additional analysis is not required if a linear model can adequately describe the experimental data. On the other hand, the study moves on to the application when curvature is present and nonlinear behavior is seen. Additional analysis is not required if a linear model can adequately describe the experimental data. On the other hand, the study moves on to the application of RSM when curvature is present and nonlinear behavior is noted.

The substantial cost associated with conducting a large number of experimental trials to obtain reliable results can be significantly reduced through the application of Response Surface Methodology (RSM), which employs both linear and second-order polynomial models. The adequacy of a selected model is commonly evaluated using the lack-of-fit test, which quantifies the discrepancy between experimentally observed values and those predicted by the model. The lack-of-fit becomes statistically significant when the pure error representing variability among replicated experiments under identical conditions is considerably smaller than the residual error, indicating that the chosen model may not appropriately describe the process. To address such deficiencies, several strategies can be implemented, including increasing the number of center-point replications, adopting higher-order models, applying suitable transformation functions to

better capture the relationship between input and output variables, removing outliers, or reducing the number of input factors. The choice of an appropriate RSM model depends on both the number of variables under investigation and the complexity of the process. For most optimization problems involving two or three variables, a second-order polynomial model incorporating linear, interaction, and quadratic terms is generally sufficient to accurately represent the response surface.

As mentioned before, testing the adequacy of a second-order model against a higher-order model represents one way to determine whether a higher-order model needs to be used. This can be done by comparing the R^2 or adjusted R^2 values for the two models. If the higher-order model proves to be significantly better than the second-order model in describing the data, it will be necessary to consider the use of a higher-order model. Another way to check on model order involves plotting the response surface and examining the data for curvature and nonlinear trends. If the response surface seems to be highly nonlinear with significant curvature, a higher-order model may be required to adequately model the response of the system. Also, one has to consider whether using a higher-order model would be viable within the optimization configuration.

The optimization process may take longer and require more resources due to the complexity and additional trial runs required to mimic more complicated models. As a result, it is frequently beneficial to begin with a second-order problem and only raise complexity when absolutely necessary. Interestingly, RSM can also be used to simulate several answers at once. Finding a factor level set that simultaneously optimizes a set of responses or finding a trade-off among numerous responses are the process's goals for multiple response problems.

To produce data across the whole experimental design, the experimental structure is meticulously planned. Various factor settings are included in the design matrix, and the corresponding answers are then noted. The associations between factors and responses can be ascertained by using a regression analysis based on the experimental results. Several strategies, including multi-objective optimization techniques, response optimization techniques, and Pareto optimization techniques, can be taken into consideration and applied to the problem when dealing with multiple replies. It is crucial to comprehend and keep in mind that the objectives in a multiple response optimization problem must be prioritized according to their significance and applicability to the problem at hand.

2.7.3. Response surface design for RSM

Once the factors and responses have been determined, the next critical step is to design the experiments by choosing the points at which the desired responses can be accurately predicted and assessed. Once the number of factors has been determined, multiple DOEs can be formulated to create a response surface, and these response surface designs are categorized according to their principal characteristics (e.g., variance and the number of experiments). As a result, the choice of an appropriate design strategy plays a significant role in the overall process. Nevertheless, it is noteworthy that in the majority of previously published studies, the rationale for selecting response surface design is often inadequately addressed, typically accompanied by only a cursory explanation. The three primary categories of response surface design include FFD, CCD, and BBD.

A variable that may influence a system's or process's reaction is referred to as a factor in the context of experimental design. The different values or settings at which a factor is adjusted throughout the experiment are referred to as its levels. It is essential to comprehend the idea of levels because it allows researchers to methodically examine the link between causes and responses under a variety of circumstances. The particular goals of the experiment and the range in which the factor is expected to affect the response determine the levels for a factor. The experiment can investigate how temperature affects the response variable at different locations within the area of interest by identifying these precise levels. The levels must encompass a spectrum that accurately reflects the practical operating conditions or the area of interest. Furthermore, the quantity of levels selected for each factor can influence the precision and accuracy of the experimental outcomes. It is essential to choose an adequate number of levels to effectively represent the behavior of the response variable throughout the range of the factors (Veza et al., 2023).

2.7.3.1. Full factorial design (FFD) RSM

An experiment utilizing a FFD examines every possible combination of levels across all factors. This RSM leads to experimental procedures where at least one trial must be conducted for each conceivable combination of factors and their respective levels. Such an exhaustive approach guarantees that all interactions are accounted for, with every factor interaction being included in the analysis. The total number of trials or repetitions is a vital aspect to consider. The required number of repetitions is influenced by several factors, including the level of precision desired in

the results, the variability present, and the resources available, such as time and funding. Increasing the number of repetitions diminishes the impact of random variation, resulting in a more accurate estimation of the true effects of the factors involved.

It is crucial to document the number of repetitions performed in the study to reflect the reliability and robustness of the experimental outcomes. However, conducting a large number of repetitions may not be feasible due to practical limitations. In such cases, it is important to acknowledge these constraints and their potential implications on the precision and generalizability of the results. Consequently, the FFD is comparatively costly and labor-intensive for multi-factor experimental studies. Its complexity escalates exponentially with an increase in the number of factors and levels.

A brief overview of FFD is illustrated in Figure 2.4. A more prevalent form of FFD is the three-level FFD, which accommodates three distinct values for the factors: low, center, and high. Thus, the total number of experiments required to investigate k factors at three levels will amount to 3^k . Nevertheless, a significant limitation of the three-level FFD is its demand for a large number of experimental runs, which frequently leads to the emergence of superfluous high-order interactions (Karimifard & Moghaddam, 2018).

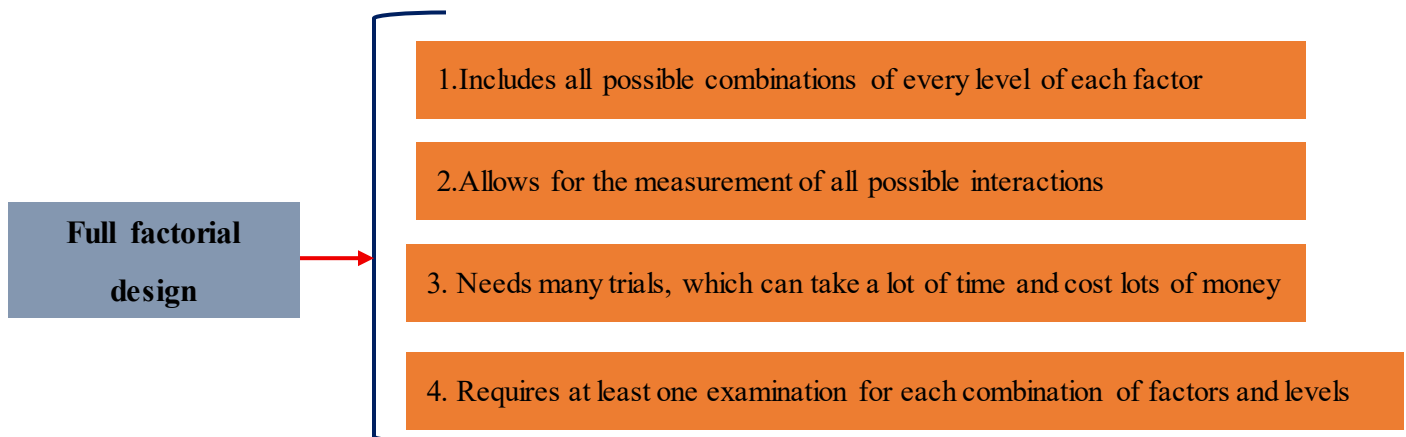


Figure 2.2 A brief summary of FFD

2.7.3.2. Central composite design (CCD)

RSM employing a CCD is widely recognized as a predominant approach in experimental design. CCD is particularly advantageous for sequential experimental investigations, as it allows for the enhancement of previous factorial experiments by incorporating additional axial and center points. This design facilitates the effective approximation of both first and second-order terms, enabling the modeling of a response variable that exhibits curvature through the integration of center and

axial points into a factorial framework. A CCD can serve to (i) accurately estimate first- and second-order terms; and (ii) to represent a response variable through curvature by incorporating center and axial points into a factorial design, as illustrated in Figure 2.5. The curvature of the response surface can be assessed by utilizing points situated at the midpoint of the experimental domain alongside "star" points positioned outside this domain. In a factorial design, the levels of the points are set at ± 1 , whereas the "star" points are designated at $\pm\alpha$, where $|\alpha|$ is greater than or equal to 1. The efficacy of predictions is influenced by the spatial arrangement of these points, highlighting the significance of the α value and the number of trials conducted at the center of the domain in determining the precision of the estimations. CCD can be classified into three distinct categories, as demonstrated in Figure 2.6 (Veza et al., 2023).

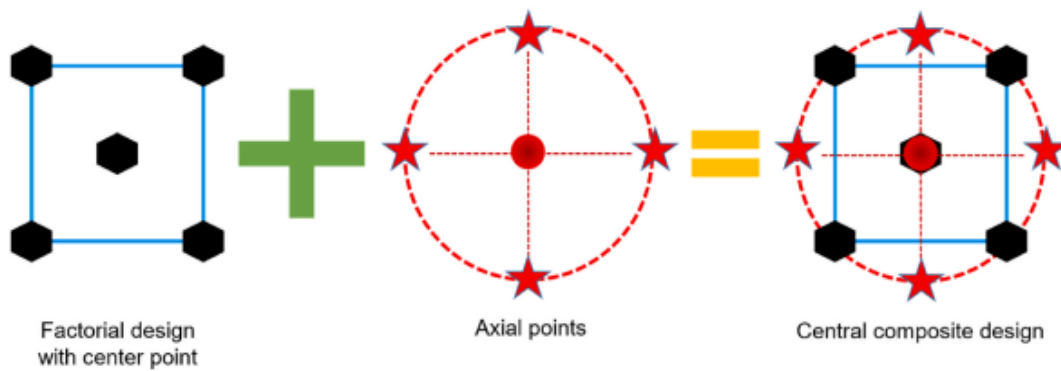


Figure 2.3 CCD graphical representation

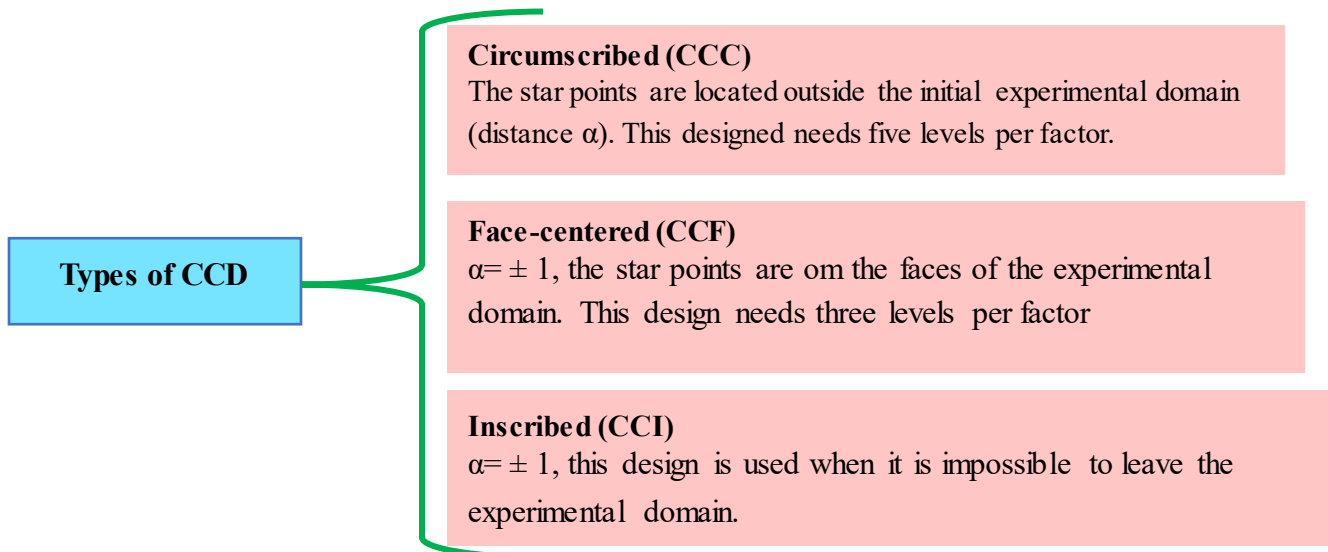


Figure 2.4 Three types of CCD

2.7.3.3. Box-Behnken design (BBD)

Another variant of RSM is referred to as BBD. This design type is distinct from factorial designs, as it does not rely on either full or fractional factorial approaches. The BBD is particularly advantageous for estimating first- and second-order coefficients due to its typically reduced number of design points, which can lead to significant savings in both time and cost. However, it is important to note that BBD lacks the inherent factorial structure found in CCD, making it less suitable for experiments that require a chronological approach. Despite its limitations in covering the corners of the nonlinear design space, BBD is often regarded as more effective than other response surface designs, such as three-level FFD and CCD. It allows for the exploration of higher-order responses with fewer experimental runs compared to traditional factorial methods. Like CCD, BBD is designed to maintain a higher-order surface by strategically selecting runs and is characterized by its rotatability and the necessity for three levels per factor, enabling it to fit a full quadratic model of the response surface (Veza et al., 2023). In the BBD, the treatment combinations are positioned at the edges of the cube, at the midpoints, and at the center, as illustrated in Figure 2.7. This design of the response surface must be considered for experimental studies involving more than two factors, particularly when the optimum is anticipated to be situated in the central region of the factor ranges.

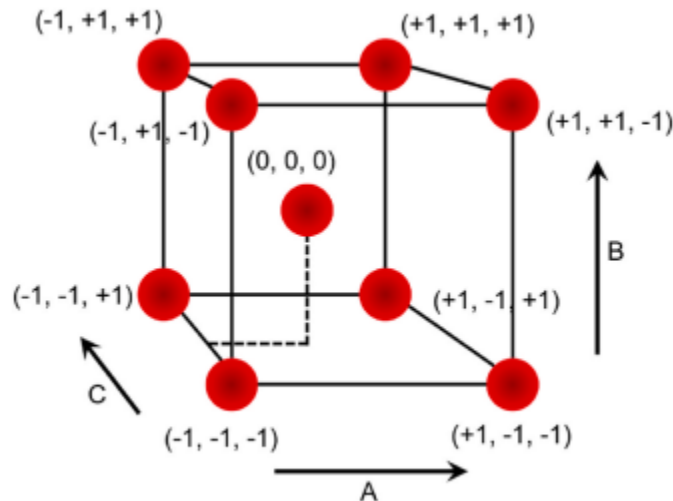


Figure 2.5 BBD graphical representation

2.8. Research Gap

The potential of TiO₂ and CuO NPs to enhance the performance and emissions of CI engines is evident; however, notable research deficiencies remain, especially concerning their synergistic effects when used in diesel-methanol blends. While there have been individual investigations into the effects of each nanoparticle, there is a lack of comprehensive understanding regarding their combined influence on combustion efficiency and emission reduction. Additionally, the use of Box-Behnken Design (BBD) for the optimization of various parameters such as the concentration of NPs, the ratios of fuel blends, and the operational conditions of the engine has not been sufficiently explored in the context of multi-nanoparticle systems. This oversight hinders the ability to achieve an optimal equilibrium between performance enhancements and emission reductions. By addressing these critical gaps, it may be possible to advance the development of nanoparticle-enhanced fuel blends, leading to more sustainable and efficient CI engine applications.

CHAPTER THREE

MATERIAL AND METHODS

3.1. Introduction

This chapter summarizes the materials, experimental setup, and methods used to study and enhance the combined impact of copper oxide (CuO) and titanium oxide (TiO₂) NPs on the operational performance and emission characteristics of a CI engine that runs on diesel-methanol blends. The objective of this study is to assess the effects of different concentrations of these metal oxide NPs on critical engine parameters like brake power (BP), brake torque (BT), brake specific fuel consumption (BSFC), and emissions like carbon dioxide (CO₂), hydrocarbons (HC), nitrogen oxides (NO_x), and carbon monoxide (CO).

In order to conduct a systematic and statistically sound investigation, the Box-Behnken Design (BBD) of RSM was utilized. This design facilitates the assessment of both the interactive and individual impacts of three independent variables: engine load, TiO₂ concentration, and CuO concentration, on various engine responses. The chapter offers a thorough explanation of the experimental procedures, the materials employed for fuel preparation, the techniques for nanoparticle dispersion, the specifications of the engine, the instruments for measurement, and the approach to statistical modeling. This methodological framework is crucial for attaining a comprehensive understanding of how nanoparticle additives interact with alcohol-diesel blends, thereby affecting engine performance across different operating conditions.

3.1. Materials

Due of its wide application in CI engines, commercial-grade diesel fuel served as the main fuel in this investigation. Because of its high oxygen content, low carbon-to-hydrogen ratio, and ability to reduce emissions when combined with diesel, methanol was selected as the alcohol addition. CuO and TiO₂ NPs (NPs) were introduced as fuel additives to improve combustion properties and increase the stability of the diesel-methanol mixture. These NPs are known for their enormous surface area and catalytic qualities, which improve atomization, combustion efficiency, and emission reduction. The diesel fuel was purchased from a nearby provider in compliance with relevant fuel quality regulations, and the methanol used in the mixture was of analytical grade with a purity of more than 99%. The TiO₂ and CuO NPs were synthesized in powdered form, exhibiting an average particle size between 20 and 50 nanometers. These NPs were subsequently dispersed

into the diesel-methanol mixture utilizing a magnetic stirrer, followed by ultrasonication to achieve a uniform distribution and mitigate agglomeration. The concentrations of the NPs were determined based on prior research outcomes, with the objective of identifying optimal levels that enhance performance and reduce emissions without leading to negative consequences such as injector blockage or fuel instability. All chemicals and materials were managed in accordance with safety protocols, and the fuel blends were freshly prepared prior to each test to ensure consistency and prevent phase separation.

The study utilized various supplementary materials and equipment, including laboratory glassware like beakers and measuring cylinders, to facilitate precise fuel blending. A digital balance with high precision was also employed to weigh the necessary amounts of TiO₂ and CuO NPs. The diesel-methanol mixture's homogeneity was enhanced, and agglomeration was avoided by using an ultrasonic cleaner to guarantee adequate dispersion of the NPs. Lab coats, gloves, and goggles were among the personal protective equipment worn during the fuel production process to ensure safety and reduce exposure to chemicals and NPs. The experimental setup included a multi-gas exhaust analyzer to measure key emission metrics like CO, HC, NO_x, and CO₂, as well as a test rig with a single-cylinder diesel engine to assess performance and emissions. These devices allowed for precise data collecting and monitoring under a variety of load conditions. A comprehensive inventory of the materials and equipment employed in the research is detailed in Table 3.1, which offers a succinct summary of all necessary components for fuel preparation, experimental evaluation, and analysis.

Table 3.1 List of materials and equipment used for the study

No.	Items	No.	Items
1	Methanol	9	Ultrasonic cleaner
2	Diesel	10	Measuring cylinders
3	TiO ₂ NPs	11	Glass ware
4	CuO NPs	12	Gloves
5	Digital balance	13	Engine test rig
6	Surfactant	14	Exhaust gas analyzer
7	Beakers	15	Data acquisition system

3.2. Methods

The approach employed in this work included the fabrication of diesel-methanol fuel blends, the development of nanoparticle-based nanofluid blends, the laboratory setup of the test engine, and the subsequent performance and emissions analysis. Initially, specific proportions of methanol were combined with diesel fuel to create a stable base fuel mixture. Following this, TiO₂ and CuO NPs were quantified, dispersed, and ultrasonically mixed into the fuel blends to yield homogeneous nano-fuel samples. The TMBC 8 test bench, an air-cooled, single-cylinder, four-stroke diesel engine located at AASTU, was used for experimental investigations. In order to evaluate the effects of the nano-fuel blends on performance metrics like brake thermal efficiency and BSFC, as well as emissions like CO, HC, NO_x, and CO₂, the engine was run under a variety of load conditions. To measure emissions accurately, an exhaust gas analyzer was used. The flowchart in Figure 3.1 illustrates the entire methodological workflow, from fuel preparation to data analysis.

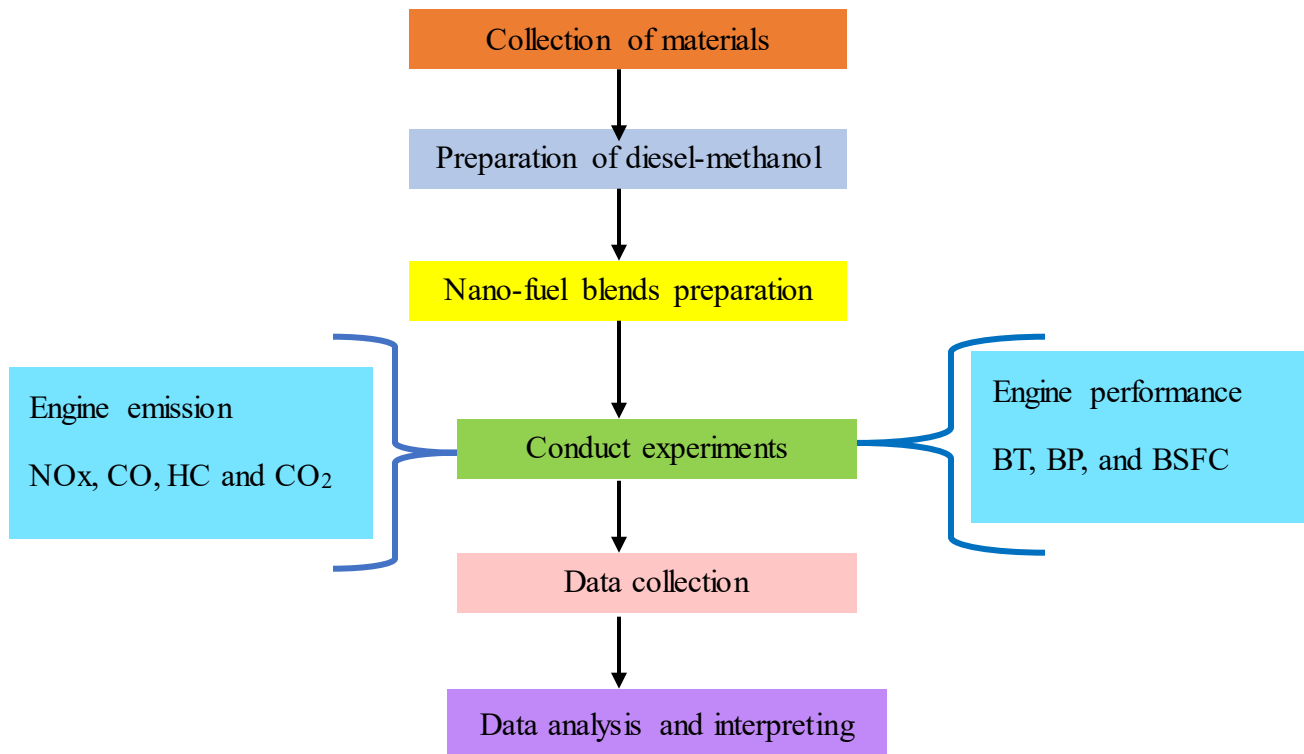


Figure 3.1 The comprehensive methodological workflow of the study

3.3. Design of experiment using Response Surface Methodology (RSM)

RSM is a set of sophisticated statistical and mathematical techniques that are frequently applied to the modelling and optimization of complicated engineering processes. This methodology is particularly useful when multiple input variables interact to affect one or more output replies. In the current study, RSM was used to comprehensively assess the performance and emission characteristics of a CI engine operating on diesel-methanol-nanoparticle mixtures. Fifteen experimental runs were conducted using the Box-Behnken Design (BBD), a dependable and efficient design technique inside the RSM framework. This approach necessitates fewer trials compared to full factorial designs while still effectively capturing essential interactions. The investigation concentrated on three independent variables: engine load (A), titanium dioxide (TiO₂) nanoparticle concentration (B), and copper oxide (CuO) nanoparticle concentration (C). These variables were selected due to their established influence on combustion and emission behavior, and their levels were meticulously chosen within practical and technically relevant ranges. The specific upper, middle, and lower levels for each variable are outlined in Table 3.2, which serves as the basis for constructing the experimental matrix utilized for optimization and analysis.

Table 3.2 Range of process factors used in Box Behnken design

Input variables	Coded	High	Average	Low
Engine load	A	80	60	40
TiO ₂ nanoparticle	B	90	60	30
CuO nanoparticle	C	60	40	20

3.4. Preparation of diesel-methanol

Many studies have been conducted on the use of methanol in CI engines, particularly when it comes to its combinations with conventional diesel fuel. Investigations have shown that the incorporation of methanol into diesel can enhance combustion properties and diminish specific emissions, attributable to methanol's elevated oxygen content and its low carbon-to-hydrogen ratio. Methanol-diesel blends ranging from M5 (5% methanol and 95% petro-diesel by volume) to M80 (80% methanol and 20% petro-diesel) have been tested; mixes up to M40 are generally suitable without requiring engine changes. Three distinct blend ratios were developed and used in this study's experiments:

1. M10: 10% methanol and 90% petro-diesel
2. M20: 20% methanol and 80% petro-diesel
3. M30: 30% methanol and 70% petro-diesel

These blends were selected to assess how methanol concentration affects engine performance and emissions while making sure they stay within the safe operating ranges for unmodified CI engines.

Procedure for Blending Diesel and Methanol (Example: M10)

The following steps detail the preparation of a 1-liter sample of the M10 blend:

Measurement of Diesel: A 1000 mL graduated beaker was utilized to accurately measure 900 mL of standard petro-diesel.

Measurement of Methanol: A separate 500 mL beaker was used to measure 100 mL of methanol.

Initial Mixing: The diesel was poured into a clean, dry 1-liter glass or plastic bottle that has a securely sealable cap.

Addition of Methanol: The pre-measured methanol was subsequently added to the bottle containing the diesel.

Homogenization: The bottle was tightly sealed and shaken vigorously for at least 2 minutes to ensure thorough mixing and homogeneity of the blend.

The same procedure was applied for the preparation of M20 and M30 blends, with adjustments made to the volumes of methanol and diesel in proportion. All blending activities were carried out at room temperature in well-ventilated areas to reduce vapor exposure and enhance safety. It is crucial to highlight that due to the potential immiscibility issues that can arise with alcohol-diesel blends, particularly at lower ambient temperatures, the blends were visually examined for any phase separation before to use. Should any stratification be observed, further agitation was conducted before fueling.

3.5. Preparation of Nano-methanol-diesel fuel blends

In order to enhance the performance and emission profiles of methanol-diesel mixes, TiO₂ and CuO NPs were used as fuel additives. These metal oxide NPs were selected because of their strong catalytic activity, thermal stability, and proven capacity to improve combustion efficiency while reducing hazardous emissions in internal combustion engines. Commercial sources provided the TiO₂ and CuO nanoparticles used in this investigation, which had a purity level of 99.5% and particle diameters between 15 and 20 nm and 20 and 30 nm, respectively. TiO₂ nanoparticle concentrations in the blended fuels were adjusted to 30 ppm, 60 ppm, and 90 ppm, while CuO

nanoparticle concentrations were set at 20 ppm, 40 ppm, and 60 ppm, all determined by their weight relative to the fuel's total mass.

3.5.1. Materials and equipment used

- a) **TiO₂ nanoparticles:** Used to catalyze fuel oxidation and improve combustion properties. Detailed characteristics are provided in Appendix A.
- b) **CuO nanoparticles:** Function as oxidation catalysts, aiding in complete combustion and reducing carbon monoxide and hydrocarbon emissions. Specifications are summarized in Appendix B.
- c) **Cetyletrimethyl ammonium bromide (CTAB):** A cationic surfactant is employed to stabilize nanoparticles in the fuel. CTAB adheres to the surfaces of the NPs, creating a negatively charged protective layer that inhibits agglomeration and improves uniform dispersion.
- d) **Analytical Precision balance:** An electronic scale with high precision, featuring a resolution of 0.00001 g, is utilized for the accurate measurement of NPs and surfactants.
- e) **Ultrasonic cleaner:** Employed to guarantee comprehensive distribution of NPs throughout the diesel-methanol mixture by utilizing ultrasonic waves (20–40 kHz), which facilitate de-agglomeration and consistent suspension of particles. Figures 3.2 and 3.3 depict the equipment and materials needed to prepare the nano-diesel-methanol fuel blend.



a) TiO₂ nanoparticles



b) CuO nanoparticles



c) CTAB



d) Digital electronic balance

Figure 3.2 Equipment and material used for nano-methanol-diesel blends preparation



Figure 3.3 Ultrasonic cleaner

3.5.2. Fuel Preparation Procedure (Example: M10 + TiO₂ 90 ppm + CuO 60 ppm)

The steps involved in preparing the nano-methanol-diesel blends are detailed below:

- 1. Fuel Measurement:** Utilize a clean 500 mL beaker to measure 100 mL of the M10 fuel blend, which consists of 10% methanol and 90% diesel.
- 2. Nanoparticle Weighing:** Precisely weigh 0.09 g of TiO₂ and 0.06 g of CuO nanoparticles using an analytical balance for accuracy.
- 3. Surfactant Addition:** Measure out 0.15 g of CTAB surfactant.
- 4. Initial Mixing:** Introduce the weighed NPs and CTAB into the 100 mL of M10 fuel. Stir the mixture thoroughly for a minimum of 15 minutes to ensure proper initial dispersion.

5. Bulk Blending: Pour the 100 mL nanoparticle-fuel suspension into a 900 mL M10 blend that is contained within a 1-liter vessel to create a uniform 1-liter sample.

6. Ultrasonic Homogenization: Transfer the final mixture into an ultrasonic cleaner and sonicate it for 30 minutes at a high frequency to guarantee complete dispersion and to avoid the agglomeration of NPs.

This procedure was uniformly implemented for all samples of nanoparticle-doped fuel, with the dosage levels modified in accordance with the desired formulation. Figure 3.4 depicts the blending process utilizing the ultrasonicator for the preparation of nano-methanol-diesel fuel.



Figure 3.4 blending process utilizing the Ultrasonicator

3.6. Engine experimental setup and test procedure

The TBMC 8 test bench, located at AASTU's engine testing lab, was used for the experimental investigation. It has a single-cylinder, four-stroke, air-cooled diesel engine with a direct injection (DI) system. The engine has a 24:1 CR and generates 5.1 kW of output power at 3000 rpm. The engine shaft was attached to an air-cooled asynchronous motor that functioned as a dynamometer in order to assess engine performance. A frequency converter was used to introduce load

fluctuations while keeping the engine speed constant at 2400 rpm throughout every experiment. Table 3.3 contains comprehensive engine specifications.

To evaluate the effects of various fuel combinations, performance parameters such as brake power (BP), brake torque (BT), and brake specific fuel consumption (BSFC) were recorded under a variety of load scenarios. To ensure accuracy and consistency, the engine was allowed to reach a steady-state operating temperature prior to data collection. Each experiment was performed at several load levels, with all measurements averaged over a minimum of three repetitions to minimize experimental variability. In order to assess exhaust emissions, a KANE-EGA exhaust gas analyzer was utilized, which is capable of real-time monitoring of the concentrations of CO, HC, CO₂, and NO_x. This facilitated a thorough assessment of how the fuel mixtures and nanoparticle additives affected the engine's environmental performance. The experimental test matrix is presented in Table 3.4, and a schematic representation of the setup is illustrated in Figure 3.5 to visually depict the experimental arrangement.

Table 3.3 Specification of the test engine

Company/model	Kubota/ E300-ES01(TBMC 8)
Type of engine	CI
Fuel	Diesel
Cylinders No.	1
Stroke No.	4
Intake air type	Naturally aspirated
Cooling type	Water
Swept volume (cm ³)	309
CR	24:1
power output(kW)	5.1 at 3000 rpm
Cylinder bore	77 mm
Stroke	70 mm

Table 3.4 Experimental test matrix

Engine operating conditions	Test fuels	Parameters
Fixed CR (24:1) Fixed speed (2400 rpm) Varying load	D100, M10, M20, and M30 For optimization: M10+ varying nanoparticle	Engine performance: BT, BP, and BSFC Emission: CO, CO ₂ , HC, and NO _x

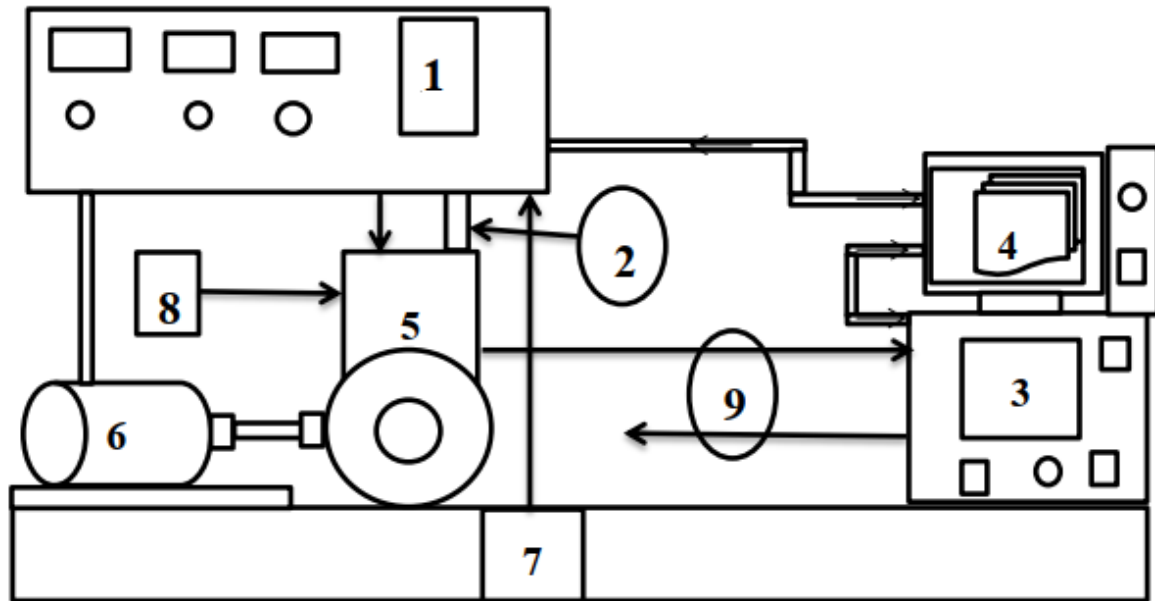


Figure 3.5 Schematic diagram of the experimental setup

- | | | |
|--------------------------|------------------------|------------------------------------|
| (1) Test stand | (4) Desktop computer | (7) Fuel tank and fuel intake line |
| (2) Fuel flow tube | (5) Diesel engine | (8) Air filter and air intake line |
| (3) Exhaust gas analyzer | (6) Asynchronous motor | (9) Exhaust gas line |

Before conducting the tests, the engine underwent a comprehensive inspection and was permitted to warm up under no-load conditions to guarantee stable operating temperatures and proper oil circulation. The fuel tanks were cleaned and filled with the designated test fuels—standard diesel, methanol-diesel blends (M10, M20, M30), and nano-additive blends (TiO₂ and CuO at various ppm levels). Before taking measurements, the engine was run for a few minutes on each fresh fuel sample in order to remove the old fuel from the system and promote the formation of stable combustion characteristics.

During the testing procedure, the engine was run at a steady 2400 rpm while the load conditions were changed, usually in increments of 20% to 80%. BP, BT, and BSFC were recorded for each load level. These metrics were derived from torque and fuel consumption readings. To ensure consistency and minimize errors, each measurement was recorded after the engine had reached a stable state, and results were averaged over three trials. Emissions analysis was performed utilizing the KANE-EGA exhaust gas analyzer, a sophisticated device capable of identifying key pollutants in the exhaust gas. This instrument measured CO, HC, CO₂, and NO_x. The sampling probe was inserted directly into the exhaust outlet, and readings were taken once the values stabilized. All emission data were digitally logged for subsequent processing and comparison across various fuel formulations and load conditions. To ensure the reliability of the experiments, environmental factors such as room temperature and air pressure were maintained at relatively constant levels throughout the testing process. The test bench was operated in a controlled laboratory environment with sufficient ventilation.

3.7. Data analysis

A desktop monitoring device was used to collect engine performance and exhaust emissions data straight from the TMBC 8 engine test bench during the trial runs. Key performance indicators: Using a linked exhaust gas analyzer, real-time exhaust gas concentrations were automatically recorded together with BT, BSFC, and BP. These measurements were recorded and stored for each test point that corresponded to varying load levels at a constant engine speed of 2400 rpm. Subsequently, the raw data were processed and arranged into tables, facilitating further analysis of engine behavior under different fuel and additive conditions.

Brake power (BP): A crucial measure of engine efficiency, it signifies the effective mechanical power output that can be harnessed at the flywheel. This value is derived from the multiplication of torque and angular velocity. The brake power was ascertained through the conventional mechanical power formula:

$$BP = \frac{2\pi NT}{60} \quad (3.1)$$

Where BP is brake power (kW): N is angular speed (rpm): T is torque in (Nm)

Brake torque (BT): refers to the rotational force exerted by the engine and transferred to the dynamometer. It is another critical performance parameter and was derived from the brake power and rotational speed using the rearranged form of the above equation:

$$BT = \frac{BP \times 60}{2\pi N} \quad (3.2)$$

Where: BT is brake torque (Nm): BP is brake power (kW): N is angular speed (rpm)

BSFC: measures the efficiency of the engine in converting fuel energy into useful work. It represents the mass of fuel consumed to generate one kilowatt of brake power per hour. BSFC is calculated using the ratio of fuel mass flow rate to brake power.

$$BSFC = \frac{\dot{m}_f}{BP} \quad (3.3)$$

However, $\dot{m}_f = \dot{v} \times \rho_f$

Where: BSFC is brake specific of fuel consumption (kg/kW-hr): BP is brake power: \dot{m}_f is mass flow rate: \dot{v} is volumetric flow rate: ρ_f is density of fuel.

Exhaust gas emissions: denote the byproducts that are discharged into the atmosphere via the exhaust outlet of an internal combustion engine during its operation. Ideally, under conditions of perfect or stoichiometric combustion: where the air-to-fuel ratio is optimally balanced, the primary outputs would consist of CO₂ and H₂O. These substances are the anticipated final products of complete combustion when the fuel undergoes full oxidation. Nevertheless, in practical engine scenarios, achieving perfect combustion is seldom realized due to various factors such as fluctuations in the air-fuel mixture, flame quenching occurring near the cylinder walls, temperature variations, and incomplete oxidation.

Consequently, the exhaust gases comprise numerous undesirable pollutants, including CO, which is a toxic, partially oxidized byproduct; HC, which arise from fuel that does not undergo combustion; and oxides of nitrogen (NO_x), which are produced at elevated temperatures when nitrogen and oxygen in the air react. These emissions not only impair engine performance but also significantly contribute to air pollution, thereby posing health and environmental hazards. The control and reduction of these emissions have emerged as a critical focus in the design of engines

and the formulation of fuels, particularly through the implementation of cleaner fuels, exhaust after-treatment systems, and fuel additives such as NPs or alcohol-based mixtures.

CHAPTER FOUR

RESULTS AND DISCUSSIONS

4.1. Engine performance and Exhaust emission characteristics

This part of the study looked at how changes in engine load affected tailpipe emissions and engine performance metrics. Brake Power (BP), Brake Torque (BT), and Brake Specific Fuel Consumption (BSFC) were the three engine performance metrics that were examined in connection to engine load using the equations (3.1, 3.2, and 3.3) from the preceding chapter. Furthermore, four types of exhaust gases were analyzed in relation to engine speed: carbon monoxide (CO), carbon dioxide (CO₂), nitrogen oxides (NO_x), and hydrocarbons (HC). D100, M10, M20, and M30 fuel samples were prepared for the engine performance and exhaust gas emission tests. The baseline diesel fuel (D100) was used to compare the test results.

4.1.1 Performance Characteristics

Brake power (kW): Brake power (BP), defined as the effective power output accessible at the engine crankshaft, was determined utilizing Equation 3.1. Table 4.1 presents the measured BP values obtained from the engine test stand under different loading conditions for each fuel blend.

Table 4.1 The brake power data recorded from the test

Engine brake power (kW)				
Engine load (%)	Fuel sample			
	D100	M10	M20	M30
20	0.57	0.55	0.52	0.50
40	1.25	1.23	1.18	1.16
60	1.91	1.89	1.84	1.81
80	2.62	2.61	2.57	2.53

The BP output of the tested fuels at different engine loads, all recorded at a constant engine speed of 2400 rpm, is shown in Figure 4.1. As would be predicted given the higher fuel input and increased combustion energy at higher loads, the figure clearly demonstrates that BP increases gradually with engine load for all fuel types. At 80% engine load, the D100's max BP was measured at 2.62 kW. Reductions of roughly 1.73%, 5.33%, and 7.02% were seen for M10, M20, and M30 when comparing the average BP of the methanol-diesel blends to D100. Among these blends, M30 demonstrated the lowest BP, likely attributable to methanol's reduced calorific value and elevated L_v , which can inhibit peak combustion temperatures and diminish overall energy output.

Conversely, D100 exhibited superior performance owing to its lower viscosity and greater energy content, facilitating more complete and efficient combustion.

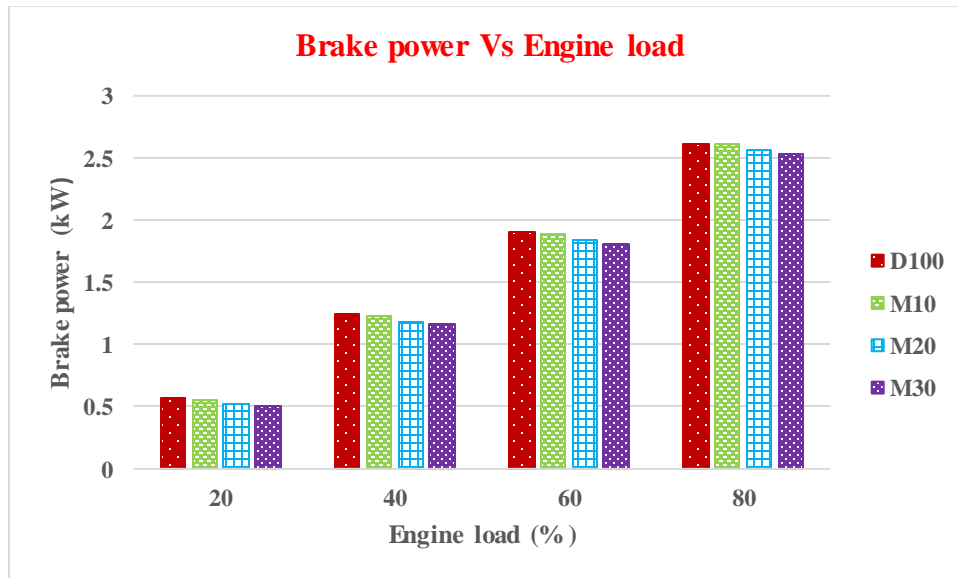


Figure 4.1 Variation of brake power with engine load

Brake torque (Nm): Brake torque (BT), denoting the rotational force generated by the engine at the crankshaft, was determined using Equation 3.2. This parameter is essential for evaluating the mechanical performance and load-bearing capacity of the engine across various fuel types. Table 4.2 displays the BT values for a variety of test fuels that were recorded at various engine loads.

Table 4.2 The brake torque data recorded from the test

Engine brake torque (Nm)				
Engine load (%)	Fuel sample			
	M0 (D100)	M10	M20	M30
20	2.40	2.37	2.31	2.21
40	4.05	4.01	3.96	3.87
60	5.17	5.12	5.04	4.98
80	7.11	7.03	6.95	6.90

The BT output of the test fuels at different engine loads all recorded at a constant engine speed of 2400 rpm is shown in Figure 4.2. BT for all fuels rises steadily with increasing engine load, as the figure illustrates. This is normal behavior as more fuel is injected and burned to satisfy the increased power requirement. The D100 had the greatest BT, measuring 7.11 Nm at 80% engine load. The methanol-diesel blends M10, M20, and M30 all had BT values that were, on average, 1.06%, 2.68%, and 4.74% lower than D100. The lower energy density and higher L_v of methanol,

which may lower combustion temperatures and postpone ignition, are responsible for the decrease in BT with increasing methanol content. These factors can lead to less efficient combustion and, consequently, lower torque output. In contrast, D100 delivers higher torque due to its favorable fuel properties, such as lower viscosity and higher heating value, which promote rapid ignition and complete combustion.

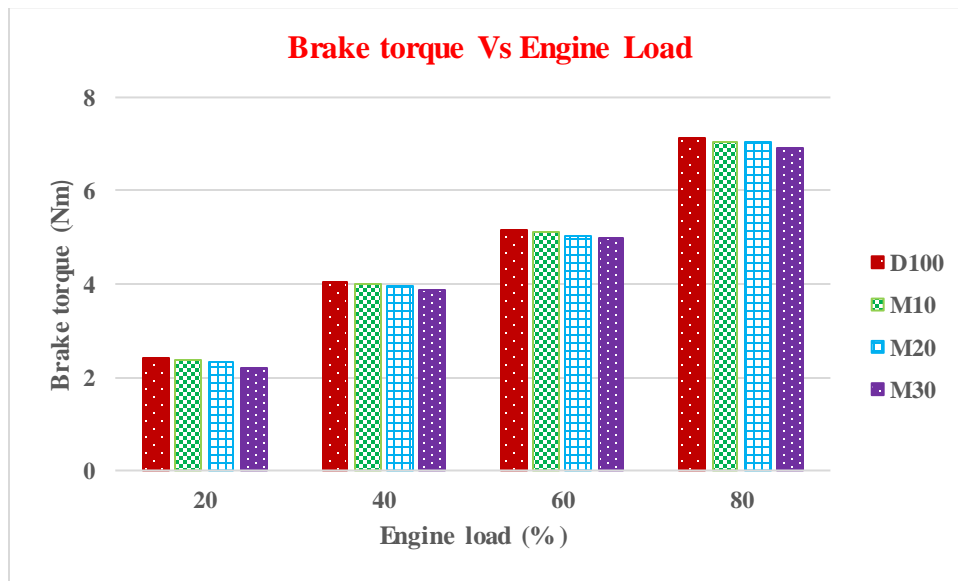


Figure 4.2 Brake torque variation with engine load

BSFC (kg/kWh): A crucial factor in evaluating engine performance is the assessment of BSFC in relation to engine load. The BSFC of a diesel engine is primarily affected by factors such as fuel density, the higher heating value of the fuel, viscosity, and the volumetric rate of fuel injection. Below, Table 4.3 presents the output data for BSFC in conjunction with engine load, which was acquired from the test stand. The BSFC for the engine at various speeds was calculated in accordance with Equation 3.3.

Table 4.3 The BSFC data recorded from the test

Engine BSFC (kg/kWh)				
Engine load (%)	Fuel sample			
	M0 (D100)	M10	M20	M30
20	0.530	0.545	0.552	0.561
40	0.405	0.417	0.423	0.429
60	0.368	0.375	0.381	0.394
80	0.379	0.386	0.399	0.402

BT variation with engine load Engine load variations affect BSFC, a measure of the engine's fuel efficiency in transforming chemical energy into mechanical effort. As engine load increases, BSFC first drops and eventually reaches an ideal minimum point, as seen in Figure 4.3. This happens because the engine runs more effectively at moderate loads, which maximizes the amount of energy generated per unit of fuel used. However, at higher load levels, BSFC begins to rise again due to increased fuel demand and potential limitations in combustion efficiency. From the data, the average BSFC of the D100 was found to be 2.45% lower than that of the M10 blend, indicating slightly better fuel efficiency for the under most conditions. Interestingly, the M20 and M30 blends demonstrated average BSFC values that were 4.35% and 6.12% lower than D100, respectively. This higher BSFC of methanol-diesel blends could be attributed to that methanol produces less energy per unit mass, and its physical and chemical characteristics (such as high L_v and low cetane number) have a detrimental effect on engine combustion efficiency.

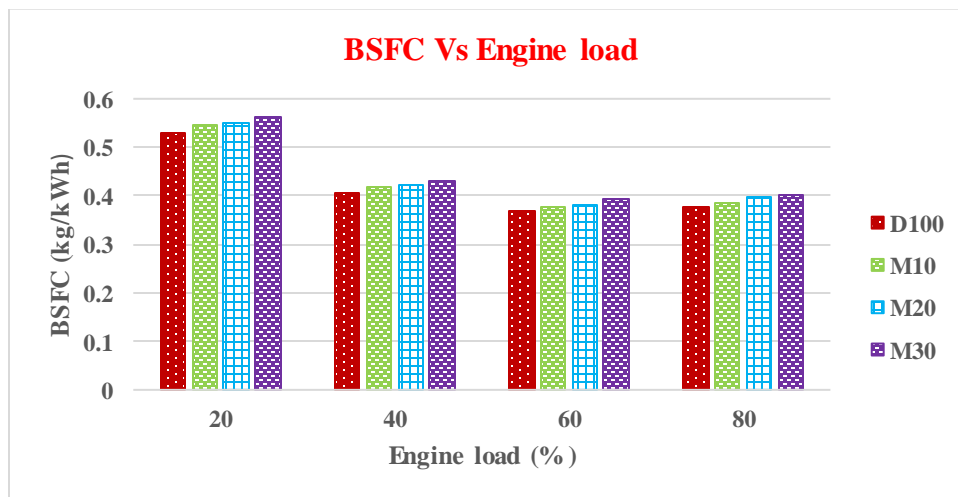


Figure 4.3 Variation of BSFC with engine load

4.1.2 Exhaust Emission Characteristics

This section of the research discusses how engine load affects exhaust emissions. NO_x, hydrocarbons, CO, and CO₂ are the many exhaust characteristics that are being examined.

Carbon monoxide (CO): Incomplete combustion of fuels contributes to elevated levels of CO emission. For combustion to be complete, several critical conditions must be satisfied: an adequate supply of oxygen, effective mixing of the air-fuel mixture, sufficient time for combustion reaction, and high enough oxygen concentration within the combustion chamber. A deficiency in any of these factors can result in the formation of CO due to the partial oxidation of carbon-

containing compounds. Table 4.4 presents the recorded CO emission values obtained from the engine test stand.

Table 4.4 The carbon monoxide data recorded from the test

Carbon monoxide (%vol)				
Engine load (%)	Fuel sample			
	M0 (D100)	M10	M20	M30
20	0.037	0.041	0.043	0.044
40	0.034	0.036	0.039	0.040
60	0.028	0.030	0.031	0.034
80	0.030	0.033	0.035	0.038

The variation in CO emissions for the studied gasoline mixes at various engine loads is displayed in Figure 4.4. Under all loading scenarios, the M30 blend had the highest CO emission values among the fuels assessed. This increase is caused by the incomplete oxidation of carbon compounds caused by methanol's higher L_v and lower cetane number, which tend to impede combustion and lower flame temperatures. With reductions of roughly 7.57%, 14.68%, and 21.16% in comparison to M10, M20, and M30, respectively, D100 demonstrated noticeably lower CO emissions. This trend implies that as the content of methanol in the blend increases, the likelihood of incomplete combustion also rises.

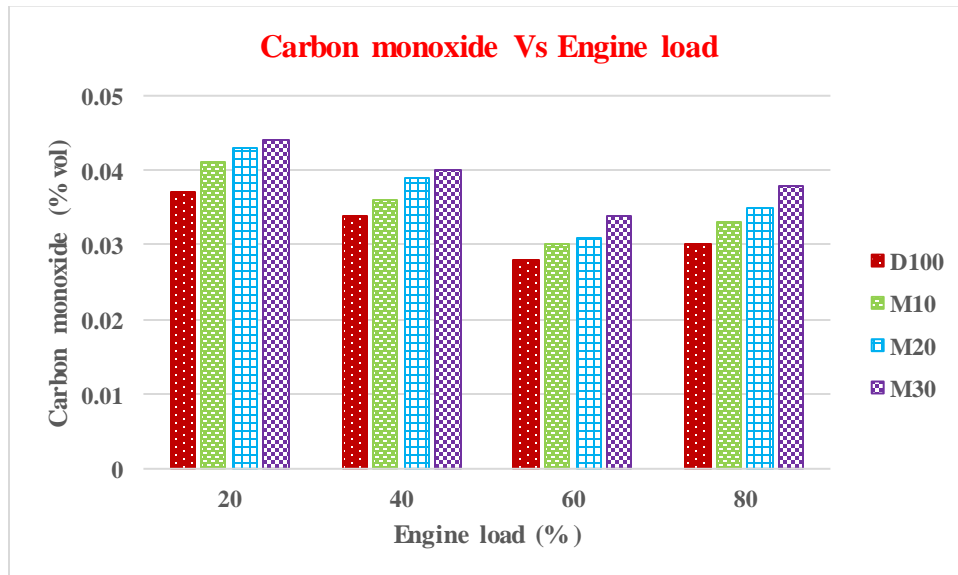


Figure 4.4 Variation of carbon monoxide with engine load

Carbon dioxide emission (CO₂): A higher concentration of CO₂ in the exhaust emissions is indicative of a more complete combustion of the air-fuel mixture. This is because, during efficient combustion, the carbon content in the fuel is fully oxidized to CO₂ rather than forming CO. The elevated CO₂ levels observed can also be ascribed to the presence of oxygen-rich components in the blended fuels, which enhance oxidation reactions and facilitate the conversion of CO to CO₂. Additionally, this process is supported by ideal combustion circumstances, which include suitable in-cylinder temperatures, adequate oxygen availability, and optimum air-fuel mixing. Table 4.5 presents the CO₂ emission data recorded during the engine tests.

Table 4.5 The carbon dioxide data recorded from the test

Carbon dioxide (%vol)				
Engine load (%)	Fuel sample			
	M0 (D100)	M10	M20	M30
20	2.71	2.55	2.49	2.44
40	3.22	3.06	3.01	2.98
60	3.75	3.53	3.48	3.44
80	4.21	4.01	3.94	3.90

Figure 4.5 displays the trend of CO₂ emissions for the different test fuels with varying engine loads. The graph shows that CO₂ emissions usually increase with engine load. Among the fuels under evaluation, pure diesel (D100) consistently produced higher CO₂ emissions than methanol-diesel blends. The average CO₂ emissions from D100 were 5.38%, 7.08%, and 8.26% greater than those from M10, M20, and M30. Because methanol has a lower carbon-to-hydrogen (C/H) ratio than diesel, there is a decrease in CO₂ emissions as the amount of methanol increases. Because methanol has a lower carbon-to-hydrogen (C/H) ratio than diesel, CO₂ emissions fall as the amount of methanol increases. Because methanol contains less carbon, it burns with less CO₂. Because methanol contains less carbon per unit of energy produced, it burns with less CO₂. Additionally, methanol's high oxygen content promotes cleaner burning but reduces the amount of carbon mass available for oxidation. Therefore, combining methanol with diesel results in more oxygenated, less carbon-rich combustion, which accounts for the observed drop in CO₂ emissions.

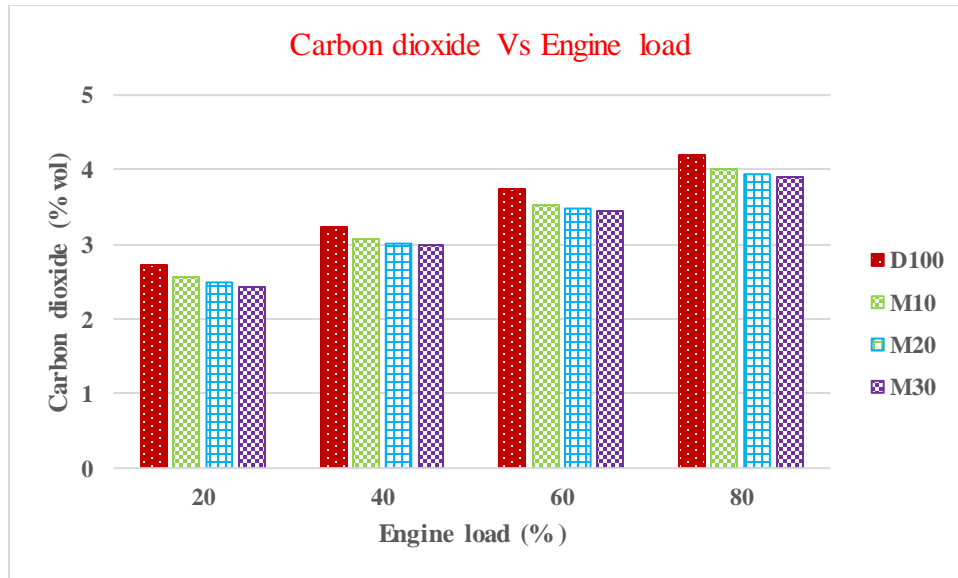


Figure 4.5 CO₂ variation with engine load

Hydrocarbon emission (HC): The main cause of HC emissions is incomplete fuel combustion in the engine cylinder. Because of things like inadequate air-fuel mixing, flame quenching close to the cylinder walls, or insufficient combustion duration, these unburned or partially consumed fuel components manage to evade the combustion process. The amount of HC emissions is significantly influenced by the engine's operating characteristics, including load, speed, and temperature, as well as the chemical composition of the test fuels. Blended fuels, especially those with a high oxygen percentage or lower cetane numbers, may change the ignition delay and combustion characteristics under certain conditions, boosting the production of HC. Table 4.6 displays experimental data on HC emissions from the engine test stand.

Table 4.6 The hydrocarbon data recorded from the test

Hydrocarbon (ppm)				
Engine load (%)	Fuel sample			
	M0 (D100)	M10	M20	M30
20	43	47	49	53
40	34	36	38	41
60	28	30	31	35
80	40	42	45	48

The relationship between HC emissions and engine load for various test fuels is shown in Figure 4.6. The findings demonstrate that HC emissions initially decline with increasing load, reach a minimum value, and then increasing once more at higher loads. Both plain diesel (D100) and methanol-diesel mixes exhibit this behavior. Improved combustion efficiency at medium loads, where higher in-cylinder temperatures and better air-fuel mixing encourage more thorough fuel oxidation, is responsible for the initial decrease in HC emissions. However, at very high engine loads, the additional fuel supply may cause oxygen-deficient areas and locally rich mixes, which can contribute to incomplete combustion and a rise in HC emissions. Overall, D100 continuously provided fewer HC emissions than the blended fuel out of all the fuels tested. Overall, among all the fuels tested, D100 consistently produced lower HC emissions compared to the blended fuels. In comparison to M10, M20, and M30, D100 specifically showed decreases of roughly 6.83%, 12.23%, and 22.21%, respectively. The higher HC levels in the methanol-diesel blends are probably caused by the higher L_v and lower number of cetane in methanol, which might result in incomplete combustion by delaying ignition and lowering flame temperatures. This implies that adding more methanol to the fuel blend could have a detrimental effect on combustion efficiency, particularly when there is a high load.

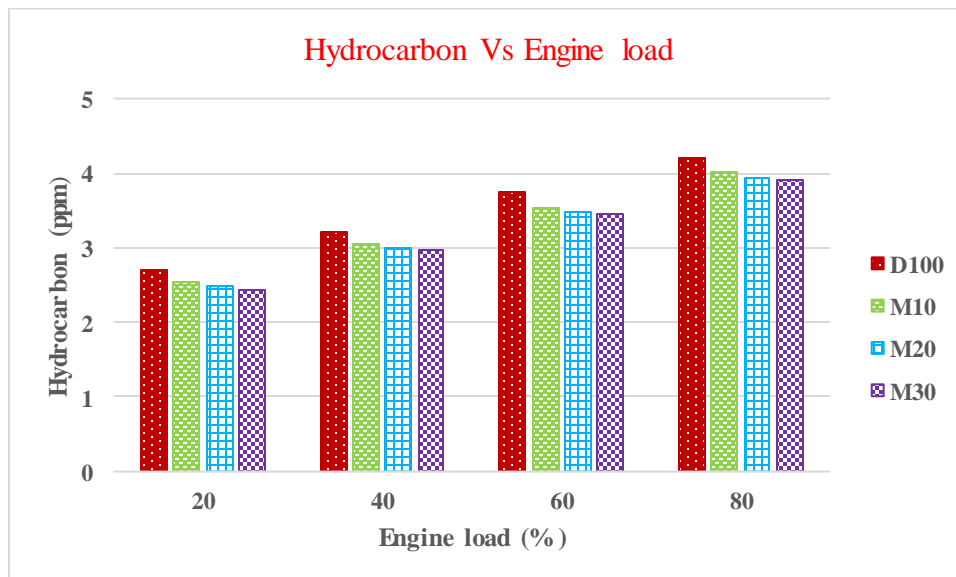


Figure 4.6 Variation of hydrocarbon with engine load

Nitrogen Oxides (NOx): NOx is mainly produced due to elevated combustion temperatures within the engine cylinder, where nitrogen and oxygen from the intake air interact under thermal conditions. The generation of NOx is significantly affected by the maximum in-cylinder temperatures, the presence of oxygen, and the duration of exposure to high temperatures. Particularly in the premixed combustion phase, higher combustion temperatures enhance the thermal NOx production process. The recorded NOx emission levels from the engine test stand are shown in Table 4.7.

Table 4.7 The nitrogen oxides data recorded from the test L_v

Nitrogen oxides (ppm)				
Engine load (%)	Fuel sample			
	M0 (D100)	M10	M20	M30
20	40	36	33	30
40	117	110	105	101
60	194	181	178	173
80	240	226	221	216

Figure 4.7 illustrates the variation in NOx emissions with engine loads for the different test fuel blends. The data clearly show that the M30 blend consistently produced the lowest NOx emissions across all loading conditions. In contrast, D100 generated the highest level of NOx, which increased by 7.43%, 10.94%, and 14.87% compared to M10, M20, and M30, respectively. The observed decline in NOx emissions as methanol content rises can be linked to the fundamental characteristics of methanol—most notably its elevated L_v and reduced flame temperature, which together help to decrease the maximum in-cylinder temperature. Given that the production of NOx is significantly influenced by temperature, the cooler combustion conditions fostered by methanol effectively diminish the thermal NOx generation mechanism. Furthermore, the oxygen-rich composition of methanol promotes more efficient combustion while concurrently inhibiting NOx production.

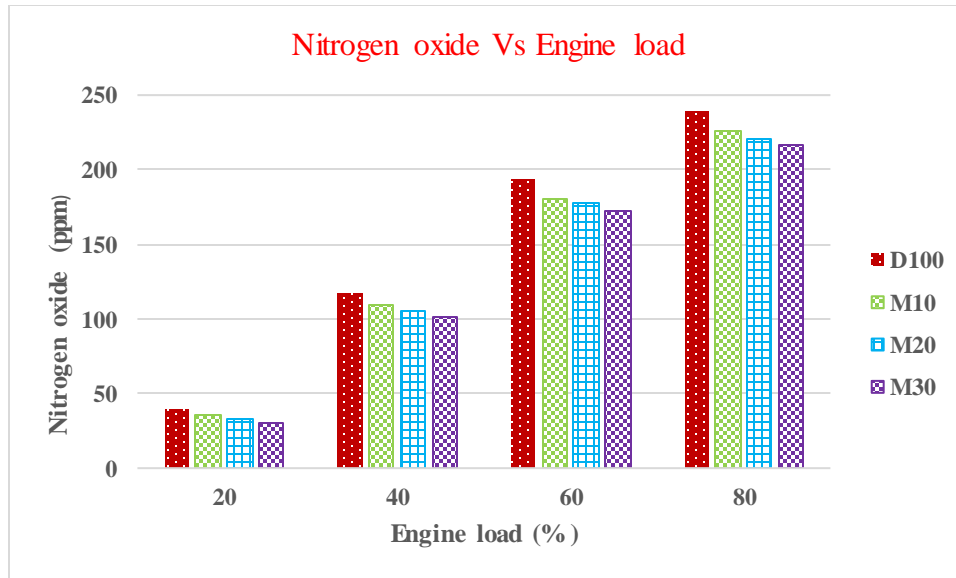


Figure 4.7 Variation of nitrogen oxide with engine load

Among the tested fuel blends, M10 (10% methanol and 90% diesel) demonstrated the most balanced performance by achieving a noticeable reduction in harmful emissions while maintaining engine output characteristics close to that of pure diesel (D100). Higher methanol blends, such as M20 and M30, increased HC and CO emissions due to incomplete combustion, which is probably driven by methanol's lower cetane number and high L_v , even if they also provided additional reductions in other pollutants, such as NO_x and CO₂. M10, on the other hand, produced lower CO, HC, and NO_x emissions than D100 while maintaining combustion efficiency and engine output due to its moderate oxygen content and no interruption to combustion stability.

Overall, M10 emerges as the most effective compromise between emission control and performance retention among the tested fuels. It leverages the environmental benefits of methanol blending without significantly compromising engine output or combustion completeness. This makes M10 a promising candidate for real-world applications where reducing emissions is essential, yet operational efficiency and reliability must still be preserved.

4.2. Optimization of engine performance and emissions

4.2.1 Response surface methodology model (RSM) analysis

A design matrix made with the Box-Behnken Design (BBD) of RSM(RSM) established the foundation for a total of fifteen experimental trials. Three main parameters were the focus of this study: engine load (A), copper oxide NPs (CuO NPs) (C), and titanium dioxide NPs (TiO₂ NPs)

(B). Using RSM for this analysis, the study's goal was to look at these components' individual and combined effects on engine performance and emissions. The numerical link between the output factors and the process factors was determined using a quadratic polynomial model. Furthermore, as shown in Equations 4.1-4.7, a mathematical formulation for multiple regression analysis was created, allowing for the development of predictive models. The statistical technique of Analysis of Variance (ANOVA) was used to evaluate the correlations and ascertain the impact of the input variables on the response variables. Table 4.8 summarizes the results of an ANOVA analysis of engine performance, including BT, BP, and BSFC, as well as emissions, including NO_x, CO₂, CO, and HC.

Several statistical metrics, such as the F – value, P – value, R², and Adj-R², were used to assess the model's quality. A higher Adj-R² number that closely matches the R², particularly when the R² is near to 1, indicates a good fit of the model. R² can be used to compare experiment outcomes to expected models. For BT, BP, BSFC, CO₂, CO, NO_x, and HC, the corresponding R² values are 99.99%, 99.99%, 99.80%, 99.97%, 94.15%, 99.85%, and 99.64%. In comparison to analytical results, these values show a high degree of precision and are very close to 1. The P-value can be used to assess the model's validity. For any given model, a P-value of less than 0.05 indicates statistical significance, suggesting a departure from the null hypothesis. In contrast, a P-value greater than 0.05 suggests that the model does not possess significance. Furthermore, the ANOVA results indicate that higher F-values further substantiate the model's significance (Ramachandran, Krishnaiah, Perumal Venkatesan, et al., 2023). The ANOVA findings regarding the variables BP, BSFC, and BT are detailed in Table 4.9. Additionally, Table 4.10 presents the ANOVA results pertaining to the emission characteristics.

A summary of the important analytical measures utilized to evaluate the generated response surface model's validity and reliability is given in Table 4.11. One of the main metrics is the R², which measures the accuracy and goodness of fit of the model by showing how well it explains the variation shown in the experimental data. A higher R² value typically implies that the model closely aligns with the actual data points. Furthermore, the variance between the adj-R² and the pred-R² provides information about the predictive power and resilience of the model. The model's generalizability is confirmed by a minimal difference between these two values, which shows that it consistently performs well on both training and validation datasets. Another significant statistic

in the table that shows the degree of data dispersion around the mean answer is the standard deviation (Std. Dev). Lower standard deviation values, which show that the model predictions are reliable and closely grouped, support the model's accuracy in predicting the output response under different input conditions.

$$\begin{aligned} \text{BT (Nm)} = & 4.196 - 0.04212A - 0.00204B - 0.00119C + 0.000978A * A + 0.000015B * \\ & B + 0.000009 C * C + 0.000017 A * B - 0.000000 A * C + 0.000021 B * C \end{aligned} \quad (4.1)$$

$$\begin{aligned} \text{BP (kW)} = & 0.0087 + 0.0285A + 0.000958B + 0.00006C + 0.000047A * A + 0.0000001B * \\ & B + 0.000003 C * C - 0.0000001 A * B - 0.000000 A * C + 0.000004 B * C \end{aligned} \quad (4.2)$$

$$\begin{aligned} \text{BSFC (kg/kWh)} = & 0.6849 - 0.009825A + 0.0002B + 0.000075C + 0.000074A * A - 0.000002B * \\ & B - 0.000003 C * C - 0.000002 A * B + 0.000004 A * C - 0.000001B * C \end{aligned} \quad (4.3)$$

$$\begin{aligned} \text{CO (% vol)} = & 0.0991 - 0.001763A - 0.000193B - 0.000377C + 0.000013A * A - 0.000001B * \\ & B - 0.000001 C * C - 0.000001 A * B + 0.000002 A * C + 0.000001B * C \end{aligned} \quad (4.4)$$

$$\begin{aligned} \text{CO}_2(\% \text{ vol)} = & 2.3038 + 0.02069A + 0.00039B - 0.00223C + 0.00004A * A - 0.000002B * B + \\ & 0.000015 C * C - 0.000038 A * B + 0.000001 A * C + 0.000004B * C \end{aligned} \quad (4.5)$$

$$\begin{aligned} \text{HC (ppm)} = & 103.5 - 2.775A + 0.0181B - 0.0354C + 0.025833A * A - 0.000463B * B - \\ & 0.000208 C * C - 0.00125A * B - 0.000625 A * C + 0.0000001B * C \end{aligned} \quad (4.6)$$

$$\begin{aligned} \text{NO}_x \text{ (ppm)} = & -149 + 8.231A + 0.304B - 0.175C - 0.04406A * A - 0.00014B * B + 0.00406C * \\ & C - 0.00542A * B - 0.00125 A * C - 0.00417B * C \end{aligned} \quad (4.7)$$

Table 4.8 Experimental matrix with the results of the engine performance and emission

Run	Variables			Results						
	load	TiO ₂	CuO	BT	BP	BSFC	CO	CO ₂	HC	NO _x
1	80	90	40	7.18	2.69	0.371	0.025	3.90	32	193
2	40	90	40	4.11	1.32	0.409	0.031	3.03	25	98
3	80	60	60	7.13	2.66	0.379	0.029	3.99	36	204
4	60	60	40	5.19	1.94	0.366	0.024	3.51	22	170
5	60	30	60	5.17	1.92	0.368	0.028	3.55	24	175
6	40	30	40	4.05	1.25	0.415	0.035	3.11	31	107
7	40	60	60	4.08	1.30	0.411	0.032	3.05	27	101
8	80	30	40	7.08	2.62	0.382	0.031	4.07	41	215
9	40	60	20	4.06	1.28	0.413	0.034	3.08	29	105
10	60	60	40	5.20	1.96	0.365	0.025	3.52	22	172
11	60	60	40	5.21	1.95	0.367	0.025	3.51	23	171
12	80	60	20	7.11	2.64	0.374	0.027	4.02	39	210
13	60	30	20	5.15	1.90	0.369	0.033	3.59	26	179
14	60	90	60	5.31	2.01	0.356	0.020	3.45	18	161
15	60	90	20	5.24	1.98	0.360	0.022	3.48	20	175

Table 4.9 ANOVA for engine performance

Source	BT		BP		BSFC	
	F-value	P-value	F-value	P-value	F-value	P-value
Model	9479.37	0.0001	5541.92	0.0001	280.34	0.0001
Load (A)	82688.89	0.0001	49686	0.0001	1050.21	0.0001
TiO ₂ NPs (B)	84.50	0.0001	160.17	0.0001	75.21	0.0001
CuO NPs (C)	9.39	0.028	13.50	0.014	0.21	0.667
A*A	2512.03	0.0001	17.31	0.009	1350.22	0.0001
B*B	3.10	0.138	0.08	0.793	2.91	0.149
C*C	0.23	0.651	0.08	0.793	2.91	0.149
A*B	1.78	0.240	0.00	1.00	2.60	0.168
A*C	0.00	1.00	0.00	1.00	5.10	0.073
B*C	2.78	0.156	0.33	0.589	0.94	0.377

Table 4.10 ANOVA for engine emissions

Source	CO		CO ₂		HC		NO _x	
	F – value	P – value	F – value	P – value	F – value	P – value	F – value	P – value
Model	8.93	0.013	1645.23	0.0001	153.31	0.0001	369.27	0.0001
A	14.78	0.012	1539.54	0.0001	335.17	0.0001	3082.50	0.0001
B	31.07	0.003	223.52	0.0001	188.53	0.0001	43.81	0.001
C	1.81	0.236	17.85	0.008	20.95	0.006	14.31	0.013
A*A	30.56	0.003	7.82	0.038	815.70	0.0001	167.44	0.0001
B*B	0.32	0.596	0.09	0.78	1.33	0.302	0.01	0.930
C*C	0.71	0.584	1.06	0.35	0.05	0.827	1.42	0.286
A*B	0.30	0.610	17.11	0.009	4.66	0.083	6.17	0.056
A*C	1.18	0.327	0.00	1.00	0.52	0.504	0.15	0.718
B*C	0.67	0.452	0.21	0.665	0.00	1.00	3.65	0.114

Table 4.11 Evaluation of the ANOVA model

Parameter	BT	BP	BSFC	CO	CO ₂	HC	NO _x
R ²	99.99	99.99	99.80	94.15	99.97	99.64	99.85
Adj-R ²	99.98	99.97	99.45	83.16	99.91	98.99	99.58
Pred-R ²	99.92	99.91	97.29	9.49	99.51	95.59	97.72
Std. Dev	0.015	0.0087	0.00155	0.0018	0.011	0.695	2.617

4.2.2. Optimization of engine performance analysis

4.2.2.1 Brake Torque

Brake torque refers to the torque available at the engine crankshaft (or input shaft) after accounting for internal losses such as friction. The ANOVA results presented in Table 4.9 indicate that all three main factors (A, B, and C) significantly influence brake torque, as evidenced by their very low P-values (0.001, 0.0001, and 0.028, respectively) along with high F-values. Among these, factor A² shows the strongest influence, with an exceptionally large F-value of 2512.03 and a P-value of 0.0001, making it the most dominant factor affecting BT. In contrast, terms B², C², and the interaction effects AB, AC, and BC exhibit P-values greater than 0.05, suggesting that their contributions to brake torque are statistically insignificant.

Fig.4.8 and Fig.4.9 visually represent how BT varies with engine load and TiO₂ and CuO NPs, with values ranging from 5.11 Nm to 7.18 Nm. The increase in brake torque with higher engine load and TiO₂ and CuO NPs concentration can be attributed to enhanced combustion efficiency and improved mechanical performance. At elevated engine loads, the greater fuel-air density and cylinder pressure lead to more complete combustion, while TiO₂ and CuO act as combustion catalysis, promoting faster hydrocarbon oxidation and energy released during the combustion. Furthermore, Fig. 4.10 illustrates that adding TiO₂ and CuO NPs can be beneficial for increasing the brake torque, predominantly under higher load conditions.

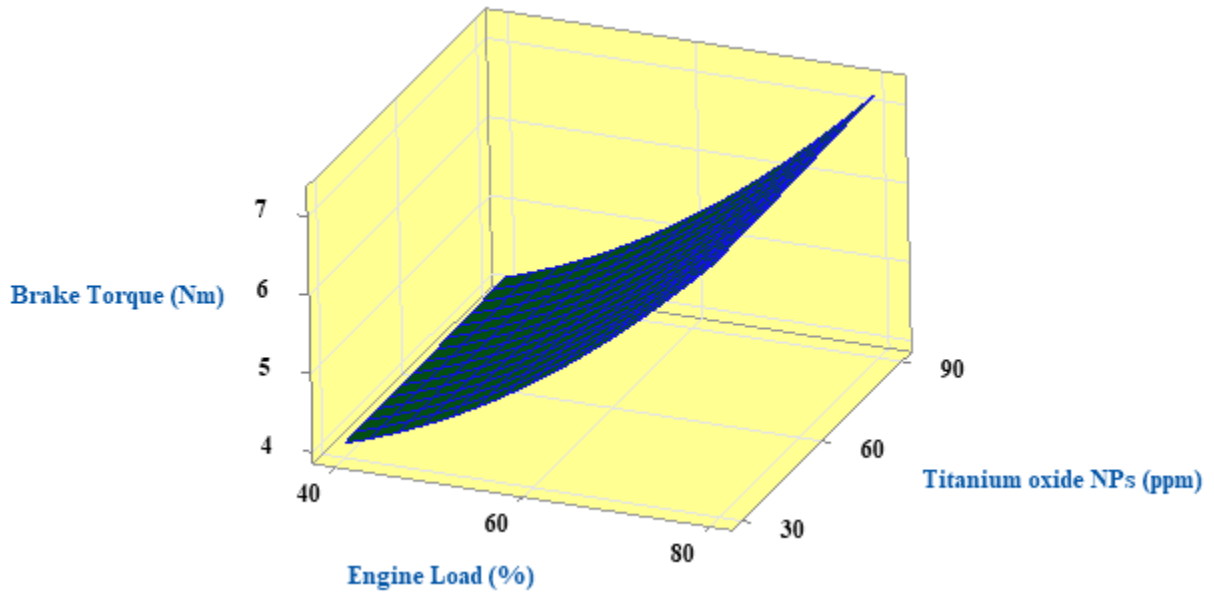


Figure 4.8 Surface plot of BT vs engine load and TiO₂ NPs

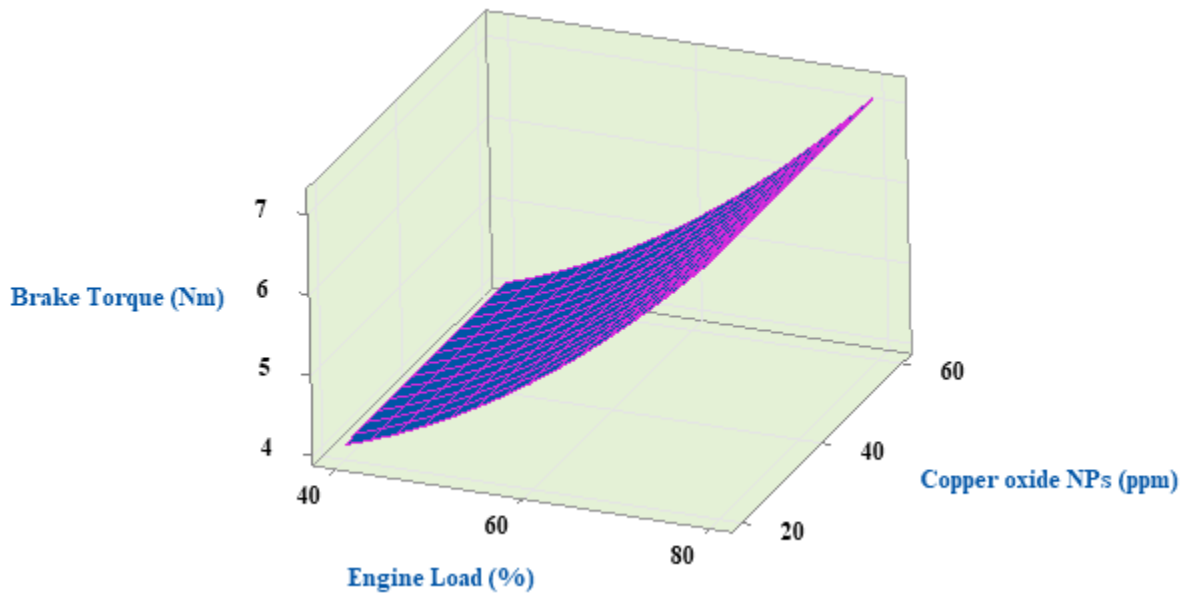


Figure 4.9 Surface plot of BT vs engine load and CuO NPs

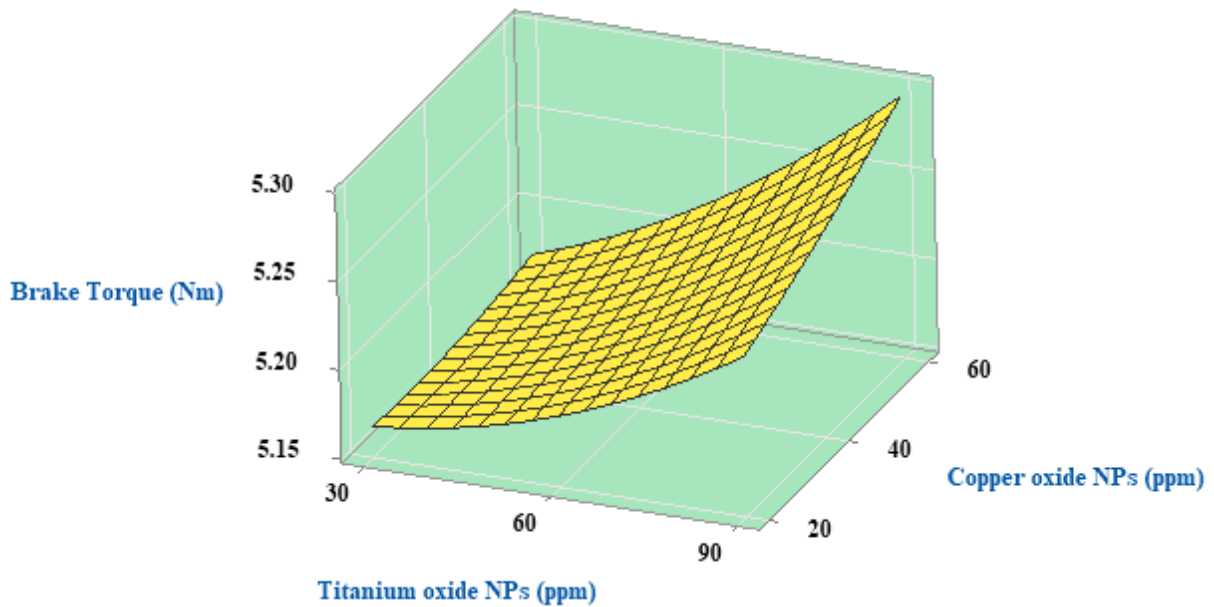


Figure 4.10 Surface plot of BT vs TiO₂ and CuO NPs

4.2.2.2. Brake Power (BP)

BP represents the actual usable power delivered by an engine at its output shaft, accounting for energy losses from friction and other internal mechanical resistances. The ANOVA results in Table 4.9 demonstrate that factors A, B, and C all exert statistically significant effects on BP, as indicated by their extremely low P – values (0.0001 for each) and substantial F – values of 49,689, 160.17, and 13.50, respectively. Among these, engine load (factor A) shows the most pronounced influence on BP, as higher loads enable greater fuel combustion rates, thereby increasing power output. This is further supported by the significant quadratic effect of engine load (A^2 term), which shows an F-value of 17.31 and a P – value of 0.009. In contrast, the quadratic terms of other factors (B^2) and their interaction effects (AB, AC, BC) demonstrate negligible influence on BP.

Fig.4.11 and Fig.4.12 surface plots illustrate how brake power output varies with changes in engine load and the concentration of TiO₂ and CuO NPs. As engine load increases from 40% and 80%, the brake power also rises, which is a typical trend due to the higher fuel input and combustion energy required to meet the increased load demand. Similarly, increasing the TiO₂ NP concentration from 30 ppm to 90 ppm and CuO NP concentration from 20 ppm to 60 ppm also results in a noticeable improvement in brake power. The combined effect of higher engine load and TiO₂ and CuO NPs concentration shows a synergistic enhancement in engine performance.

Fig 4.13 shows that TiO_2 and CuO NPs play a role in improving combustion efficiency, likely promoting more complete fuel oxidation or enhancing thermal properties. Overall, the figure indicates that adding TiO_2 and CuO NPs can be beneficial for increasing the brake power output of an engine, particularly under higher load conditions.

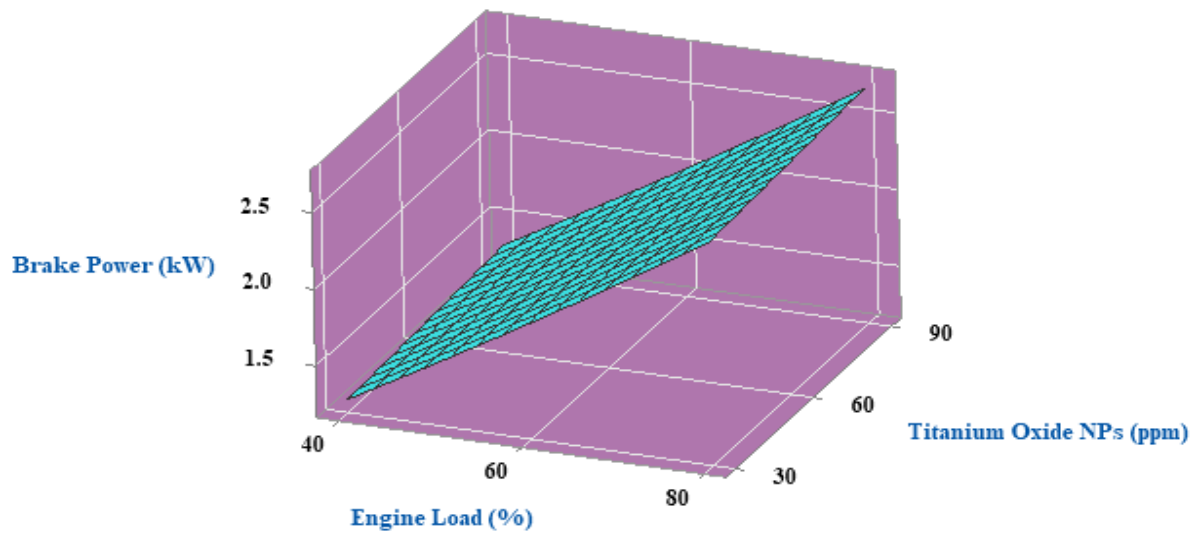


Figure 4.11 Surface plot of BP vs engine load and TiO_2 NPs

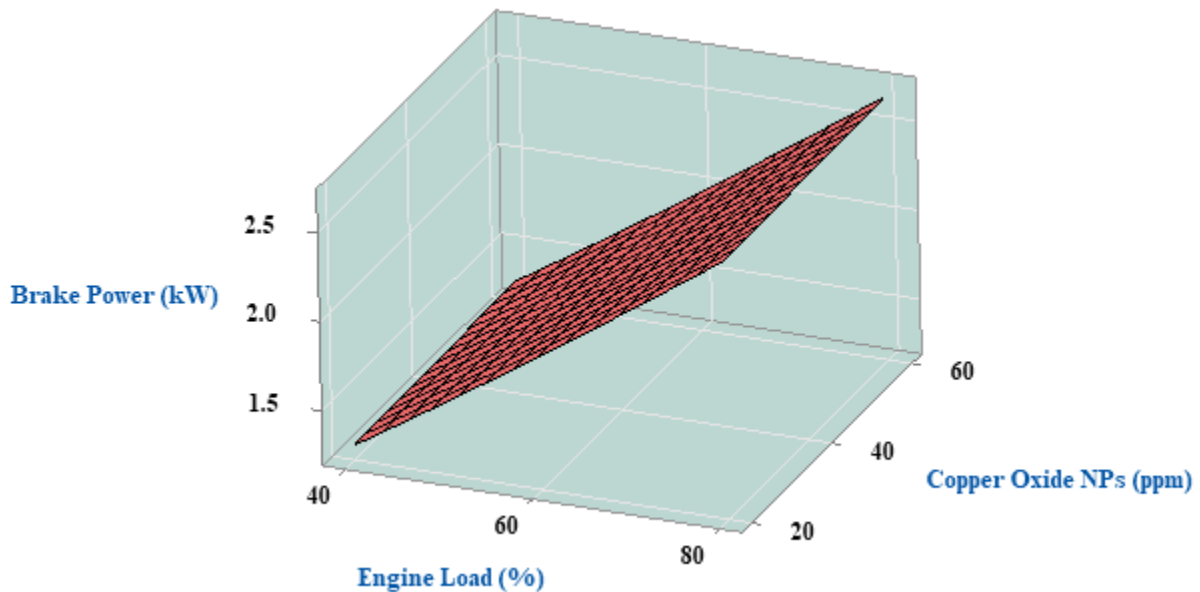


Figure 4.12 Surface plot of BP vs engine load and CuO NPs

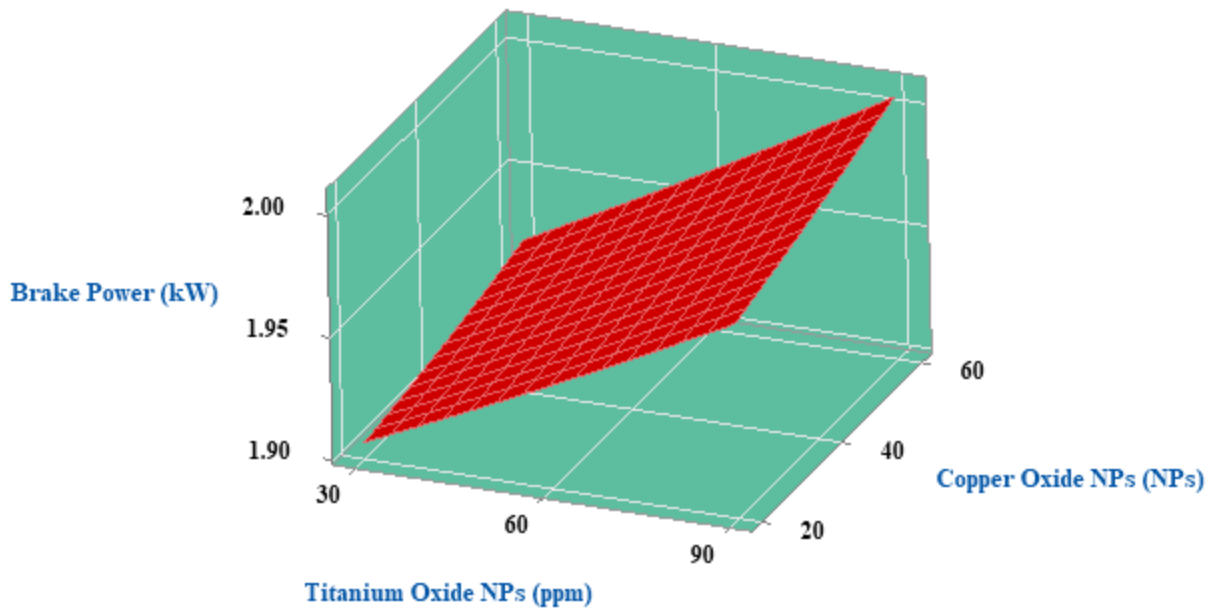


Figure 4.13 Surface plot of BP vs TiO₂ and CuO NPs

4.2.2.4. Brake specific energy consumption (BSFC),

BSFC is a key indicator of engine efficiency, representing the amount of fuel consumed to generate a unit of brake power. It is primarily governed by the fuel's energy content (heating value) and its rate of consumption, which makes BSFC especially useful for evaluating and comparing fuels with differing characteristics, such as heating value and cetane number. The statistical results presented in Table 4.9 indicate that BSFC is significantly affected by the main factors A and B, with factor A exerting the most pronounced influence, as reflected by its high F-value of 1050.21. The quadratic term A² (F-value=1350.22) and factor B (F-value=75.21) also show substantial impacts, while B², C², and all interaction (AB, AC, BC) prove statistically insignificant. Fig.4.14 and Fig.4.15 illustrate how BSFC varies with engine load and nanoparticle concentrations, demonstrating that higher loads and increased TiO₂/CuO NPs concentrations lead to improved efficiency, with the optimal BSFC of 0.356 kg/kWh achieved at 80% engine load.

The impact of TiO₂ and CuO NPs on BSFC is displayed in Figure 4.16. BSFC is a crucial measure that shows how much fuel is required for each unit of power generated. As the concentrations of TiO₂ and CuO NPs rise in the plot, BSFC falls. The downward trend in BSFC with increasing NPs concentrations suggests that the combined use of TiO₂ and CuO NPs improves the combustion process, possibly by acting as a catalyst or enhancing thermal conductivity and atomization. This

enhanced combustion leads to more complete fuel burning and better energy conversion efficiency, resulting in reduced fuel consumption for the same power output. Additionally, Fig.4.16 highlights the potential of using a dual-nanoparticle blend to optimize fuel efficiency in engine applications.

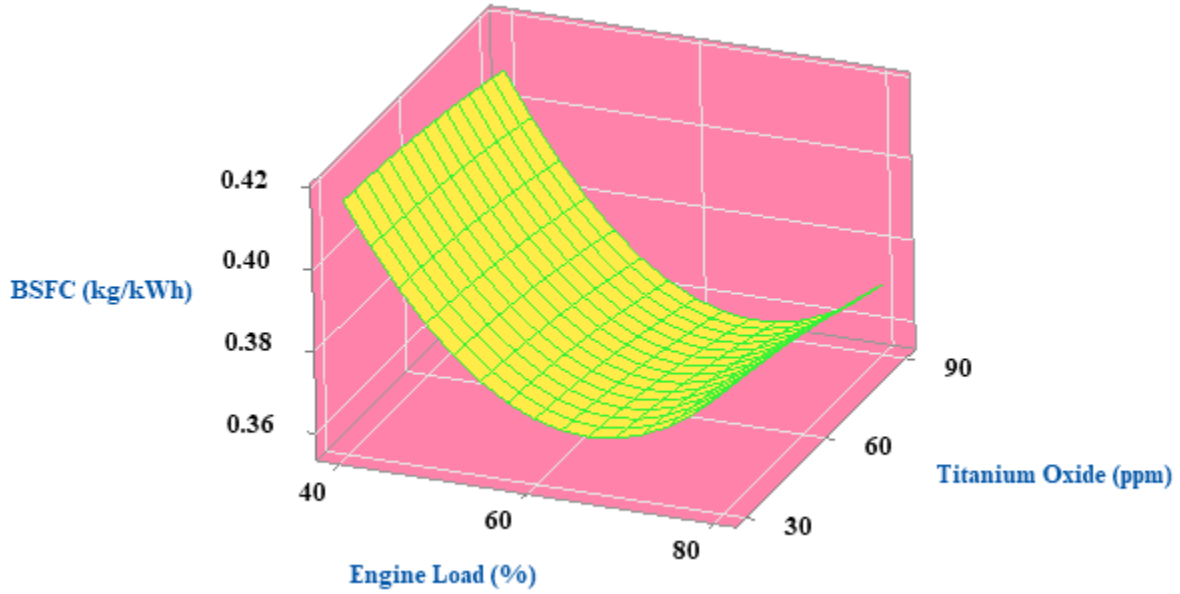


Figure 4.14 Surface plot of BSFC vs engine load and TiO₂ NPs

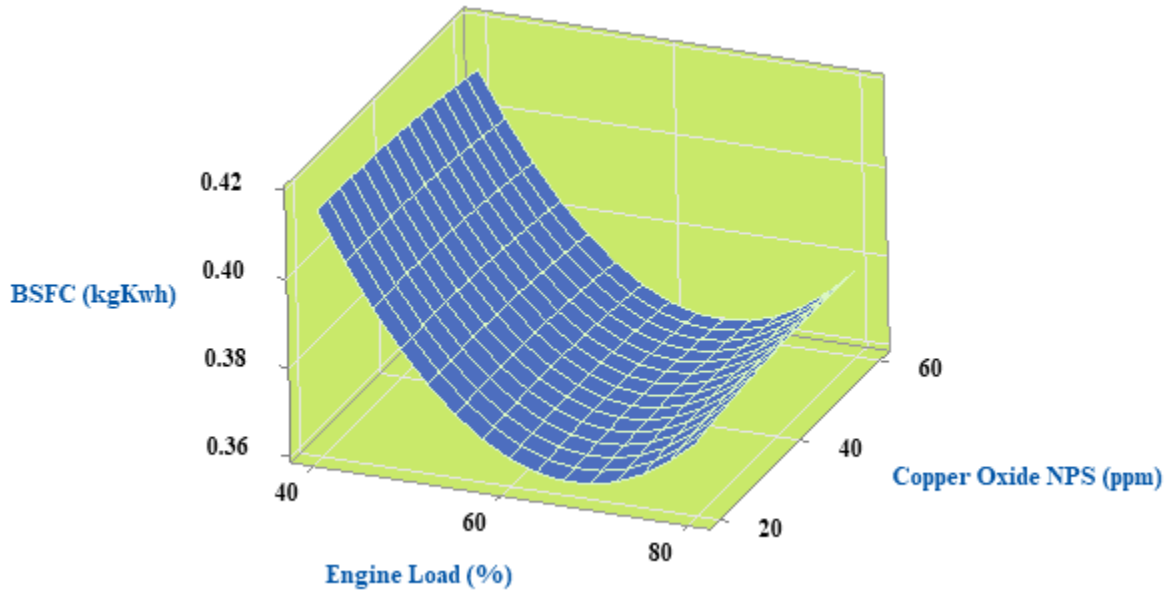


Figure 4.15 Surface plot of BSFC vs engine load and CuO NPs

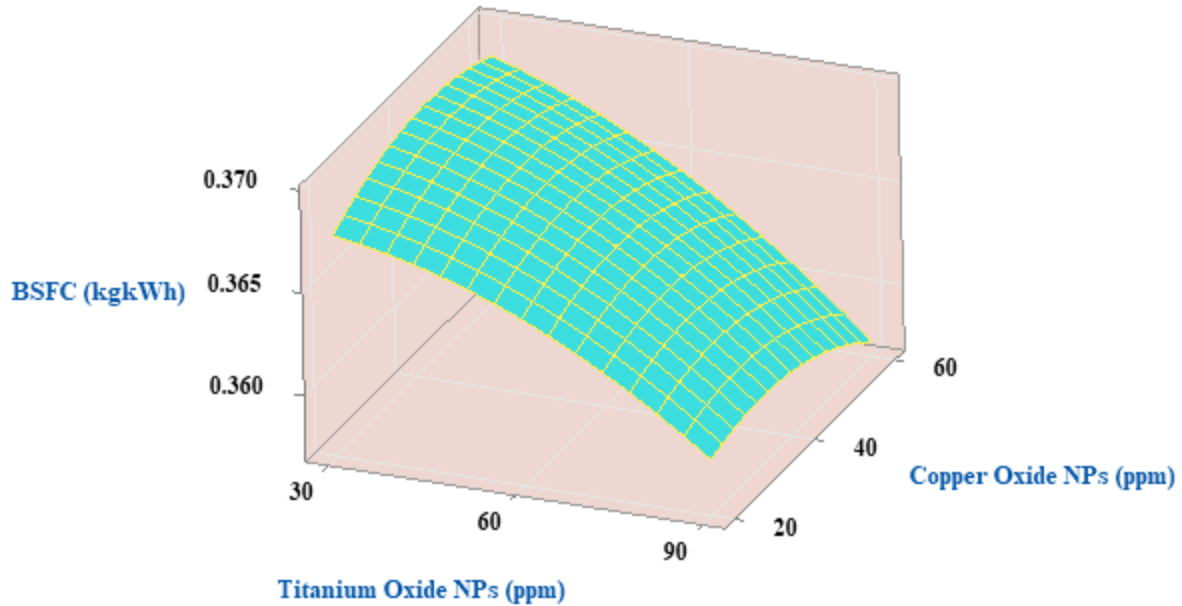


Figure 4.16 Surface plot of BSFC vs TiO₂ and CuO NPs

4.2.3. Optimization of engine exhaust emission analysis

4.2.3.1. Carbon monoxide

With P-values of 0.012 and 0.003, respectively, and F-values of 14.18 for A and 31.07 for B, showing strong linear effects, the ANOVA analysis from Table 4.10 shows that the A and B terms had the greatest impact on CO emissions. While B₂, C₂, and all interactions (AB, AC, and BC) are statistically insignificant, the quadratic term A₂ (F-value=30.56) likewise exhibits significant effects.

Figures 4.17 and 4.18 illustrate how engine load, TiO₂, and CuO NPs affect carbon monoxide emissions. Carbon monoxide emissions decrease as engine load and NPs increase. The plots suggest that the combination of higher engine loads and NPs contributes to lower CO output, highlighting their synergistic effect. Additionally, Figure 4.19 shows the dual inclusion of TiO₂ and CuO NPs hints at their combined catalytic potential in CO emission reduction. The plot implies that both types of NPs may contribute to lower CO emissions, through their individual or synergistic effects. Copper oxide is known for its oxidation-promoting properties, while titanium oxide may enhance thermal stability and catalytic activity. The decreasing CO trend across increasing engine loads suggests that these NPs may further optimize combustion when combined with higher operational loads.

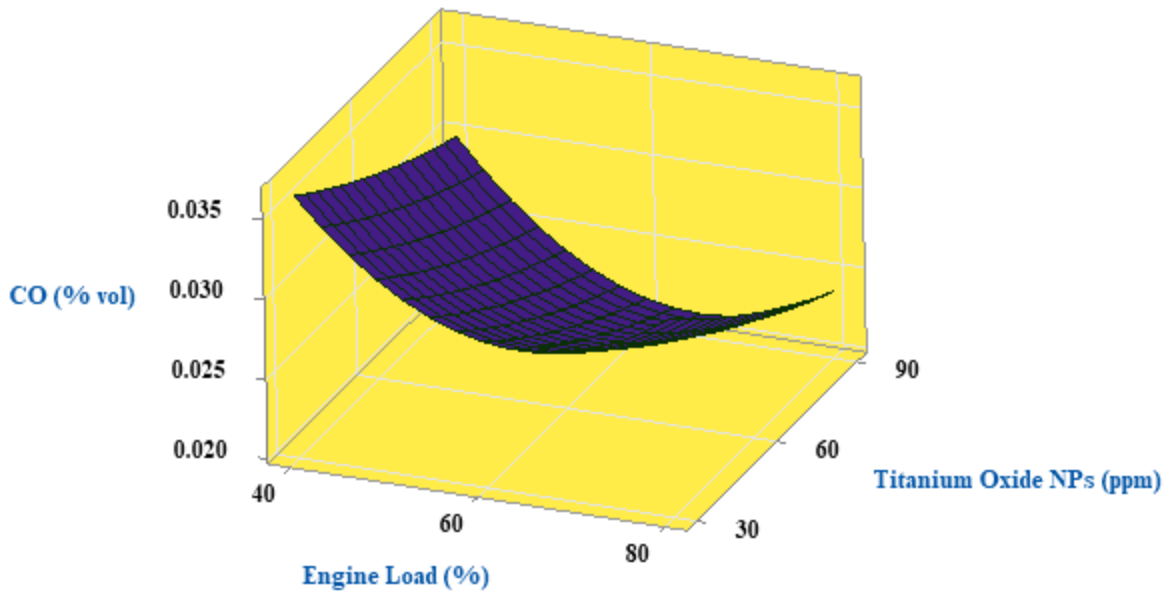


Figure 4.17 Surface plot of CO vs engine load and TiO₂ NPs

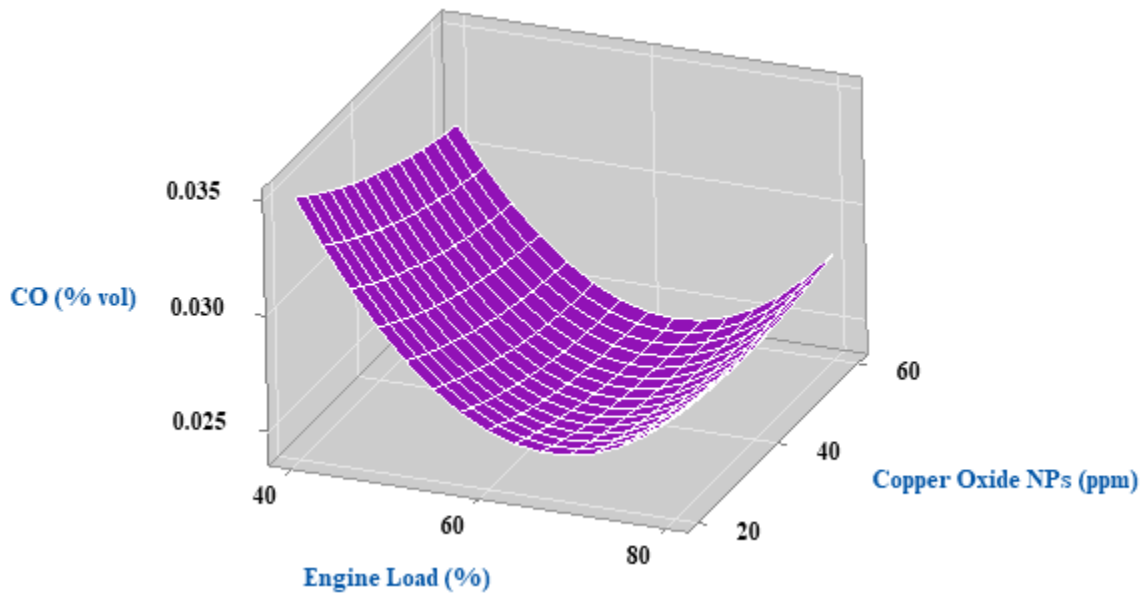


Figure 4.18 Surface plot of CO vs engine load and CuO NPs

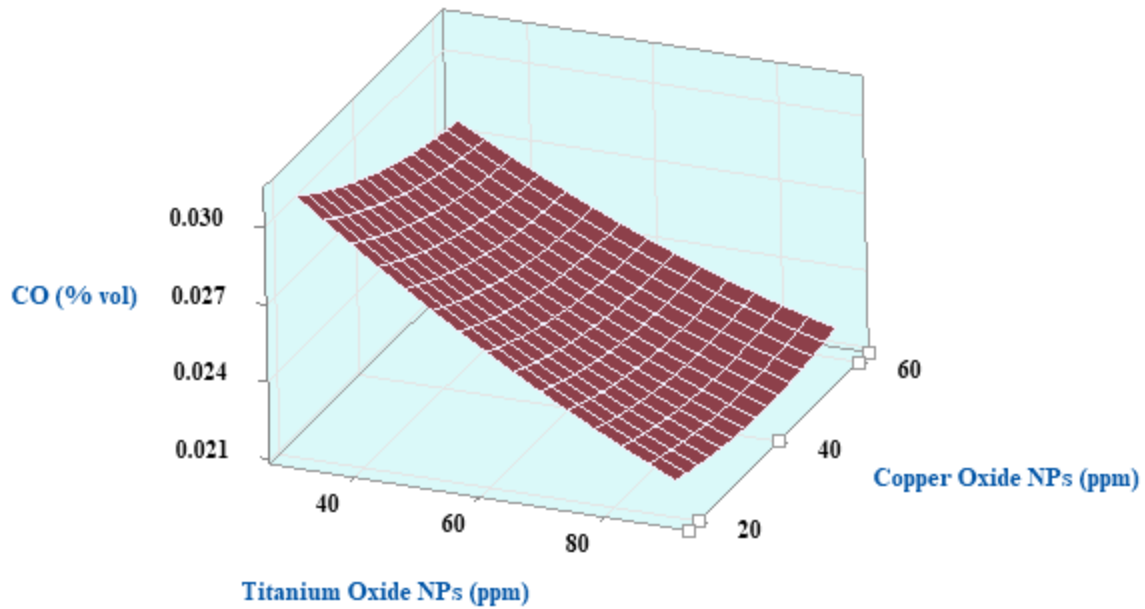


Figure 4.19 Surface plot of CO vs TiO₂ and CuO NPs

4.2.3.2. Carbon dioxide Emission

With P-values of 0.0001, 0.0001, and 0.008, respectively, and an F-value of 1539.54 for A, 223.52 for B, and 17.85 for C, the ANOVA analysis from Table 4.10 shows that the terms A, B, and C had the greatest impact on CO₂ emissions. The quadratic term A² (F-value=7.82) and interaction term AB (F-value=17.11) also show substantial impacts, while B², C², and interaction (AC and BC) prove statistically insignificant.

Fig 4.20 and Fig.4.21 illustrate the relationship between CO₂ and input factors (engine load, TiO₂, and CuO nanoparticle). The plots likely depict how CO₂ emissions change as the engine load increases. At lower engine loads (40%), the CO₂ concentration is relatively low, around 3.03 % vol. As engine load rises to 80%, the CO₂ levels increase significantly, reaching 4.07 % vol. This trend suggests that higher engine loads lead to greater fuel combustion, resulting in elevated CO₂ emissions. Fig 4.22 examines the relationship between CO₂ emission and the effect of TiO₂ and CuO NPs. It suggests that variations in nanoparticle concentrations influence CO₂ emissions, a higher concentration of TiO₂ and CuO NPs reduces CO₂ levels, possibly due to the catalytic or combustion modifying effect of NPs.

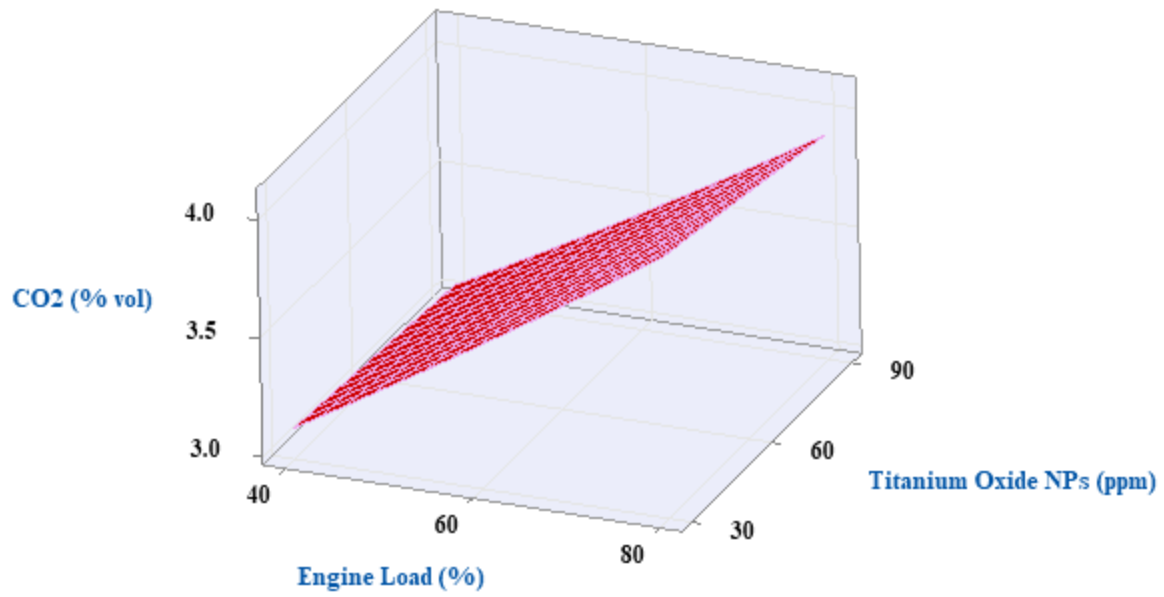


Figure 4.20 Surface plot of CO₂ vs engine load and TiO₂ NPs

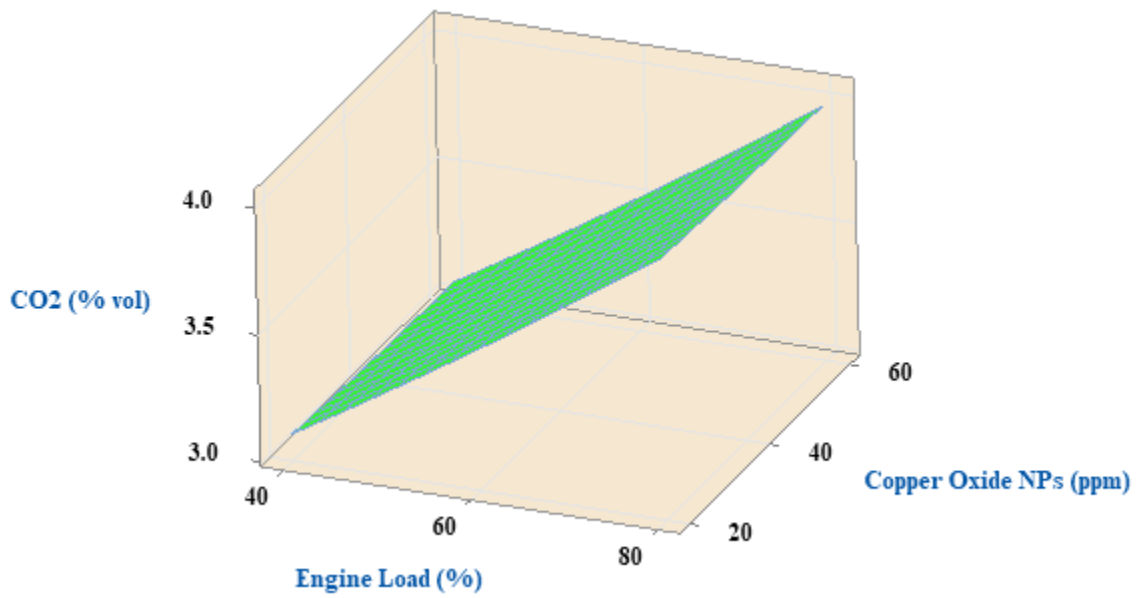


Figure 4.21 Surface plot of CO₂ vs engine load and CuO NPs

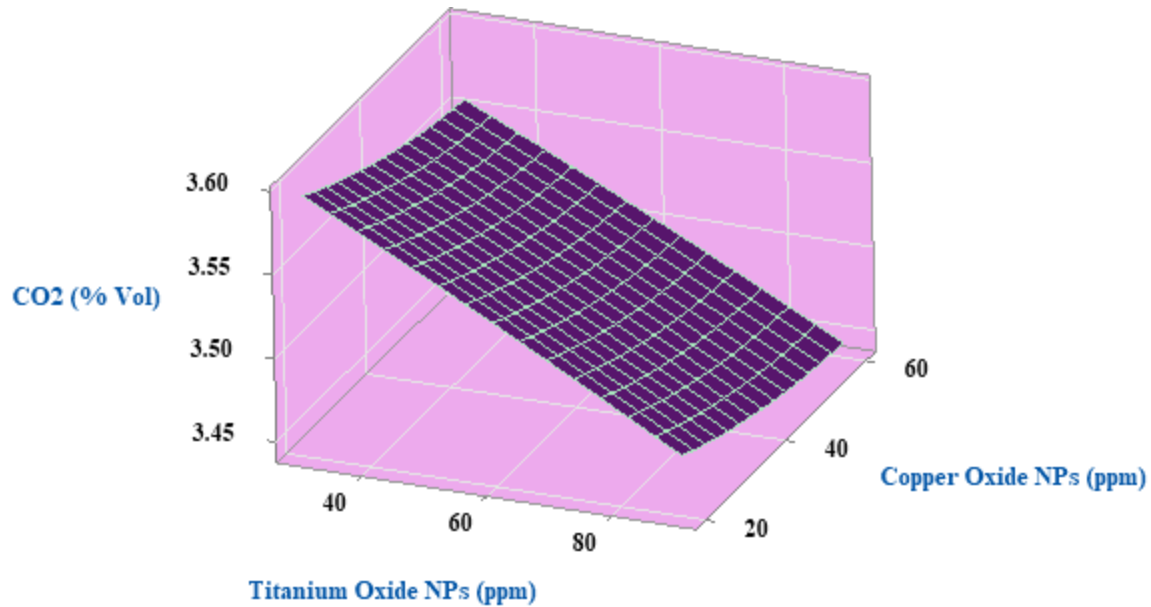


Figure 4.22 Surface plot of CO₂ vs TiO₂ and CuO NPs

4.2.3.3. Hydrocarbons Emission

The ANOVA results summarized in Table 4.10 show that the main factors A, B, and C have a statistically significant effect on HC emissions, as reflected by their very low P-values of 0.0001, 0.0001, and 0.006, respectively. Their corresponding F-values 335.17 for factor A, 188.53 for factor B, and 20.95 for factor C confirm the presence of strong linear influences. In addition, the quadratic term A² exhibits a pronounced effect on HC emissions, with a high F-value of 815.70. In contrast, the quadratic terms B² and C², along with all interaction terms (AB, AC, and BC), have P-values exceeding the significance threshold, indicating that their effects on HC emissions are not statistically significant.

Figures 4.23 and 4.24 show how engine load, TiO₂, and CuO NPs affect hydrocarbon emissions. Hydrocarbon emissions decrease as engine load and NPs increase. The figures demonstrate the synergistic effect of NPs and increased engine loads, suggesting that the latter reduces HC output. Furthermore, the joint inclusion of TiO₂ and CuO NPs in Figure 4.25 suggests that they may have a combined catalytic capability for reducing HC emissions. According to the plot, both kinds of NPs may have a role in reducing HC emissions, either alone or in combination. While titanium oxide may improve thermal stability and catalytic activity, copper oxide is well-known for its capacity to promote oxidation. These NPs may improve combustion even further, as indicated by the declining HC trend as engine loads increase.

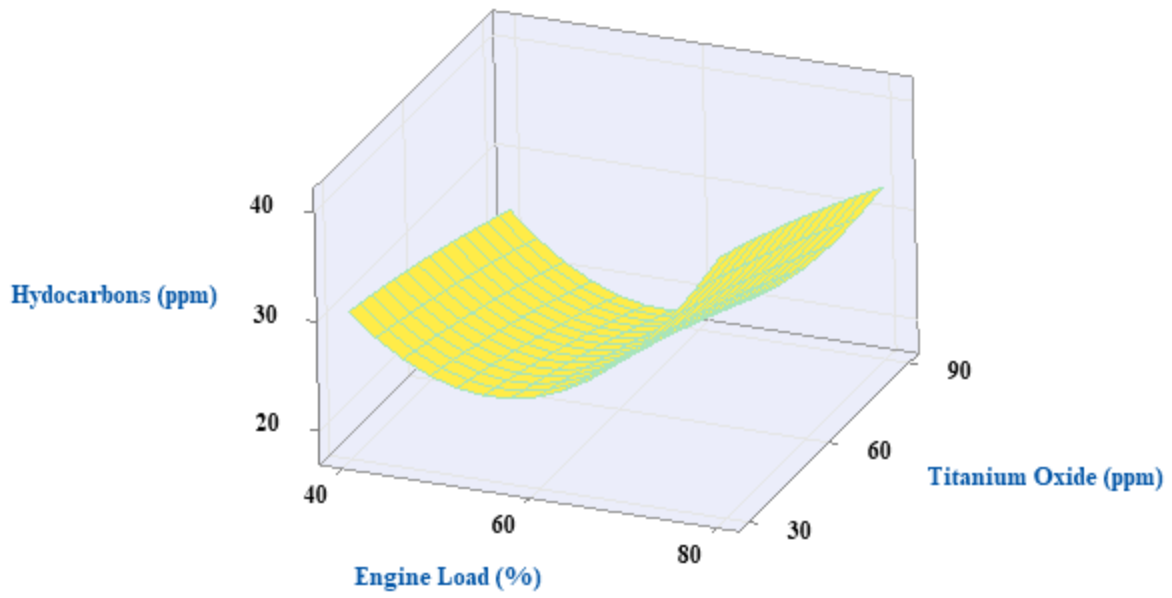


Figure 4.23 Surface plot of HC vs engine load and TiO₂ NPs

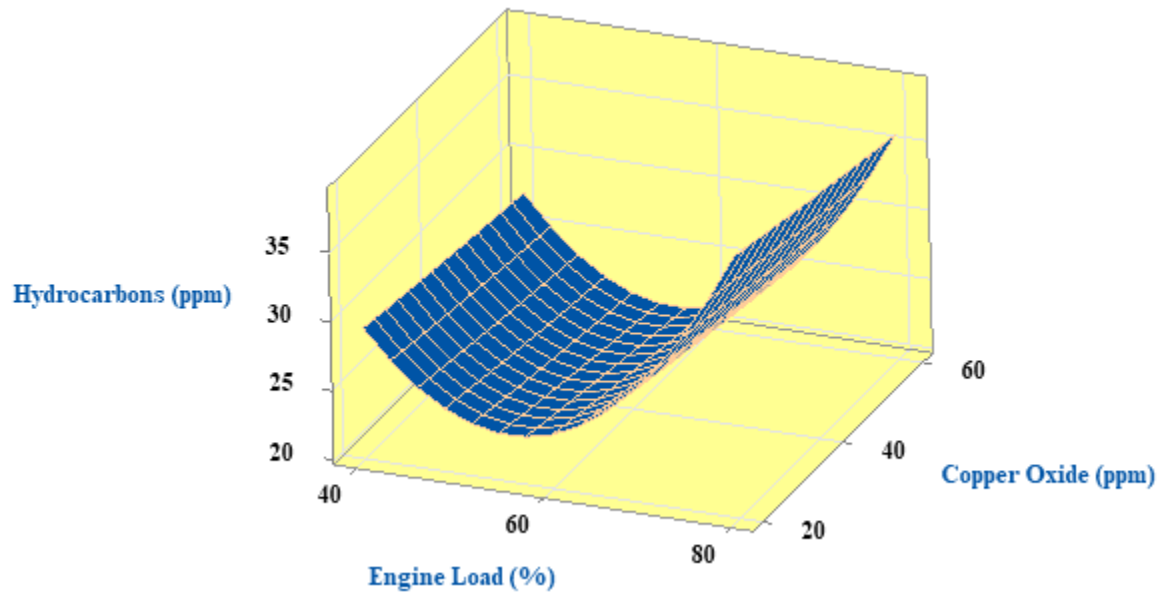


Figure 4.24 Surface plot of HC vs engine load and CuO NPs

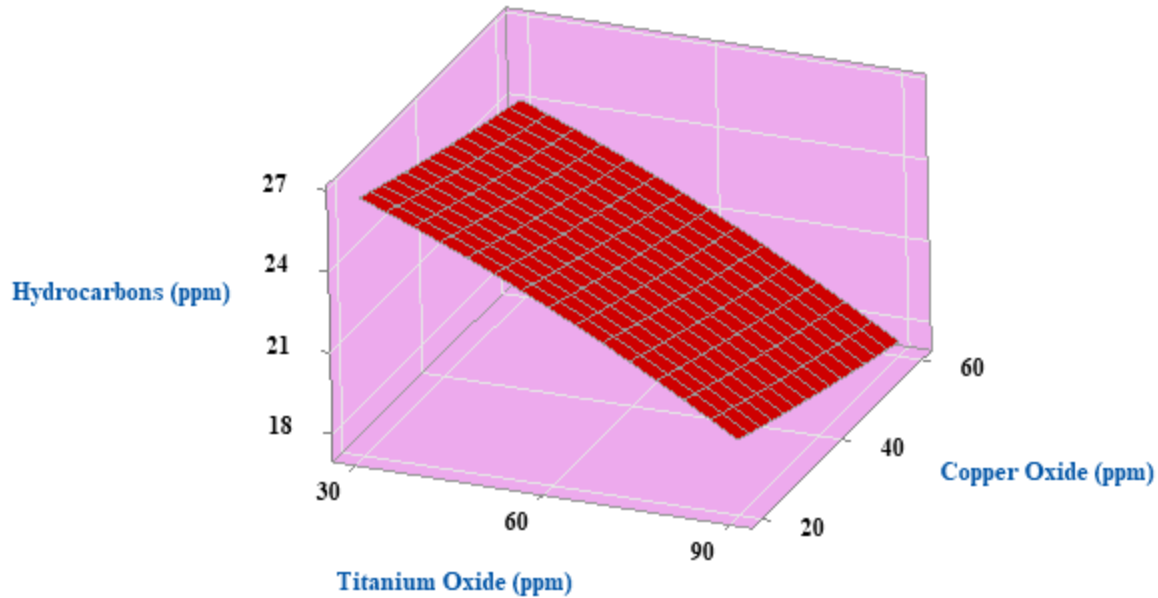


Figure 4.25 Surface plot of HC vs TiO₂ and CuO NPs

4.2.3.4. Nitrogen Oxides Emission

The ANOVA results presented in Table 4.10 reveal that the primary factors A, B, and C have a significant effect on NO_x emissions, as evidenced by their low P-values of 0.0001, 0.0001, and 0.013, respectively. The corresponding F-values 3082.5 for factor A, 43.81 for factor B, and 14.31 for factor C indicate strong linear relationships, with factor A exerting the most dominant influence on NO_x formation. The quadratic term A² (F-value=167.44) also shows substantial impacts, while B², C² and all interactions (AB, AC, and BC) prove statistically insignificant.

Fig 4.26 and Fig.4.27 illustrates the relationship between NO_x and input factors (engine load, TiO₂, and CuO NPs). The plots likely depict how NO_x emissions change as the engine load increases. At lower engine loads (40%), the NO_x concentration is relatively low, around 98 ppm. As engine load rises to 80%, the NO_x levels increase significantly, reaching 215 ppm. This trend suggests that higher engine loads lead to greater fuel combustion, resulting in elevated NO_x emissions. Fig 4.28 examines the relationship between NO_x emission and the effect of TiO₂ and CuO NPs. It suggests that variations in nanoparticle concentrations influence NO_x emissions, higher concentration of TiO₂ and CuO NPs reduces NO_x levels, possibly due to the catalytic or combustion modifying effect of NPs.

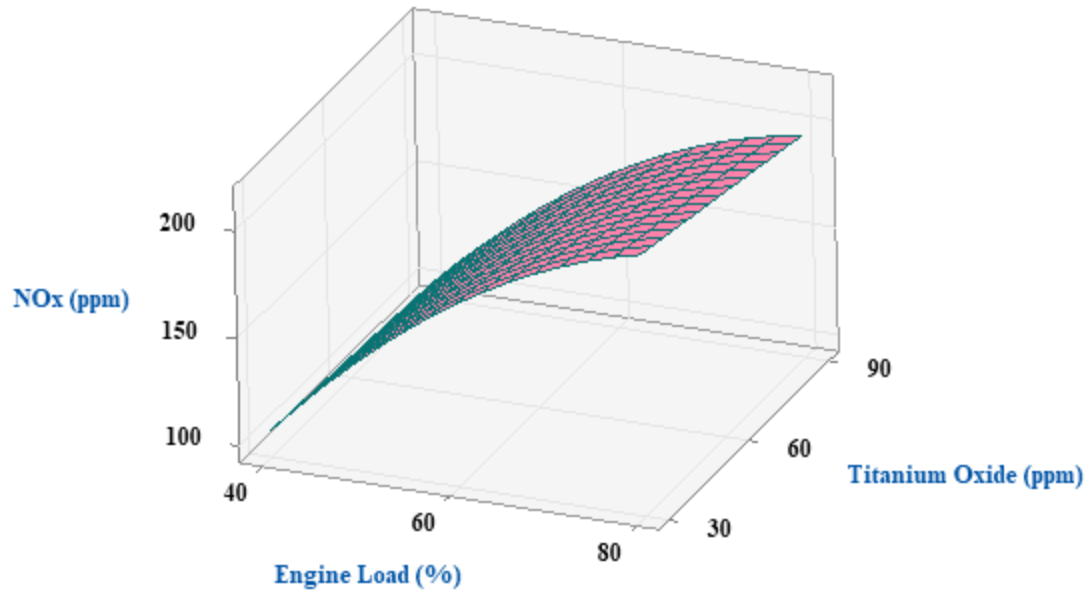


Figure 4.26 Surface plot of NOx vs engine load and TiO₂ NPs

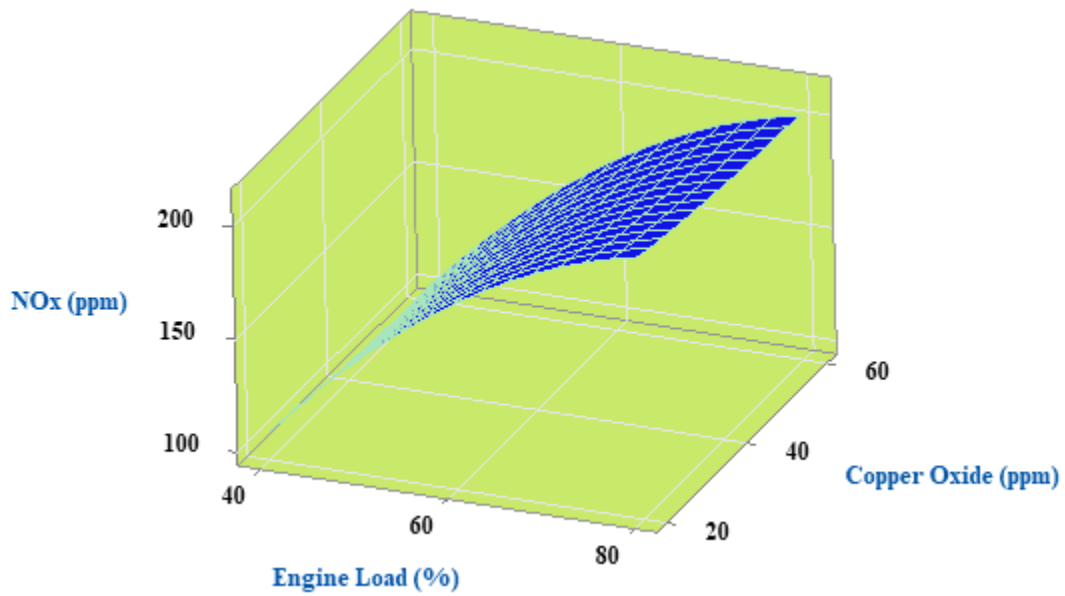


Figure 4.27 Surface plot of NOx vs engine load and CuO NPs

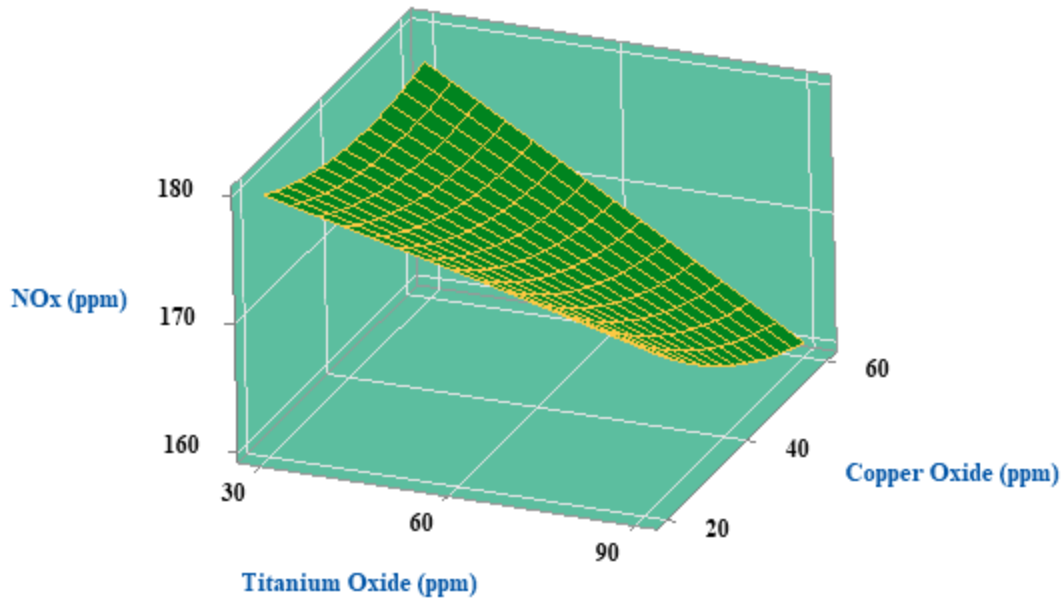


Figure 4.28 Surface plot of NO_x vs TiO₂ and CuO NPs

4.3. Optimizer for response surface methodology

In order to improve compression ignition engine's performance characteristic while reducing harmful emissions, this study used a numerical optimization approach. By utilizing statistical software and computational techniques, the research aimed to optimize a set of seven variables. The optimization strategy prioritized increasing brake power and brake torque, while simultaneously aiming to reduce BSFC, CO, CO₂, HC, and NO_x.

Table 4.12 presents the optimization framework, which involved adjusting key input parameters—namely engine load, TiO₂ nanoparticle concentration, and CuO nanoparticle concentration within specified ranges defined by the RSM model. The RSM optimizer identified the optimal conditions at 63% engine load, 90 ppm TiO₂, and 60 ppm CuO. Under these settings, the engine achieved a BT of 5.54 Nm and a BP of 2.11 kW, along with a BSFC of 0.356 kg/kWh. Emission outputs were also minimized, with CO₂ at 3.514 %vol, CO at 0.022 %vol, NO_x at 167 ppm, and HC at 18 ppm. Figure 4.29 shows the response optimization for performance and emission characteristics. These results highlight the significant impact of engine load, TiO₂, and CuO NPs on both performance and emission characteristics.

Table 4.12 Optimization setup

Response	Upper limit	Lower limit	Goal
BSFC (kg/kWh)	0.415	0.356	Minimize
NOx (ppm)	215	98	Minimize
CO ₂ (%vol.)	4.07	3.03	Minimize
CO (%vol.)	0.035	0.02	Minimize
HC (ppm)	41	18	Minimize
BT (Nm)	7.18	4.05	Maximize
BP (kW)	2.69	1.25	Maximize

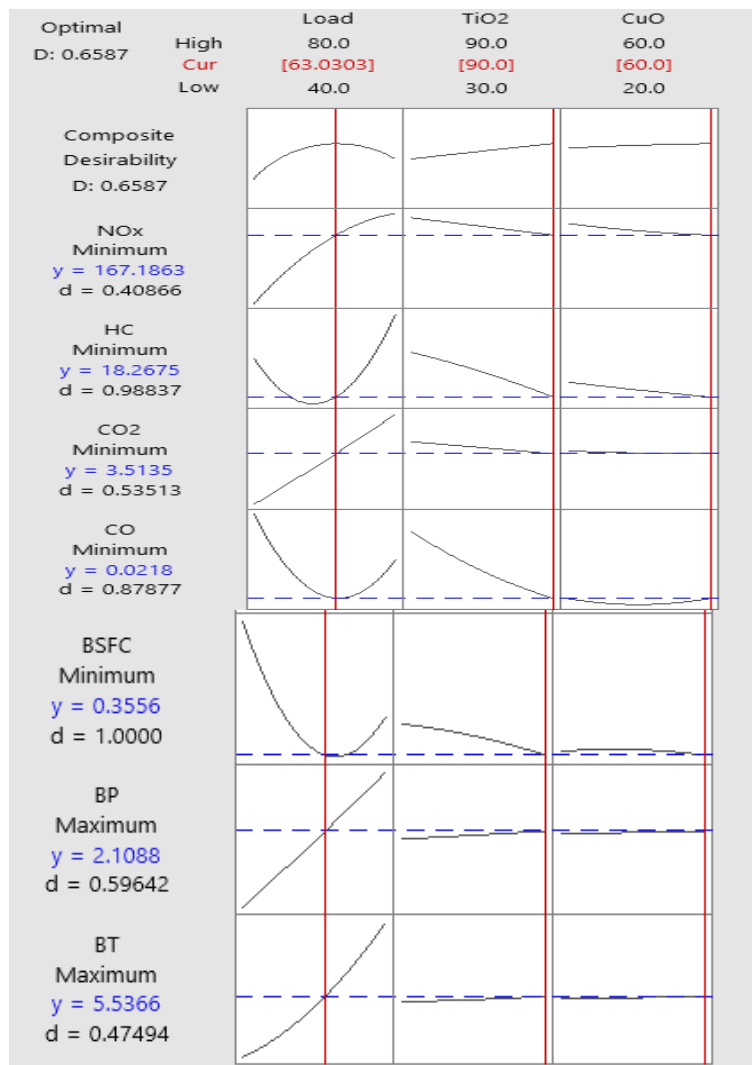


Figure 4.29 Response optimization for performance and emission characteristics

CHAPTER 5

CONCLUSION AND RECOMMENDATION

5.1. Conclusions

The purpose of this study was to examine how metal oxide NPs additions and diesel-methanol fuel blends affected the emissions and performance of CI engines, with an emphasis on statistical optimization of these parameters. All experimental studies were carried out in the Department of Mechanical Engineering laboratory at AASTU. An ultrasonicator cleaner was used during the fuel blend preparation process to guarantee that the TiO₂ and CuO NPs were evenly distributed throughout the methanol-diesel blends, with the use of CTAB as a surfactant to avoid agglomeration. Pure diesel (D100), M10, M20, and M30 blends, as well as M10 augmented with different amounts of metal oxide NPs, were among the test fuels.

Among the methanol-diesel blends tested, M10 (10% methanol, 90% diesel) demonstrated the most promising and well-balanced performance. It significantly reduced emissions, especially CO, HC, and NO_x, while maintaining engine power and combustion efficiency comparable to that of standard diesel (D100). Although blends with higher methanol content, such as M20 and M30, further reduced CO₂ and NO_x, they were associated with elevated CO and HC emissions due to methanol's lower cetane number and high L_v, which led to incomplete combustion. Thus, M10 emerged as the optimal compromise between emission reduction and engine stability, offering moderate oxygen enrichment without significantly disrupting combustion dynamics.

A numerical optimization framework based on the BBD of RSM was an essential component of this study. Finding the ideal mix of engine operating conditions and nanoparticle concentrations to maximize performance outputs brake power (BP) and brake torque (BT) while minimizing hazardous emissions (CO, CO₂, HC, and NO_x) and brake specific fuel consumption (BSFC) was the goal. 63% engine load, 90 ppm TiO₂, and 60 ppm CuO were found to be the ideal input parameters by the RSM-based optimization. Under these conditions, the engine achieved a BT of 5.54 Nm, a BP of 2.11 kW, and a BSFC of 0.356 kg/kWh. Emission levels were significantly reduced, with CO₂ at 3.514 %vol, CO at 0.022 %vol, NO_x at 167 ppm, and HC at 18 ppm. Overall, the findings demonstrate that the combined use of TiO₂ and CuO NPs, when properly optimized using a statistical approach, can substantially improve the combustion performance and reduce emissions in CI engines operating with methanol-diesel blends. This integrated strategy offers a

viable pathway toward cleaner and more efficient internal combustion engines, supporting broader efforts in sustainable fuel development and pollution reduction.

5.2. Recommendations and Future Directions

Several recommendations and potential directions for future research are proposed to enhance the applicability and understanding of nanoparticle-assisted diesel-methanol fuel blends in CI engines in light of the experimental results and optimization outcomes reported in this study:

- The current study has demonstrated the immediate benefits of TiO₂ and CuO NPs in reducing pollutants and improving engine efficiency. Further research is suggested to look at the long-term effects on engine components, such as valves, injectors, and piston rings. To ensure the durability and safety of these fuels augmented with NPs during prolonged engine usage, wear, deposits, and lubrication characteristics must be evaluated.
- Future research ought to concentrate on assessing the efficacy of diesel-methanol-nanoparticle mixtures in non-steady-state scenarios, which encompass start-up, acceleration, and deceleration phases, in order to guarantee uniform reliability throughout all operational conditions.
- Although TiO₂ and CuO demonstrated efficacy in this research, other NPs like Al₂O₃, CeO₂, ZnO, or combinations of multi-metal oxides could provide further advantages. It is advisable to conduct comparative studies utilizing various types and combinations of NPs, along with exploring methanol ratios that extend beyond M10, M20, and M30, to enhance the optimization of fuel formulations tailored for diverse engine types and applications.
- It is advised to incorporate a combustion analysis, paying special attention to ignition delay and combustion duration, in order to obtain a more thorough understanding of the combustion behavior in CI engines running with diesel-methanol-nanoparticle mixes.
- To improve the correlation between engine performance and combustion phenomena, future research should use heat release rate (HRR) analysis and in-cylinder pressure data.
- It is highly recommended to incorporate machine learning models or genetic algorithms alongside traditional RSM could further enhance predictive accuracy and optimization robustness, especially in complex engine-fuel interaction studies.

REFERENCES

- Adelkhani, A., Nooripour, P., & Daneshkhah, E. (2024). The Effects of Adding TiO₂ and CuO Nanoparticles to Fuel on Engine and Hand–Arm Driver Vibrations. *Machines*, *12*(10), 724.
- Ağbulut, Ü., Sarıdemir, S., Rajak, U., Polat, F., Afzal, A., & Verma, T. N. (2021). Effects of high-dosage copper oxide nanoparticles addition in diesel fuel on engine characteristics. *Energy*, *229*, 120611.
- Azad, A. K., Doppalapudi, A. T., Khan, M. M. K., Hassan, N. M. S., & Gudimetla, P. (2023). A landscape review on biodiesel combustion strategies to reduce emission. *Energy Reports*, *9*, 4413–4436.
- Azizzadeh Hajlari, S., Najafi, B., & Faizollahzadeh Ardabili, S. (2019). Castor oil, a source for biodiesel production and its impact on the diesel engine performance. *Renewable Energy Focus*, *28*(00), 1–10. <https://doi.org/10.1016/j.ref.2018.09.006>
- Barai, D. P., Bhanvase, B. A., & Żyła, G. (2022). Experimental investigation of thermal conductivity of water-based Fe₃O₄ nanofluid: an effect of ultrasonication time. *Nanomaterials*, *12*(12), 1961.
- Berber, A. (2019). The effect of diesel-methanol blends with volumetric proportions on the performance and emissions of a diesel engine. *Mechanics*, *25*(5), 363–369.
- Bermúdez, J. M., Arenillas, A., & Menéndez, J. A. (2012). Equilibrium prediction of CO₂ reforming of coke oven gas: suitability for methanol production. *Chemical Engineering Science*, *82*, 95–103.
- Bobadilla, L. F., Azancot, L., González-Castaño, M., Ruíz-López, E., Pastor-Pérez, L., Durán-Olivencia, F. J., Ye, R., Chong, K., Blanco-Sánchez, P. H., & Wu, Z. (2024). Biomass gasification, catalytic technologies and energy integration for production of circular methanol: New horizons for industry decarbonisation. *Journal of Environmental Sciences*, *140*, 306–318.
- Boretti, A. (2013). Renewable hydrogen to recycle CO₂ to methanol. *International Journal of Hydrogen Energy*, *38*(4), 1806–1812.
- D’Silva, R., Binu, K. G., & Bhat, T. (2015). Performance and emission characteristics of a CI

- engine fuelled with diesel and TiO₂ nanoparticles as fuel additive. *Materials Today: Proceedings*, 2(4–5), 3728–3735.
- D’Silva, R., Hafeez, M., Fernandez, J., Paloth, F., Rahiz, I. A., Binu, K. G., Raju, K., & Thirumaleshwara, B. (2017). Effect of copperoxide nanoadditives on the performance and emissions characteristics of a CI engine. *Energy and Power*, 7(4), 99–104.
- Deka, T. J., Abd Elaziz, M., Osman, A. I., Ibrahim, R. A., Baruah, D. C., & Rooney, D. W. (2024). Optimising novel methanol/diesel blends as sustainable fuel alternatives: Performance evaluation and predictive modelling. *Energy Conversion and Management*, 321, 118943.
- Edor, G. (2024). *RECENT PROGRESS ON THE DIRECT CONVERSION OF METHANE TO METHANOL*.
- Elsaidy, A., Vallejo, J. P., Salgueiriño, V., & Lugo, L. (2021). Tuning the thermal properties of aqueous nanofluids by taking advantage of size-customized clusters of iron oxide nanoparticles. *Journal of Molecular Liquids*, 344, 117727.
- García, A., Monsalve-Serrano, J., Micó, C., & Guzmán-Mendoza, M. (2023). Parametric evaluation of neat methanol combustion in a light-duty compression ignition engine. *Fuel Processing Technology*, 249, 107850.
- Gharehghani, A., Asiaei, S., Khalife, E., Najafi, B., & Tabatabaei, M. (2019). Simultaneous reduction of CO and NO_x emissions as well as fuel consumption by using water and nano particles in Diesel–Biodiesel blend. *Journal of Cleaner Production*, 210, 1164–1170.
- Gülcan, H. E., Gültekin, N., & Cıvız, M. (2022). The effect of methanol-Dodecanol addition on performance and smoke emission in a CI engine with diesel fuel. *International Journal of Automotive Science And Technology*, 6(2), 207–213.
- Hasan, A. O., Osman, A. I., Ala’a, H., Al-Rawashdeh, H., Abu-jrai, A., Ahmad, R., Gomaa, M. R., Deka, T. J., & Rooney, D. W. (2021). An experimental study of engine characteristics and tailpipe emissions from modern DI diesel engine fuelled with methanol/diesel blends. *Fuel Processing Technology*, 220, 106901.
- Hassan, Q. H., Ridha, G. S. A., Hafedh, K. A. H., & Alalwan, H. A. (2021). The impact of

- Methanol-Diesel compound on the performance of a Four-Stroke CI engine. *Materials Today: Proceedings*, 42, 1993–1999.
- Huang, J., Xiao, H., Yang, X., Guo, F., & Hu, X. (2020). Effects of methanol blending on combustion characteristics and various emissions of a diesel engine fueled with soybean biodiesel. *Fuel*, 282, 118734.
- Kalaimurugan, K., Karthikeyan, S., Periyasamy, M., Mahendran, G., & Dharmaprabakaran, T. (2023). Experimental studies on the influence of copper oxide nanoparticle on biodiesel-diesel fuel blend in CI engine. *Energy Sources, Part A: Recovery, Utilization, and Environmental Effects*, 45(3), 8997–9012.
- Karimifard, S., & Moghaddam, M. R. A. (2018). Application of RSM in physicochemical removal of dyes from wastewater: a critical review. *Science of the Total Environment*, 640, 772–797.
- Karvounis, P., Theotokatos, G., Vlaskos, I., & Hatziapostolou, A. (2023). Methanol combustion characteristics in compression ignition engines: a critical review. *Energies*, 16(24), 8069.
- Klejnowski, M., & Stolecka-Antczak, K. (2024). The Influence of Hydrogen Concentration on the Hazards Associated with the Use of Coke Oven Gas. *Energies (19961073)*, 17(19).
- Koca, S., Zincirci, O., & Aktaş, F. (n.d.). Investigation of the Effect of TiO₂ Nanoparticles on Engine Performance and Emission Characteristics in Diesel Engines. *International Journal of Automotive Science And Technology*, 8(2), 242–251.
- Li, H., Hong, H., Jin, H., & Cai, R. (2010). Analysis of a feasible polygeneration system for power and methanol production taking natural gas and biomass as materials. *Applied Energy*, 87(9), 2846–2853.
- Ma, S., Guo, Q., Wei, J., Yin, Z., Zhuang, Y., Zhang, Y., Dai, Q., & Qian, Y. (2024). Analyzing the effect of carbon nanoparticles on the combustion performance and emissions of a DI diesel engine fueled with the diesel-methanol blend. *Energy*, 300, 131616.
- Malik, M. A. I., Kalam, M. A., Abbas, M. M., Silitonga, A. S., & Ikram, A. (2024). Recent advancements, applications, and technical challenges in fuel additives-assisted engine operations. *Energy Conversion and Management*, 313, 118643.

- Modi, V., Rampure, P. B., Babbar, A., Kumar, R., Nagaral, M., Bhowmik, A., Pandey, S., Hasnain, S. M. M., Ali, M. M., & Bashir, M. N. (2024). Nanoparticle-enhanced biodiesel blends: a comprehensive review on improving engine performance and emissions. *Materials Science for Energy Technologies*.
- Mofijur, M., Ahmed, S. F., Ahmed, B., Mehnaz, T., Mehejabin, F., Shome, S., Almomani, F., Chowdhury, A. A., Kalam, M. A., & Badruddin, I. A. (2024). Impact of nanoparticle-based fuel additives on biodiesel combustion: An analysis of fuel properties, engine performance, emissions, and combustion characteristics. *Energy Conversion and Management: X*, 21, 100515.
- Muniyappan, S., & Krishnaiah, R. (2024). The influence of TiO₂ nanoparticles on the performance, combustion, and emissions on ternary blends of n-heptane, mahua biodiesel and diesel-fuelled engine using response surface methodology. *Case Studies in Chemical and Environmental Engineering*, 10, 100900.
- Naik, J. V., & Kumar, K. K. (2018). Performance and emission characteristics of diesel engines with Al₂O₃ and CuO nanoparticles as additives. *International Journal of Mechanical Engineering and Technology*, 9(2), 791–798.
- Nanthagopal, K., Ashok, B., Tamilarasu, A., Johny, A., & Mohan, A. (2017). Influence on the effect of zinc oxide and titanium dioxide nanoparticles as an additive with Calophyllum inophyllum methyl ester in a CI engine. *Energy Conversion and Management*, 146, 8–19.
- Parida, M. K., Mohapatra, P., Patro, S. S., & Dash, S. (2024). Effect of TiO₂ nano-additive on performance and emission characteristics of direct injection compression ignition engine fueled with Karanja biodiesel blend. *Energy Sources, Part A: Recovery, Utilization, and Environmental Effects*, 46(1), 7521–7530.
- Pellegrini, L. A., Soave, G., Gamba, S., & Langè, S. (2011). Economic analysis of a combined energy–methanol production plant. *Applied Energy*, 88(12), 4891–4897.
- Perumal, V., & Ilangkumaran, M. (2018). The influence of copper oxide nano particle added pongamia methyl ester biodiesel on the performance, combustion and emission of a diesel engine. *Fuel*, 232, 791–802.

- Prashant, G. K., Lata, D. B., & Joshi, P. C. (2016). Investigations on the effect of methanol blend on the combustion parameters of dual fuel diesel engine. *Applied Thermal Engineering*, *103*, 187–194.
- Rajendran, S., Dhairiyasamy, R., Jaganathan, S., Murugesan, S., Muthusamy, R., Periannan, S., Muniyappan, G., Jaganathan, B., Srinivasan, K., & Elangandhi, H. (2023). Effect of injection timing on combustion, emission and performance characteristics of safflower methyl ester in CI engine. *Results in Engineering*, *20*, 101599.
- Ramachandran, E., Krishnaiah, R., Perumal Venkatesan, E., Medapati, S. R., & Sekar, P. (2023). Experimental Investigation on the PCCI Engine Fueled by Algal Biodiesel Blend with CuO Nanocatalyst Additive and Optimization of Fuel Combination for Improved Performance and Reduced Emissions at Various Load Conditions by RSM Technique. *ACS Omega*, *8*(8), 8019–8033. <https://doi.org/10.1021/acsomega.2c07882>
- Ramachandran, E., Krishnaiah, R., Venkatesan, E. P., Shaik, S., Saleel, C. A., & Hussain, F. (2023). Investigation into the Ideal Concoction for Performance and Emissions Enhancement of Jatropha Biodiesel-Diesel with CuO Nanoparticles Using Response Surface Methodology. *ACS Omega*, *8*(42), 39067–39079.
- Rufus, A., Sreeju, N., Vilas, V., & Philip, D. (2017). Biosynthesis of hematite (α -Fe₂O₃) nanostructures: size effects on applications in thermal conductivity, catalysis, and antibacterial activity. *Journal of Molecular Liquids*, *242*, 537–549.
- S PRAKASH VARMA, P., & Venkata Subbaiah, K. (2024). Biofuel blends and nano-additives: a sustainable approach to diesel engine performance and emissions improvement. *Engineering Research Express*.
- Sani, M. S. M., Mamat, R., Khoerunnisa, F., Rajkumar, A. R., Razak, N. F. D., & Sardjono, R. E. (2018). Vibration analysis of the engine using biofuel blends: a review. *MATEC Web of Conferences*, *225*, 1010.
- Senthil Kumar, J., Ramesh Babu, B. R., & Gagan, R. (2020). Emission examination on nanoparticle blended diesel in constant speed diesel engine. *Petroleum Science and Technology*, *38*(2), 98–105.

- Shamsul, N. S., Kamarudin, S. K., Rahman, N. A., & Koffi, N. T. (2014). An overview on the production of bio-methanol as potential renewable energy. *Renewable and Sustainable Energy Reviews*, 33, 578–588.
- Soudagar, M. E. M., Nik-Ghazali, N.-N., Kalam, M. A., Badruddin, I. A., Banapurmath, N. R., & Akram, N. (2018). The effect of nano-additives in diesel-biodiesel fuel blends: A comprehensive review on stability, engine performance and emission characteristics. *Energy Conversion and Management*, 178, 146–177.
- Srinivasan, S. K., Kuppusamy, R., & Krishnan, P. (2021). Effect of nanoparticle-blended biodiesel mixtures on diesel engine performance, emission, and combustion characteristics. *Environmental Science and Pollution Research*, 28(29), 39210–39226.
- Srivastava, N., Srivastava, M., Pandey, H., Mishra, P. K., & Ramteke, P. W. (2018). *Green nanotechnology for biofuel production* (Vol. 5). Springer.
- Surendrababu, K., Muthurajan, K. G., Prabhakar, M., Prakash, S., Saravana Kumar, M., & Jayakumar, M. (2022). Performance, emission, and study of DI diesel engine running on pumpkin seed oil methyl ester with the effect of copper oxide nanoparticles as an additive. *Journal of Nanomaterials*, 2022(1), 3800528.
- Tirkey, J. V., & Singh, D. K. (2023). Performance and emission optimization of CI engine fueled with coconut shell-based producer gas and diesel by using response surface methodology. *Biomass Conversion and Biorefinery*, 13(11), 10243–10261.
- Tomkins, P., Ranocchiari, M., & van Bokhoven, J. A. (2017). Direct conversion of methane to methanol under mild conditions over Cu-zeolites and beyond. *Accounts of Chemical Research*, 50(2), 418–425.
- ul Haq, M., Jafry, A. T., Ali, M., Ajab, H., Abbas, N., Sajjad, U., & Hamid, K. (2024). Influence of nano additives on Diesel-Biodiesel fuel blends in diesel engine: A spray, performance, and emissions study. *Energy Conversion and Management: X*, 100574.
- Vargün, M., Yılmaz, I. T., & Sayın, C. (2022). Investigation of performance, combustion and emission characteristics in a diesel engine fueled with methanol/ethanol/nHeptane/diesel blends. *Energy*, 257, 124740.

- Veza, I., Spraggon, M., Fattah, I. M. R., & Idris, M. (2023). RSM(RSM) for optimizing engine performance and emissions fueled with biofuel: Review of RSM for sustainability energy transition. *Results in Engineering*, 18, 101213.
- Vigneswaran, R., Balasubramanian, D., & Sastha, B. D. S. (2021). Performance, emission and combustion characteristics of unmodified diesel engine with titanium dioxide (TiO₂) nano particle along with water-in-diesel emulsion fuel. *Fuel*, 285, 119115.
- Vishnoi, P. K., Gautam, P. S., & Gupta, V. K. (2022). Impact of using n-pentanol as a co-solvent with diesel-methanol blends on combustion, performance and emissions of CI engine. *International Journal of Ambient Energy*, 43(1), 6297–6306.
- Wang, J., Zhang, P., Zhang, C., & Jing, Z. (2020). *Performance and Emissions of a Premixed Combustion Engine Fueled by Methanol–Gasoline Blends*.
- Yusaf, T., Hamawand, I., Baker, P., & Najafi, G. (2013). The effect of methanol-diesel blended ratio on CI engine performance. *International Journal of Automotive and Mechanical Engineering*, 8, 1385–1395.
- Yusof, S. N. A., Sidik, N. A. C., Asako, Y., Japar, W. M. A. A., Mohamed, S. B., & Muhammad, N. M. (2020). A comprehensive review of the influences of nanoparticles as a fuel additive in an internal combustion engine (ICE). *Nanotechnology Reviews*, 9(1), 1326–1349.
- Zhang, H., Wang, L., Pérez-Fortes, M., Maréchal, F., & Desideri, U. (2020). Techno-economic optimization of biomass-to-methanol with solid-oxide electrolyzer. *Applied Energy*, 258, 114071.
- Zhang, W., Zhang, Z., Chen, H., Ji, Z., Ma, Y., & Sun, F. (2024). A review on performance, combustion and emission of diesel and alcohols in a dual fuel engine. *Journal of the Energy Institute*, 101760.
- Zhang, Z., Tian, J., Li, J., Ji, H., Tan, D., Luo, J., Jiang, Y., Yang, D., & Cui, S. (2021). Effects of different mixture ratios of methanol-diesel on the performance enhancement and emission reduction for a diesel engine. *Processes*, 9(8), 1366.
- Zhen, X., & Wang, Y. (2015). An overview of methanol as an internal combustion engine fuel. *Renewable and Sustainable Energy Reviews*, 52, 477–493.

APPENDICES

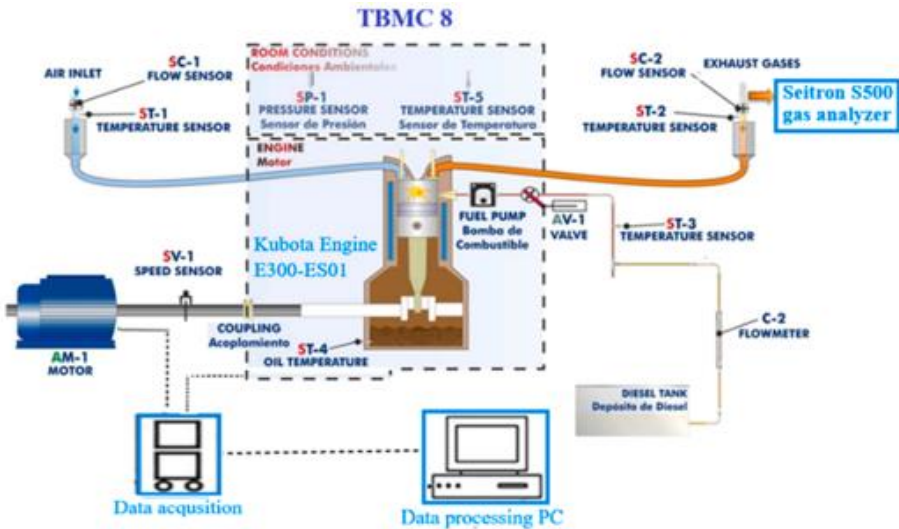
Appendix A: Structural, Chemical and Physical Properties TiO₂ properties

NO	Description	Parameters	Units
1	Density	g/cc	0.16
2	Micro strain	-	0.081
3	Purity	%	97.92
4	Surface Area	m ² /g	376
5	Color	-	White
6	Particle size average	nm	15–20
7	Dislocation density	Line ² / m ²	0.3 × 10 ¹⁵

Appendix B: Structural, Chemical and Physical Properties CuO properties

NO	Properties	Detail
1	Chemical name	Copper oxide
2	Chemical composition	Copper -79.9% Oxygen -20.1%
3	Molecular weight	32.85 g/mol
4	Thermal conductivity	0.32 W/m-k
5	Color	Pure black
6	Particle size average	20-30 nm
7	Density	6.31 g/cm ³
8	Melting point	1201 °C
9	Molar mass	79.5 g/mol
10	Boiling point	2000 °C

Appendix C: EDIBON, TBMC 8 model engine dynamometer test setup



Appendix D: Originality Declaration Form for Students

This form must be completed and signed for all works submitted to the University for Examination.

Name of student	Lelisa Alemu Gobena
Id. No.	PGE/28430/15
Department	Mechanical engineering
College	Mechanical, Chemical, and Material Engineering
Course Title	Thesis paper
Title of work / Assignment name	Optimizing the Combined Effects of TiO ₂ and CuO Nanoparticles on CI Engine Performance and Emissions with Diesel-Methanol Blends Using Box-Behnken Design

DECLARATION

1. I understand what plagiarism is and I am aware of the university's policy in this regard.
2. I declare that this dissertation entitled **“Optimizing the Combined Effects of TiO₂ and CuO Nanoparticles on CI Engine Performance and Emissions with Diesel-Methanol Blends Using Box-Behnken Design”** research project is my original work and has not been submitted elsewhere for examination or award of a degree or publication. Wherever others' work or my own work has been utilized, it has been duly acknowledged and referenced in compliance with the university's requirements.
3. I have not sought or used the services of any professional agencies to produce this work.
4. I have not permitted, nor will I permit, anyone to plagiarize my work with the intention of presenting it as their own.
5. I am aware that making any false claims regarding this work will lead to disciplinary action in accordance with the university's Anti-Plagiarism Guidelines.

Signature _____

Date _____

Lelisa Alemu

Thesis

- Quick Submit
- Quick Submit
- Adama Science and Technology University

Document Details

Submission ID
trn:oid::1:3450660781

Submission Date
Dec 25, 2025, 1:01 PM GMT

Download Date
Dec 25, 2025, 1:05 PM GMT

File Name
Thesis.docx

File Size
1.4 MB

83 Pages

21,728 Words

123,708 Characters

22% Overall Similarity

The combined total of all matches, including overlapping sources, for each database.

Match Groups

- 402 Not Cited or Quoted 19%**
Matches with neither in-text citation nor quotation marks
- 73 Missing Quotations 3%**
Matches that are still very similar to source material
- 0 Missing Citation 0%**
Matches that have quotation marks, but no in-text citation
- 0 Cited and Quoted 0%**
Matches with in-text citation present, but no quotation marks

Top Sources

- 11% **Internet sources**
- 18% **Publications**
- 4% **Submitted works (Student Papers)**

Integrity Flags

1 Integrity Flag for Review

- Replaced Characters**
125 suspect characters on 22 pages
Letters are swapped with similar characters from another alphabet.

Our system's algorithms look deeply at a document for any inconsistencies that would set it apart from a normal submission. If we notice something strange, we flag it for you to review.

A Flag is not necessarily an indicator of a problem. However, we'd recommend you focus your attention there for further review.